Universitetet i Stavanger

FACULTY OF SCIENCE AND TECHNOLOGY

MASTER'S THESIS

Study program/specialization: Petroleum Engineering/Drilling Engineering	Spring 2017 Open access
Author: **Osama Abdul-hafiz Assaf**	(signature of author)

Programme coordinator: **May Britt Myhr**

Faculty Supervisor: **Helge Hodne**

External supervisor: **Vegar Haraldsen**

Title of master's thesis:

Well P&A Tubing Compaction Method Evaluation and Modelling

Credits: 30

Keywords: Tubing Compaction, Downhole Crushing Buckling, Slot P&A, Rig-less Modelling, Method, FEM, ABAQUS	Number of pages: 116 + appendices: 9 Stavanger, July 13th, 2017

Abstract

The number of aged fields in the North Sea is increasing, and in few years, and there will be a significant increase in number of wells that need to be permanently plugged and due to low oil prices and other reasons, there is a push from the industry to reduce the cost of P&A operations as much as possible, and using rig-less equipment for P&A has proven to be a reliable alternative to drilling rigs, but this solution requires the development of new technologies to overcome the challenges that come up with it.

The presence of tubing in the area where the permeant plug should be set is still a thorny issue for P&A rig-less operation for many reasons. Recently there are many approaches for removing tubing in place without pulling it to surface, one of these alternative ideas is downhole tubing disposal (DHTD).

The main scope of this thesis is to give an insight into DHTD method, its advantages and the challenges to translate this idea into practice. In this work as well, different approaches are incorporated to estimate the required tubing crushing force, including FEM, analytical estimation and experimental work.

Results are reported for an analytical estimation and FEM (ABAQUS) analysis of a slotted tubular subjected to compression axial load. The results showed different kinds of correlations with experimental test data. On the other hand, they showed that FEM is a powerful method to solve this kind of problems.

Acknowledgments

This thesis was written for the Department of Petroleum Engineering at the University of Stavanger in cooperation with Oilfields Innovations limited.

First and foremost, praise be to God and blessing and peace be upon his prophets.

I want to express my great appreciation to Professor and mentor Helge Hodne for his great guidance and help, and a great appreciation also goes to the engineer at Oilfields innovations Norway “Vegar Haraldsen” who paved the way with his efforts and public relations and involved me in several regarding meetings to complete this work.

I am indebted to Professor Mesfin Belayneh fir his encouragement and supporting.

Special thanks to Mr. Adugna Deressa Akessa for his great helping to set up the ANSYS and Autodesk Inventor software’s work and get the access to the only one research licence in UIS which saved me a lot of time.

The thanks are connected to Mr. Giorgio Pattarini who has answered all my simple questions.

Last but not least, I would like to thank my family, friends, and those are dear to my heart who motivated me to finalize the studying successfully.

Table of Contents

Table of Figures

Table of Tables

Nomenclature

A	*Amplitude of a sine curve*
A_{cp}	*Cross section area of curved plate*
A_i	*Internal flow area of the pipe*
A_o	*Total cross-sectional area of the pipe*
A_p	*Cross section area of piston*
A_s	*Cross-sectional area of the pipe*
C_c	*Column slenderness ratio*
c_w	*Average contact force*
d	*Mean diameter*
D_i	*Well inside Diameter*
d_i	*Tubing inside diameter*
d_o	*Tubing outside diameter*
E	*Young's elastic modulus*
F	*Axial Load*
F_{avg}	*Mean axial load*
F_{cr}	*Critical buckling load*
F_{fric}	*Friction force*
F_{hel}	*Helical buckling load*
F_{sin}	*Sinusoidal buckling load*
F_{splay}	*Tubing splaying force*
F_y	*Yield load*
g	*Acceleration of gravity*
G	*Shear modulus*
g_i	*Pressure gradient of well bore Fluid (i) above the piston*
h_i	*Height of well bore Fluid column (i) above the piston*
I	*Moment of inertia*
I_{cp}	*Moment of inertia for curved plate*
J	*Polar moment of inertia*
K	*End constrain factor*
L	*length of the pipe*
L_u	*Unsupported length of the pipe or curved plate*
M_b	*Bending moment*
N	*Normal force*
p	*Pitch of the helix*

$P_{closure}$	*fracture closure pressure*
p_i	*Internal pressure of the pipe*
p_o	*External pressure of the pipe*
P_{piston}	*Pressure above Piston*
P_{surf}	*Surface presuure*
r	*Radial clearance*
R	*Radius of curvature*
r_g	*Radius of gyratio*
r_i	*Pipe inside radius*
r_o	*Pipe outside radius*
S_R	*Effective slenderness ratio*
t	*Thickness*
w	*Buoyant weight unit of the pipe*
w_c	*Contact force*
w_p	*Weight of pipe in air*
z	*Axial coordinate*
α	*Wellbore trajectory inclination angle*
Δ	*Axial displacement*
ΔL_b	*Buckling length change*
ϑ	*Plate curvature angle*
θ	*Wellbore trajectory azimuth angle*
ϑ_c	*Angle between the pipe centre and the coordinate axis*
κ	*Wellbore curvature*
μ	*Dynamic friction coefficient between casing and tubing*
ρ_i	*Density of fluid inside the pipe*
ρ_o	*Density of fluid outside the pipe*
σ_b	*Bending stress*
σ_y	*Yield strength of pipe*

Abbreviations

AISC	*American institute of steel contraction*
API	*American Petroleum institute*
BC	*Boundary condition*
BHA	*Bottom hole assembly*
BOP	*Blowout preventer*
CSG	*Casing*
CT	*Coiled tubing*
DHTD	*Downhole tubing disposal*
e-line	*Electric line*
FEM	*Finite element method*
ft	*Feet*
HBC	*Helical buckling critical load*
HWO	*Hydraulic workover*
lbs	*Pounds*
MD	*Measured depth*
NACA	*NATIONAL ADVISORY COMMITTEE FOR AERONAUTICS*
NCS	*Norwegian continental shelf*
NORM	*Naturally Occurring Radioactive Materials*
NORSOK	*Norsk Sokkels Konkuranseposisjon (Competitive Standing of the Norwegian Offshore Sector)*
OGIC	*The Oil and Gas Innovation Centre*
Oil & Gas UK	*The United Kingdom Offshore Oil and Gas Industry Association Limited*
OILtd's	*Oilfield innovation limited*
P&A	*Well Plug and Abandonment*
POOH	*Pull out of hole*
RLWI	*Riser-less Light Well Intervention*
SL	*Slick line*
TBG	*Tubing*
TTSS	*Through tubing sand screen*
UIS	*University of Stavanger*
UKOOA	*UK Offshore Operators Association*
WBE	*Well barrier elements*
XMT	*Christmas tree*

1. Introduction

1.1. Background

By the beginning of 2017, almost 4350 development wells have been completed in Norway [28]. Sometime on the future, these wells will stop production and should be plugged and abandoned (P&A).

Assuming there are at present 3,200 wells needing Rig-P&A on the NCS, and an average of 30 rig-days per well for permanent plugging, the total cost will be around 400 billion. This estimation based on a 4 million NOK/rig-day. If the plugging is performed over a 25-year period, in which about 3,000 new wells might be drilled that also need to be plugged, the total charge for P&A for the coming 40 years will be close to 900 billion NOK. This estimate is dependent on nowadays rig rates. This gives an indication of the great costs that expect ahead for P&A operations [29].

In Norway, minimizing the total cost of permanent well plugging is vital, because a great share of the costs for P&A operations represents tax deductions for operators. The income for the Norwegian state from petroleum activities is thus greatly reduced with high P&A costs. The use of rigs for P&A operations will lead to a suspension in drilling new wells, which again will lead to delayed production. The use of rigs for plugging will also lead to a higher usage rate of rigs, and it can be expected that this will increase the daily rates [29].

About 20% of wells involve a drilling rig during P&A while the rest do not, and thus, can be plugged using rig-less operations. This will be a way to reduce the cost of P&A operations by using improved and new technologies that can replace the rigs with small ships that can perform rig-less operations [30].

Oilfield Innovation has taken a patent on one of these new technologies. The idea can be titled by downhole tubing disposal (DHTD) on a rig-less concept. A general description of the method is to compact a part of the tubing instead of pulling the whole tubing out of the hole. Weakening the tubing could be required to ease its compaction, the weakening can be achieved by slicing the tubing longitudinally, and the required compacting force on the tubing can be a hydraulic force achieved using a piston positioned above the parted tubing, thus a

casing window will be created and it will enable to log cement behind casing and set a full cross section cement plug.

1.2. Scope and Objective

This new technology has never been applied in the oil fields or even in a real large-scale model, and the primary objective of this thesis work is to investigate this new technology along with its advantages and challenges, and to compare it with conventional technologies with respect to time and scope, but the main question that this work tried to answer:

- Is that possible to create a mathematical model that can predict the tubing compaction parameters within tubular and hydraulic limits of an oil/gas well?

To answer this question different approaches (analytical, experimental, and numerical using FEM) are involved in this work to addressing issues like how the slots number and length in the tubing body will affect the required crushing force.

The involved activities in this work are:

- Literature study about P&A regulations and requirements in UK and Norway including some P&A challenges and technical alternatives.
- Literature study on the new technology (principle, tools, advantages and challenges).
- A theoretical review of buckling behaviour for the pipes in the oil wells and for the column structure (Euler buckling).
- A theoretical review of the loads acting upon the piston.
- Present an analytical estimation for the initial buckling load of a slotted tubular and compare it with experimental study.
- Perform different simulations using ABAQUS/CAE and compare one of the models results with the parallel experimental work, while the other set a first step for further modelling.

2. Plug and Abandonment

2.1. Definition and standards requirements

P&A is the operation where the well is sealed off and secured with a well barrier which is defined according to NORSOK as “an envelope of one or several well barrier elements preventing fluids from flowing unintentionally from the formation into the wellbore, into another formation or to the external environment ” [6].

The main objective of the whole process is to re-establish the accepted integrity of the formation that was drilled before.

As an example, Fig. 2-1 shows the barrier envelope marked with red dashed line, the orange boxes contain the barrier elements and the blue ones contain the recommended practices [16].

In the North Sea, there are guidelines and requirements that are designed for well abandonment issued by the operators or the governmental authorities. In the UK sector, the P&A operations are being done in accordance with UKOOA (UK Offshore Operators Association) guidelines for well suspension and abandonment.

Similarly, NORSOK/D-010 standard contains those guidelines for the Norwegian sector.

All the guidelines have basically some main aims to:

- Prevent hydrocarbon escape to the surface.
- Prevent hydrocarbon transferring between different formations.
- Prevent contamination of water-bearing formations.
- Protect shallow formations from pressure collapse.

The requirements in each standard aim to achieve those goals [31].

In this work, only the overall requirements for permanent abandonment are shown, while the

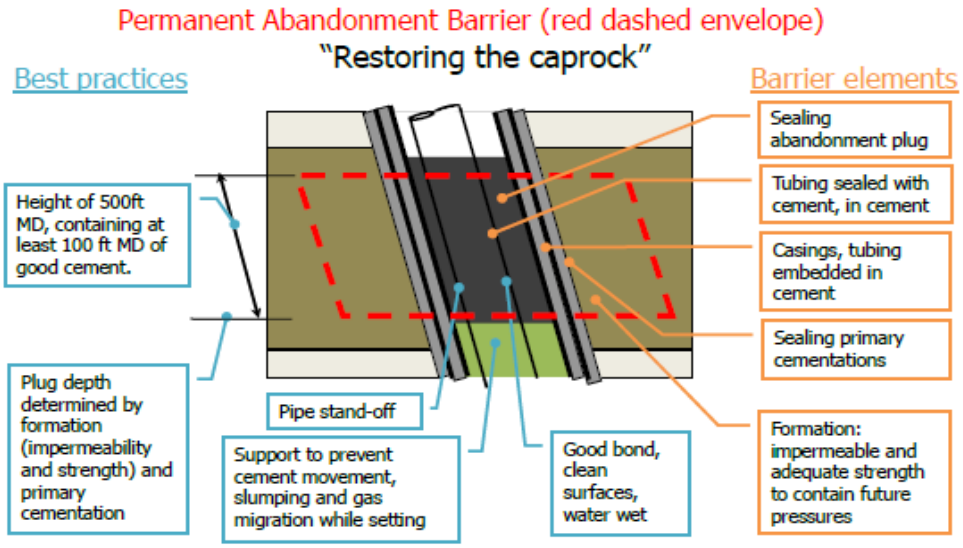

Fig. 2-1 Schematic of a permanent barrier showing the barrier envelope [16]

standards involve more details, also the requirements are stated as they are in the standards to avoid any misunderstanding of the standards.

2.1.1. Oil & Gas UK Guidelines

Oil & Gas UK guidelines contain the following requirements [16]:

- If a permeable zone is hydrocarbon-bearing or over pressured and water-bearing, then, two permanent barriers from the surface are required, and the second permanent barrier is a backup to the first.
- "The **first barrier** should be set across or above the highest point of potential inflow (top permeable zone or top perforations, whichever is shallower), or as close as reasonably possible."[16].
- The **second barrier** should be set with the following concerns when required:
  - "The same considerations in the first barrier are applied with respect to the second barrier in addition to a relative position of cement in the annulus and shallow permeable zones, Fig. 2-2" [16].

- To create a permanent barrier which is considered a good industry practice, the length of the barrier for a cement column should be at least 100 ft. MD of good cement, Fig. 2-3 as an example [16].
- When a combination permanent barrier is chosen to replace two barriers:
  - A cement column of at least 200 ft. MD of good cement is considered to constitute such a permanent barrier. But, generally an 800 ft. MD barrier is set.

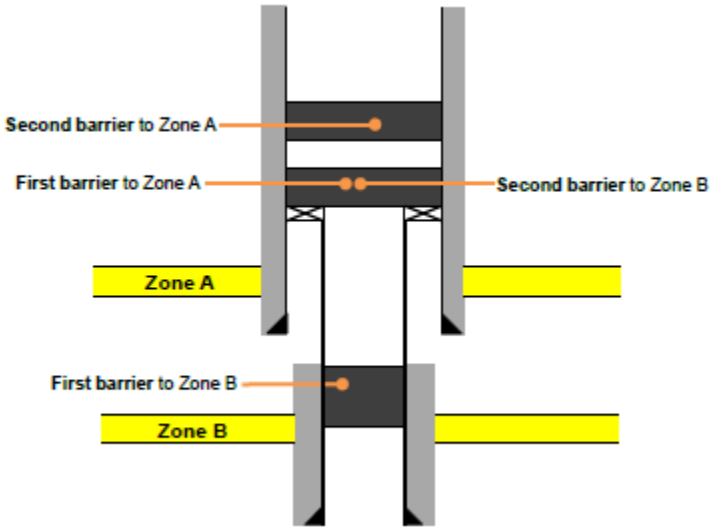

Fig. 2-2: General requirements for well abandonment [16]

  - The top of this barrier should provide at least 200 ft. MD of good cement above the highest point of any possible flow source.

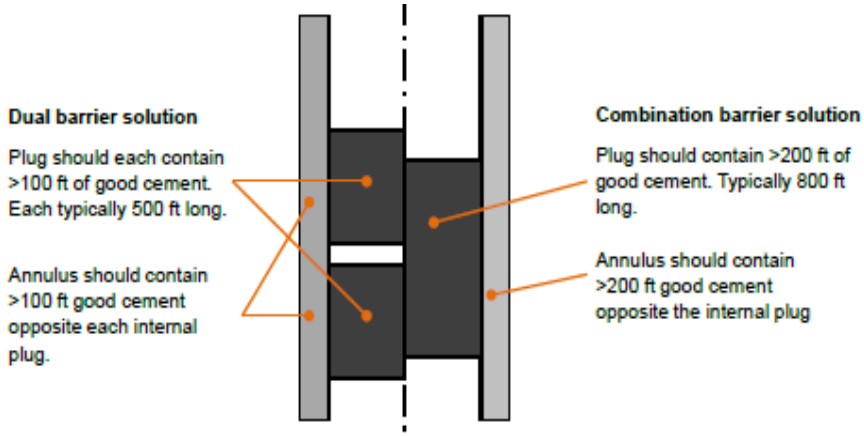

Fig. 2-3: Comparison of length for dual and combination barriers [16]

  - The internal cement plug must be adjacent to the annular good cement over a cumulative distance of 200 ft. MD of overlap. This overlap section of the plugs must be of good quality cement on both sides.

2.1.2. NORSOK Guidelines requirements

The NORSOK standard [6] principle recommendations can be condensed in:

- "Permanent abandonment shall be performed with an eternal perspective considering the effects of geological processes".
- "Two barriers shall be fulfilled in case of potential source of inflow or reservoir exposed, and one in case of formation with normal pressure or less".
- "The barrier base shall be positioned at the depth where wellbore integrity is higher than the potential pressure below, and adjacent to an impermeable formation".
- "Permanent well barriers shall extend across the full cross section of the well, include all annuli and seal both vertically and horizontally (Fig. 2-4)".

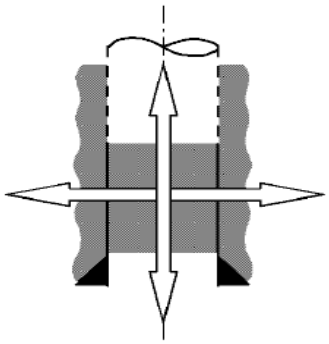

Fig. 2-4 full cross section barrier according to NORSOK [6]

- The barrier should have some characteristics like; impermeable, non-shrinkable, mechanical endurance, chemical resistance, wetting and non-harmful to steel tube.

All annular spaces are to be secured, and the surface plug should be more than 200m length and less than 50m below seabed.

2.2. Operation phases and complicity

P&A operations could be complicated and costly, especially when setting deep barriers using a rig is required. Thus, it is important to have a common approach to classify the type of P&A related to the cost estimation of it [16].

UK guideline proposes a classification of P&A planned wells according to three factors:

- The location of the well (platform, subsea or land well)
- "Abandonment Phases – reflecting the three phases of an abandonment Operation."

- “Abandonment Complexity – the methodology and equipment required.”

2.2.1. Well Abandonment Phases

The abandonment operation can be divided into three different phases, reflecting: the work-scope, equipment required, and/or the discrete timing of the different phases of work [32].

2.2.1.1. Phase 1 - Reservoir Abandonment

The aim of this phase -as the name explains- is to isolate all producing or injection zones by setting the primary and secondary barriers. In this case the tubing may be left in place, partly or fully retrieved, and the phase is finished when the reservoir section is isolated totally.

2.2.1.2. Phase 2 - Intermediate Abandonment

This phase includes: milling and retrieving casing including tubing if not done in phase 1, completed when no further plugging is required [32].

2.2.1.3. Phase 3 - Wellhead and Conductor Removal

This phase includes pull wellhead, conductor, and fill craters with cement, completed when no further operations required on the well.

2.2.2. Well Abandonment Complexity

The complexity of the work for each of the three phases mentioned earlier is defined by a digit between 0 and 4, according to the following [32]:

- **TYPE 0**: **No work required:** A phase work has been completed before.
- **TYPE 1**: **Simple Rig-less P&A:** including wireline, pumping, crane, jacks. Subsea will use Light Well Intervention Vessel.
- **TYPE 2: Complex Rig-less P&A**: Using CT, HWU, wireline, pumping, crane, jacks. Subsea will use Heavy Duty Well Intervention Vessel with Riser.
- **TYPE 3**: **Simple Rig-based P&A**: Requiring retrieval of tubing and casing.
- **TYPE 4: Complex Rig-based P&A** – May have poor access and poor cement requiring retrieval of tubing and casing, milling and cement repairs.

The complexity of the operations offshore determines the type of the unit used to perform those operations and Fig. 2-5 illustrate the main used units; RLWI (category A), heavy intervention (category B), conventional rigs (category C) [20].

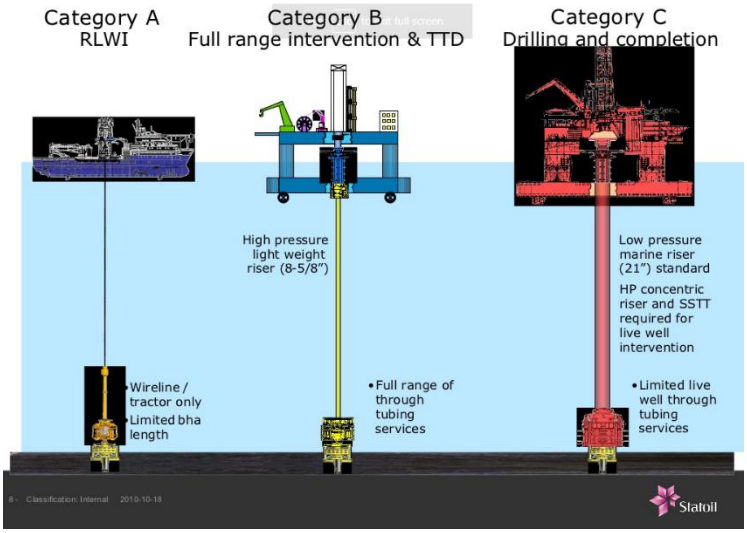

Fig. 2-5 Illustrate different kinds of platforms and vessels used in P&A operations [20]

Normally category C (semi- submersible platforms) and the heavy intervention (category B) can perform the coiled tubing operations, but till now not the riser-less vessels. Nevertheless, different efforts have been made in the last years to do that, as an example Island offshore drilled a shallow gas pilot hole using open water coiled tubing, and now they are working to enhance the technology to perform heavy well intervention with coil tubing in producing subsea wells and afterwards a whole P&A operation [33]

Usually, the cost of using Rig-less vessels is less compared to the rigs due to the lower daily rate of these units, even some studies show that the rig-less operation could consume more time, but in the outcome, the total cost will be less [34].

2.3. P&A operation challenges and the technical alternatives:

Before going into the talk about P&A challenges, it is important to mention the key steps of a conventional P&A operation performed on a well (with vertical X-mas tree as an example) which can be summarised in the following:

1. Prepare the well by checking, killing and set temporary barriers.
2. Remove Xmas tree and set BOP.

3. Removing tubing.
4. Set primary and secondary barrier plugs, with milling operations if required.
5. Cut and pull intermediate casing and the environment plug.
6. Sever and retrieve Wellhead.

The related steps to this work will be discussed in detail including the challenges and the alternative solutions:

2.3.1. Removing tubing and control lines

As mentioned before, NORSOK required a full cross section barrier for a permanent barrier, so removing tubing will be a requirement in case the tubing has control lines or the cement behind the production casing is not verified, or need to be repaired, since the industry till now is not able to perform a cement log on multiple tubes.

Removing tubing is one of the major P&A challenges due to what tubing pulling requires, thus, increasing the time and cost consuming.

Removing the tubing in the proposed barrier area could be performed in two different ways:

- Cutting and pulling the tubing to the surface.
- Locally removing the tubing by alternative methods.

2.3.1.1. Cutting and pulling the tubing to the surface

Tubing cutting operation itself is a conventional operation, and it could be performed with wireline. Even more, it does not need a tractor in the tool string. The most common way to do that is the explosive cutting where one big charge set in the centre of the tool is sent

downhole, and the explosive jet will cut the required pipe at the cutting point. Fig. 2-7 shows an example of the tubing shape after explosive cutting operation.

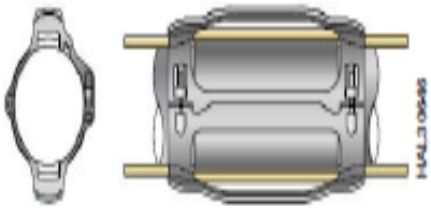

Fig. 2-6 tubing clamp and control line [11]

Fig. 2-7 tubing cross section after using explosive cutter [10]

Nowadays, attached control lines (Fig. 2-6) to the tubing could be used in deep depths with smart wells to operate some downhole devices, and according to NORSOK, "the control lines shall be removed from the areas where the barrier is to be installed". Accordingly, it is preferred to cut the control line with tubing and pull them out of the hole together, otherwise, it will break under tension, and it will stay in the well as debris, and the operation to retrieve them later will be time and cost consuming. One of the solutions for that is to push the control lines down and install mechanical plug which will be a foundation for the later cement plug, but this required a powerful pushing force due to the stiffness of the control line.

Many of the smart completion suppliers provide a cutting sub which will be used to prevent control line problems, but for old wells, this sub was not available. So, there are many companies claiming that they can provide several cutting devices or technology which can cut the tubing and the control lines together, and here are some examples:

- **<u>Mechanical pipe cutter (Baker Huges):</u>**

The tool is designed for downhole pipe cutting without damaging the outer casing, since the penetration is controlled all the time, and it can make many cut operations in one run, but if the tubing was in compression then the blade could be stuck (Fig. 2-8).

The blade moves in an eccentric circular movement around the axis of the tools that makes the cut distributed equally around the cutting surface. This tool is also used to cut control lines when the cut point is at the clamp [2].

Fig. 2-8 Baker Hughes Mechanical Pipe Cutter [2]

- **<u>Downhole Electrical Pipe cutter (GE Oil& Gas):</u>**

If the tubing is in compression, then cutting with blades will be complicated and the tubing should be set in tension first, but there are some tools that can cut the tubing in compression like the "Downhole Electrical Pipe Cutter" shown in Fig. 2-9.

Fig. 2-9 GE Downhole Electrical Cutting Tool [9]

Operated by an electrical signal, and compared to the previous tool, this tool adds more accuracy regarding cutting depth since it could be run with CCL tool, and enables to cut the tubing either in tension or compression which means the blade will not stuck [9].

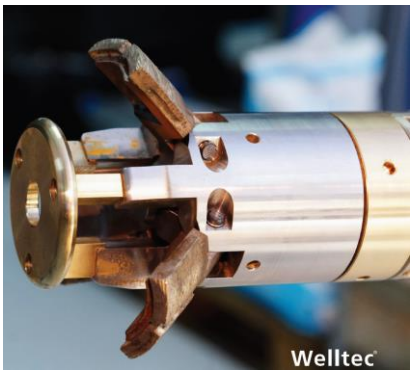

Fig. 2-10 MCCP [5]

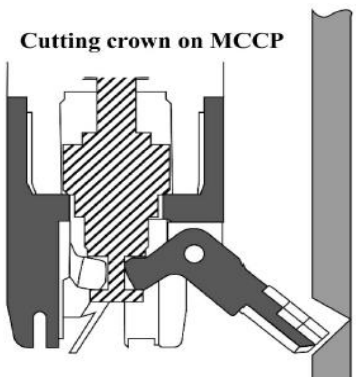

Fig. 2-11 MCCP during cutting the pipe [26]

- **Mechanical Cutter based Cutting Pad platform (Welltec):**

Using a grinding system rather than a blade (Fig. 2-10), this tool produces a smooth and polished surface with the ability to cut the pipe in tension, neutral or compressed condition,

The cutting crown (Fig. 2-11) has three arms ended with the grinding pads. The cut becomes an angled sloping surface which prevents deformation of the pipe by axial compression. Using this tool shows a lot of the advantages regarding the time and cost saving and safety [26].

After cutting the tubing, it should be pulled to the surface, and this operation is usually performed by a rig, but now a new approach is being developed to use RLWI vessels for that. Island Offshore is working now on this project [35].

2.3.1.2. Locally removing the tubing by alternative methods

Nowadays, there are new approaches to exclude the tubing POOH step, such a method could be -if proved- very cost effective and HSM considerable, because in this case there will be no pipe to handle, no milling required and low-risk probabilities...etc. Here are some of these methods, note that none of them is field proven and some of them are such ideas.

- **Downhole tubing disposal (DHTD):**

Which is the main focus in this thesis, more details about the method will be discussed in Chapter 3.

- **Chemical removing of the tubing:**

Since the tubulars are made from a corrodible material (the steel), so an idea claims that using very high corrosive chemicals could dissolve a part of tubing at a desirable depth, this idea is based on the past cases where the tubing or casing is corroded severely because of the presence of corrosive materials. The consumed reacted material should be replaced with fresh one during the operation and a circulating path is essential.

The proposed method is designed to be performed with coiled tubing, but a risk assessment should be performed to prevent CT damage, also another concern here is how to protect the rest of equipment. One of the drawbacks of this method is the long time taken to achieve the required goals [3].

- **Jet Cutter (Halliburton):**

Tested successfully and using a jet power created by sand-loaded water, this method can cut all type of steel pipes and control lines in both directions vertical and lateral [36]. Halliburton claims that “there is no limit on max section length to be cut”, so this could be a very strong point to the crushing model.

- **Remove tubing by Plasma:**

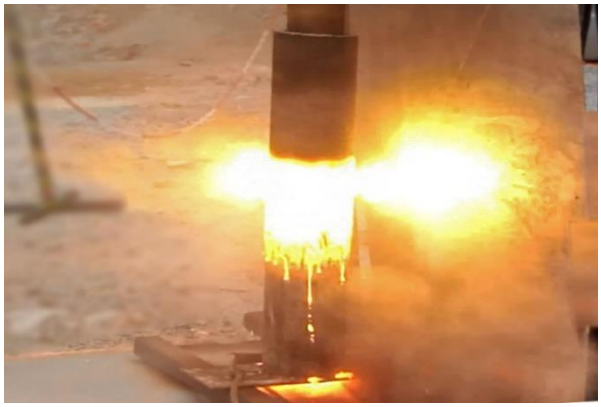

Fig. 2-12 PLASMABIT Milling [4]

In other words, remove the tubing by melting. The plasma cutter today can cut steel tube in the well by generating extremely high temperatures to melt a part of the string at the point where a cement has to be placed in P&A operation [4].

Plasma cutters can cut into all kind of well fluids. The main challenges of this kind of methods are pressure requirements, applying the technology at deep depths (it has been tested for surface cutting) and the way of BHA releasing after melting the tube.

2.3.2. Run cement log

As mentioned before, according to NORSOK, a minimum of 30 m cement interval behind casing is required to act as an external barrier, if it is to be verified by logging [6].

So, after pulling the tubing, a cement logging is performed to check the quality of cement behind the casing, this operation is performed using wireline, and the most common tools used for that are CBL (cement bond log) and USIT (ultra-sonic imager tool). Both tools use acoustic and ultrasonic waves to predict the cement condition.

Regarding this issue, it should be considered when the tubing is partially removed – by crushing for example- that the cement log tool should be adjusted to run through the tubing

first and perform the logging in the created casing window, which will add some more logging operation requirements, like:

- The casing window length should be enough to perform the logging.
- The logging tool should be centralized in the casing.
- The well fluid has a strong effect on the logging operation.

Such tools are available for example; The Baker Hughes Radial Analysis Bond Log has a diameter of 2.75" and can log cement behind between 4" to 9 5/8" casing [37]. Additionally, Schlumberger has a DSLT tool with a 3.625" diameter that will fit through the 4.5" tubing to log the bigger size casing [38].

2.3.3. Set primary and secondary barrier plugs

After getting the results of the logging, two cases could be faced:

- Casing cement condition is good and verified to be a barrier element.
- Casing cement is not present or need to be repaired.

The condition of casing cement will determine the subsequent steps to set the barrier plugs.

2.3.3.1. The validity of casing cement

In this case, a cement plug can be set inside casing directly. In many cases, a foundation for the cement plug is required, which could be mechanical (bridge plug) or high viscous pill and the length of the required cement plug is related to the type of the foundation according to the standards.

After setting the cement plug, again a verification shall be performed usually by pressure testing, tagging or both, according to the well condition.

Normally, the cement plug is set with drill pipes using semi-submersible rigs after pulling the tubing, but recently, there are different methods (some of them are still ideas) to set a sufficient barrier without using the drill pipes or rigs, here are some of these methods:

- **<u>Using the tubing itself:</u>**

Saving a lot of the costs, this method proposes to pump the cement through the severed tubing after setting a mechanical plug above the barrier required depth, here a special type of

equipment could be used at the surface to modified the well head to perform such an operation, even a bull heading can be performed using the tubing too.

With this method, a lot of cement contaminations is expected.

- **Using coiled tubing:**

Using coiled tubing to pump cement is kind of normal operation that is performed usually with no challenges if a riser is used, but without the riser, it is a challenge.

With using coiled tubing, less contamination is expected, but the small size of the CT and the presence of the package will create some challenges.

2.3.3.2. The casing cement is absent or needs to be repaired:

Then a milling operation is required to create a window to set a full cross section cement plug as a conventional solution. But milling operation has high cost and a lot of HSE concerns.

Recently, the industry provides different alternative methods/tools could be used to achieve the requirements without milling. Here are some of the tools to repair or set a cement behind the casing:

- **Perforate, wash and cement (HydraWash)**

Provided by Hydra Wash, with this technology there is no need to mill casing [39], which means no swarf problems (handling and disposal), time saving, optimum well control through all phases of plug setting, a study performed to estimate the saved time when using this method in different situations is shown in Fig. 2-14, and the difference of time-consuming is clear between the conventional way and PWC method as is illustrated [21].

As the name refer, the operation start with perforating the casing with tubing conveyed perforation guns, after firing and dropping the guns, a cup which is installed above the guns is used as a base, then washing tool uses jetting to clean the perf's and the formation from old mud and make the area behind casing clean to squeeze a cement, the cement can be verified afterwards by milling the cement inside the casing, and running a logging tool. Fig. 2-13 shows the steps of the operation [40].

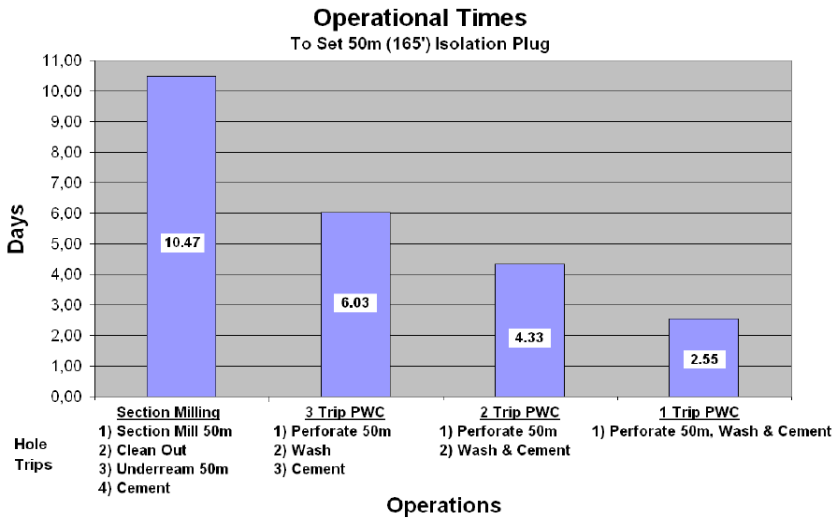

Fig. 2-14 field operational time comparison [21]

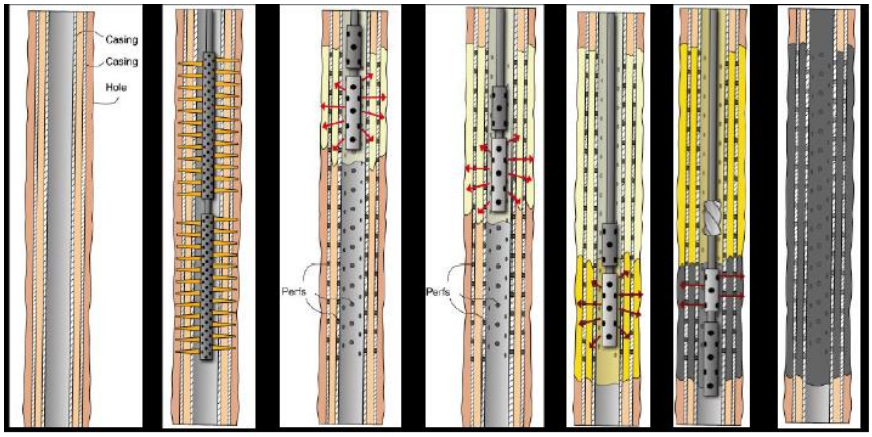

Fig. 2-13 PWC Method steps [14]

- **Cement Adapter Tool (CAT) [35]:**

This tool shown in Fig. 2-15 can be used to set surface or environment barrier where one or more casing strings need to be perforated to install the barrier, with this method no need to cut and lift the casing, the tool consists of different equipment like adapter tool, stinger assembly and cement spool.

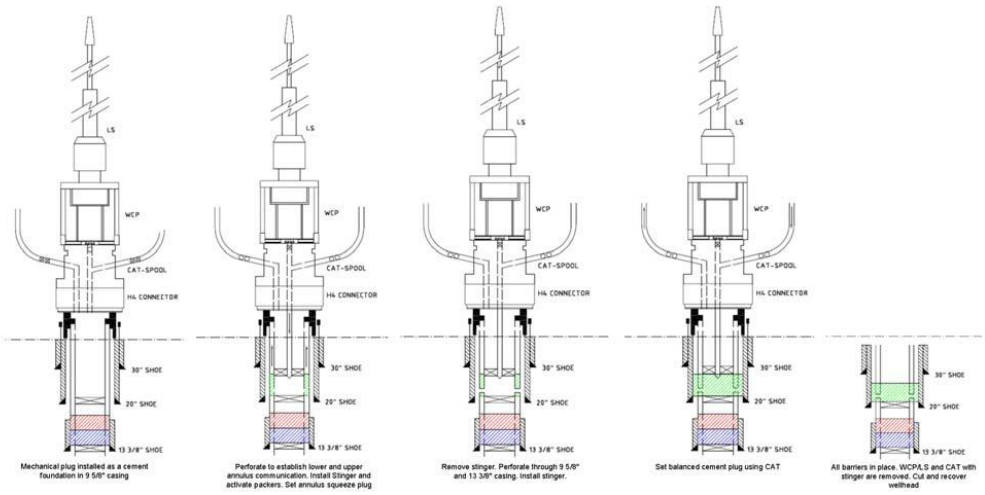

Fig. 2-15 CAT operation steps [14]

- **<u>Well Abandonment Straddle Packer (WASP) (Baker Hughes)</u>**

This tool has the same CAT tool function. WASP operation starts with perforating A- annulus, then circulating out the mud from behind the casing strings. The annuli are then cemented and tested [41].

3. The Tubing Crushing in Details

3.1. Introduction

As mentioned before, in some cases it is necessary to remove the tubing at the depth where the permanent barrier should be set. Conventionally, P&A operations use large expensive drilling rigs to pull the tubing to provide an open casing window to log casing cement, clean casing surfaces and set cement plug. In this chapter, an alternative lower cost solution will be discussed in detail.

The objective of the proposed method is to use type 1 or 2 equipment as clarified in Section 2.2.1 to perform P&A Phases 1, 2 or even 3 as clarified in Section 2.2.2.

3.2. Principle and Steps

Most of the inner volume of the casing is filled by liquid where the tubing steel occupies a small space compared to the fluid. In Table 3-1, some exmples show these volumes. When the well is plugged, one can take the advantages of this volume through filling it with tubing steel by compacting the tubing downward instead of pulling it out of the hole.

Table 3-1 Example API liquid space percentages [19]

Casing OD	9.625 in.	9.625 in.	7 in	5.5 in
Weight	53.5 ppf	53.5 ppf	29 ppf	23 ppf
Casing ID	8.535 in	8.535 in	6.184 in	4.67 in
Tubing OD	5 1/2 in	4 1/2 in	4 1/2 in.	2 3/8 in
Weight	20 ppf	12.6 ppf	12.6 ppf	4.6 ppf
Tubing ID	4.778 in	3.958 in	3.958 in	1.995 in
Liquid Space	89.8%	93.7%	88.0%	92.4%

At least 45 % compaction ratio can be achieved if the tubing is sliced and compacted [17]. Two different ways can be used to achieve that and in this work, the terms (Scenario 1) and (Scenario 2) are categorizing those two ways, which are:

- Scenario 1- wedging an upper piece of tubing into a lower split one
- Scenario 2- crushing tubing by locally deforming slotted segments

3.2.1. Scenario 1- wedging an upper piece of tubing into a lower split one

In this method, Oilfield Innovations proposes to sever the handled part of the tubing and

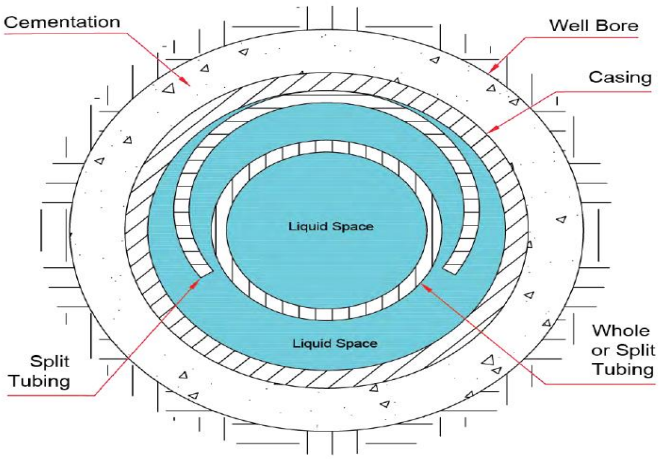

Fig. 3-1 Cross section of the well after compacting tubing- scenario 1 [19]

create a single longitudinal slot in the lower half of the tubing to allow the upper half to be easily pushed into the split part. Fig. 3-1 [19] shows the cross section of the well after pushing tubing.

In practice, as Fig. 3-2 shows, the proposal comprises the following steps:

- If a plug is set at deeper depth below the handled tubing, it is preferred to make sure that there is a relief point to formation or casing annulus for the fluid which will be trapped below the piston during compaction process, to provide a circulation through the tubing and prevent hydraulic lock-up below the piston during compaction, this can be done by punching tubing and casing at the bottom of the handled tubing.
- Longitudinally slice the lower part of the targeted tubing.
- Transversely cut the tubing above the sliced part and circulate cleaning fluid with surfactants to lubricate the piston and the compacted tubing afterwards.
- Place a bridge plug in the tubing before cutting the upper part of targeted tubing from the main tubing, and connect the inflatable packer with the bridge plug
- Inflate the packer and start pushing against the bridge plug by applying pressure above the piston, which force the upper tubing to be wedged into the void next to the lower splayed part. At this stage of the process, a repeated cycle of pressure

building up and dropping off could be observed when the tubing stores the energy to start a new step of wedging process.

- When the piston stops due to reaching the pressure limits or pressure leaks-off, perform a gauge run to check where the piston stopped. Pressure limits could be casing burst pressure or causing a micro-annulus between the casing and cement behind it during compaction.
- Perform cement logging, and the logging results will determine the next steps which are the same in a conventional operation.

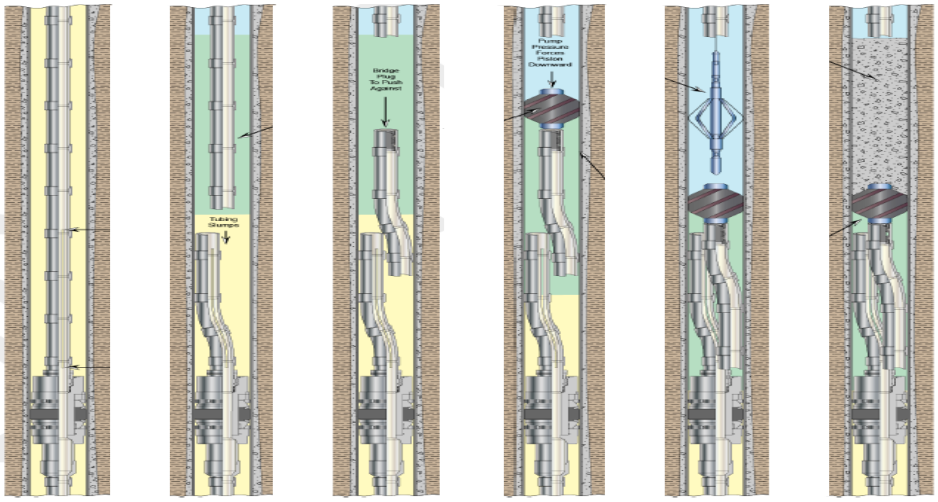

Fig. 3-2 compacting tubing- scenario 1 steps [19]

3.2.2. Scenario 2- Crushing tubing by locally deforming slotted segments

With the previous scenario, a lot of uncertainties will be faced, one of them is the presence of control lines, clamps and tubing joints which are stronger than tubing and one longitudinal cut operation could not be able to cut all the joints and the cable clamps with the tubing.

The wedging operation could create enormous friction forces between the two parts of the tubing on one hand and between the casing and the tubing on the other at early stages of the process which can stop the compaction process due to mechanical lock up.

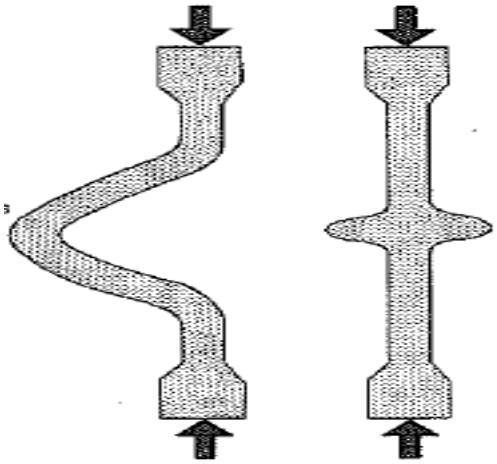

Fig. 3-3 Major contact vs local contact [8]

Based on the challenges mentioned above, the second scenario proposes to shred the tubing only axially with multiple relatively short slots at several segments. In this case, the pipe will fold locally and compact at each segment, and the outcome is the tubing will be compacted because of compacting all the segments together. The geometric architecture of the slots (number of slots in one level, length of the slot, number of segments) will be designed in such a way that minimises the friction between the tubing and casing resulted from the whole pipe contact and the segment contact (Fig. 3-3), and to prevent interaction between segments. Shredding the tubing - which will weaken it – will minimise helical buckling, claiming that helical buckling can only occur if the pipe is a whole pipe [13].

This scenario is effective in vertical and inclined part of the well, especially at the bottom of the desired compaction zone where compaction friction is not affected.

The operation steps in this scenario are very similar to those in Scenario 1, the only difference is to longitudinally slice the whole length of the targeted tubing with pre-determined number and length of slots, without severing the tubing at the middle.

3.2.3. Compaction variables

Fig. 3-4 shows the variables in Oilfield Innovation's model (Scenario 1), and the description of the variables symbols existing in Fig. 3-4 are listed in (Appendix A)

The target of any design here is to maximise the open window length (z_U) over the length of the targeted tubing ($z_{P\&A}$) that has been separated into an upper part length (z_W) and a lower split tubing length (z_S) using the differential fluid pressure across an inflatable piston.

Fluid pressure, volume, specific gravity and viscosity are primary variables that can be manipulated, but the remaining variables are limited by the available tools and the well construction.

In general, the compaction process is mainly limited by the frictional lock-up due to the forces acting upon the piston along the z axis = $F(z_S, t+1)$ + $F(z_W, t+1)$. Thus, any measured and/or calculated variables using physical or mathematical models will be used at least to estimate the combined yield (Fz_W) and frictional (Fz_S) forces that resist compaction.

The geometry of the tubing and casing will play a key role in both scenarios and affect them in different ways. For example, for the same tubing size, a smaller casing size in scenario 1 results in less eccentricity and lower bending moments, thus the expected pressure to reach the ultimate yield of the tubing will be higher.

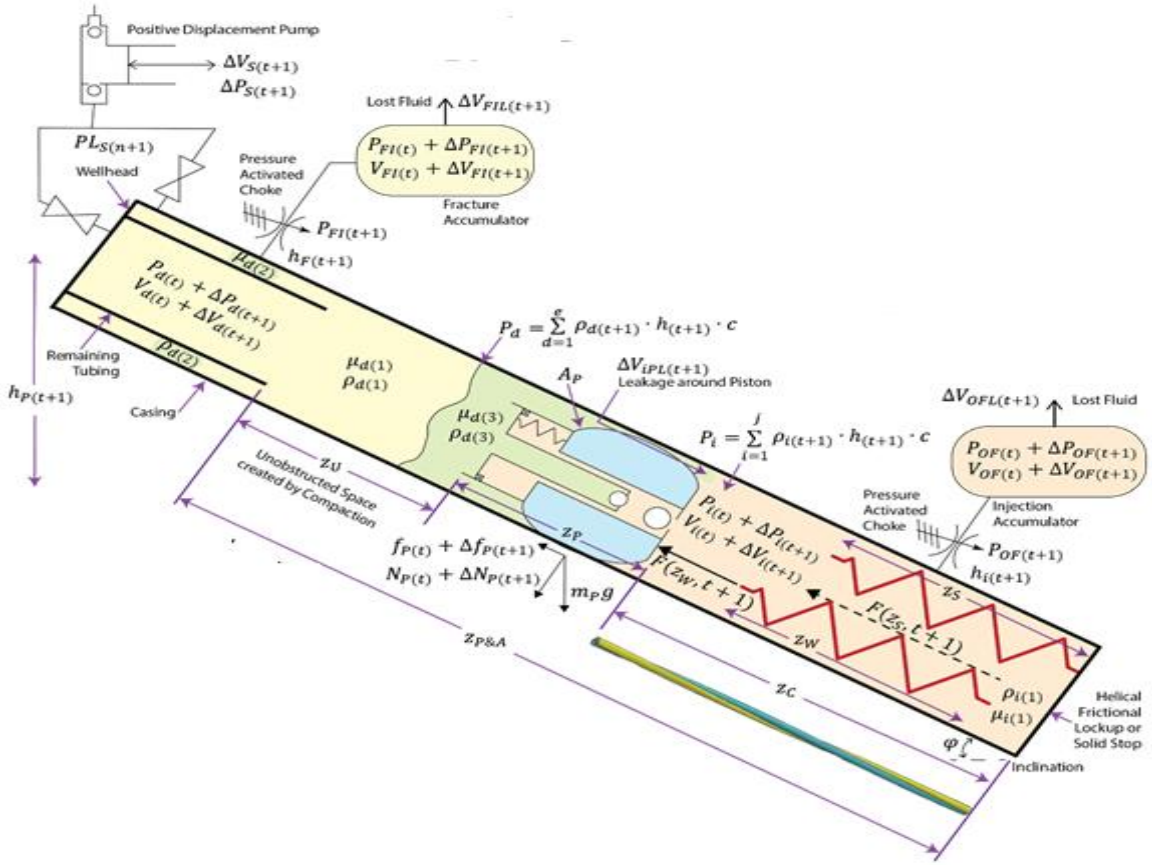

Fig. 3-4 Compaction model variables [27]

Also, well trajectory at the targeted tubing has its effects on the process in different ways. Minimum buckling loads, maximum crushing force, friction loads and other parameters will be affected by well inclination angle. As an example, the maximum compaction force in a vertical well will be concentrated at the bottom of the tubing since the whole weight of the pipe will contribute to this load, which induces a compaction at the bottom first. But in horizontal hole, the maximum force accumulates at the piston whereas the pipe weight will not contribute to the load, even it must be taken away from the induced load because it will act as drag force [13]. Friction forces calculation will be discussed in Section 4.3.3.

3.2.4. Scaling Issue

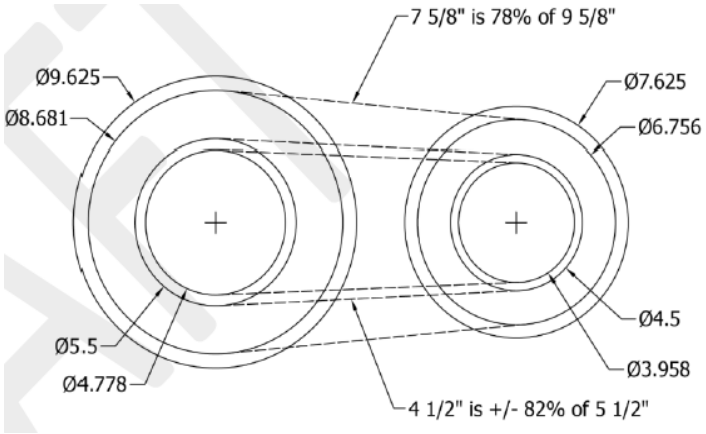

Fig. 3-5 comparison between two different geometries) [13]

Any future modelling of the method will encounter a scaling or comparison issue since each well has different conditions, including well tubulars sizes and grades, well trajectory and completion design and so on, which will add more complexity for any modelling process, but one can ease the comparison since mostly all API grades properties are known, also the contrast between some well construction combinations (Fig. 3-5 as an example) can be helpful as it can be used to estimate a wide range of results by using a scale factor.

3.3. Tools and equipment

It can be noticed clearly that DHTD method requires special tools and equipment, some of them are available now, some need to be modified and other need to be invented.

The recommended method will involve using rig-less equipment like: slick line, coiled tubing and positive pump to:

- Perform logging and drift runs before and after the compacting.

- Run the tubing cutter and the other related tools to create the casing window.
- Pump cement.

Finding the proper tools to perform the required operations downhole will be a real challenge with this method. And in this section, some of the available tools are listed and the modifications required to fit their intended purposes are discussed, in addition to the proposed invented tools.

3.3.1. Tubing Slicing tools

In Section 2.3.1.1, some of the tools and methods that can transversely sever the tubing are presented, such us explosive cutting, cutting with blade operated mechanically or electrically, or using chemical, plasma or jetting force.

Lateral tubing cutting is required in DHTD method, but also it requires to slice the tubing longitudinally, the industry has some of the tools that can do this but it is still either not compatible with the method requirements, or not invented yet. Here are some of these tools:

3.3.1.1. Gator Perforating tool

LEE Energy System (TOOLSERV as a supplier in Norway) modified a repeatable hydro-mechanical multi-use perforating system (Fig. 3-6) that replaces explosive, abrasive perforation and section milling, which means reducing the risk and the costs. The tool is

Fig. 3-6 Gator Perforator (Lee Energy)

proved and tested and it has been used in many locations to create a communication behind the casing without damaging the outer casing which could happen when using explosive perforation [42].

“The system uses coiled tubing as a work string with pressure up to 2500psi and blades to create slots in the pipe and it could perforate several sections of the same pipe size in one run as much as the blade is not blunt” [42]. The existing tool now creates four longitudinal cuts on one level and this can be repeated as much as needed with considering time factor.

This tool is proposed to be used to create slots in the upper part of the tubing to minimise its helical buckling in scenario 1.

The tool could be used in scenario 2, but some modifications are required because the maximum achievable length of the slot and the number of them (only 4) in one level are still limited because of designing issue.

The permanent mark that the blade will leave as shown in Fig.3-7 and Fig. 3-8 can be considered favourable since it reduces the required crushing force, because the crookedness has a significant effect on the buckling strength. And later, the results will show the highest applied force is the initiative one when the pipe still has its shape rigidity.

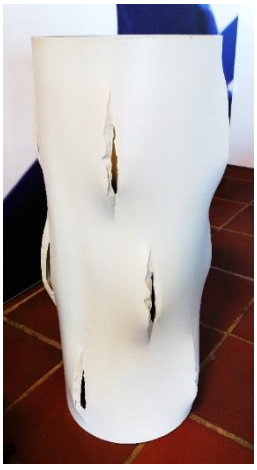

Fig.3-7 Gator tool cuts in casing (Lee Energy)

Fig. 3-8 Premature Deformation after perforating by Gator perforator (Lee Energy)

3.3.1.2. Commercial Pipe Wheel Cutters

Oilfield Innovations have cut oilfield API tubulars by hand using common cutting wheels (Fig. 3-9). Oilfield Innovations claims that these cutting wheels can be deployed by a tool conveyed on Slick line or Coiled Tubing (Fig. 3-10). The wheels are extended to begin cutting into the wall and the tool is worked up/down between selected depths in a well until the wall of the tubing is longitudinally cut [13].

Fig. 3-9 API pipe cut by wheel cutter [15]

Fig. 3-10 Oilfield innovations wheels skate [13]

3.3.2. Compaction Piston

Many service companies can supply inflatable packers that can go through a pipe and then set inside it by inflation and also retrieve it to perform certain jobs like water shut off, squeeze cementing, pressure testing casing patches, testing and treating, and set bridge plug.

Finding a suitable piston for this method will be a challenge because it should have some special specifications like:

- Piston movement: the available packers in the industry are not designed to move after setting and if that occur then it will be an indicator that the packer is failed and it is not sealing. The required piston for this method should seal and move at the same time.
- The packing element is usually made of rubber which has the highest friction coefficient with other materials (1.16) [43]. With clean dry steel the proposal solution for this is to use a special lubricant mixed with pumped water which will be placed in the wellbore, Ramex company supplies such fluids.
- The maximum allowable differential pressure across the piston: one of the main objects of the piston is to transfer the pressure above it into a force below it, and is supposed to have a high differential pressure (DP) across the piston (the lower DP the less transferred force), and there is a limit for the DP that the available packers can stand. Fig. 3-11 shows the DP ranges that (World Oil Tools) thru-tubing packers can

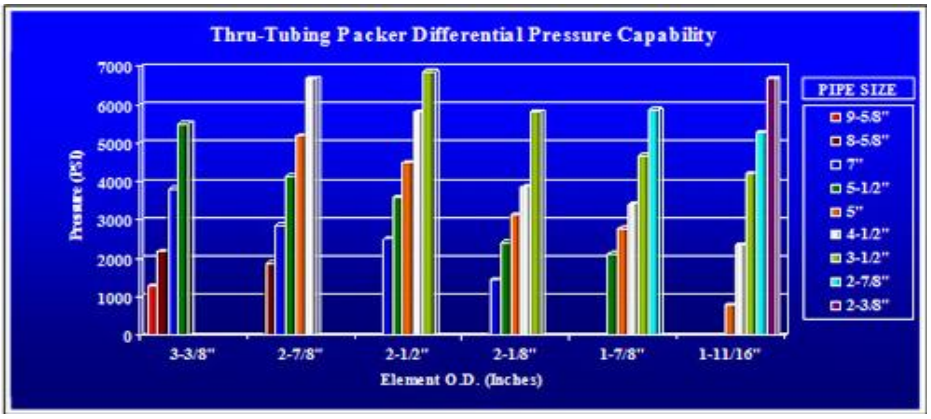

Fig. 3-11 Thru- tubing packer differential pressure capacity [7]

stand at 120°C, where it can be noticed that the higher the inflation ratio (pipe size/element OD), the lower the differential pressure rating. The differential pressure rating based on the packer's ability to seal at the rated pressure, not to resist the movement.

- The movement of the piston will imply a certain limit of leakage since a liquid should lubricate the surface between the piston and the casing. There will be no way to control the lubrication process which can develop to a type of uncontrolled leakage that may lead to operation failure.
- Size compatibility: some of the inflatable packers are designed to be run and set in the same pipe size, but the requirement for this method is to pass through the tubing and set in the casing.

- Ability to transfer from tubing to casing in the inflation condition: if the tubing was in compression, so after severing it could not drop down enough to create the required casing window length to set the packer inside the casing. In this case, the packer should start the operation inside the tubing and then move to casing. In normal cases, if that occur it will damage the packing element of the packer.
- Piston Twisting: it is noticed in the performed tests (see Section 3.4.1) that in many cases the used piston is twisted due to the tubing crushing. This issue is a reason of many test failures during the modelling especially when using the cement retainer as a piston.
- Temperature effect should be considered too, the higher the temperature the lower DP capability.

Oilfield Innovations has contacted TAM International to fabricate the piston that can meet the needs of the operation, and as a first step TAM will provide a specially fabricated piston (Fig. 3-12) that will perform the proposed real scale test (Section 3.4.2) in the near-term.

Fig. 3-12 TAM fabricated piston for large scale test [13]

Here are some examples from the companies produced inflatable packers.

3.3.2.1. Thru-Tubing Inflatable Packer (World Oil Tools)

This packer is run on coil tubing, used for the usual isolation jobs when the tubing cannot be removed or pulled, the element can inflate up to 3 times of its original size [44]. It can maintain variable differential pressures as shown in Fig. 3-11 across the packer element, the length and the temperature resistance of the elastomer compound can be varied.

3.3.2.2. TAM inflatable packers (TAM International)

This kind of packers is special in its design, it can be inflated by wellbore fluid and does not require mechanical mechanism to inflate, and it sets effectively in either cased or open hole and is available for different well sizes and differential pressures.

There are two types of the packer:

- Rubber full cover (Fig. 3-13) where only a rubber attached to the wellbore and is mostly used for the open hole.
- The packers with the anchor (Fig. 3-14) specially used in the casing to prevent movement of the inflatable packer after it has been inflated.

Fig. 3-13 TAM plug full covered rubber [27]

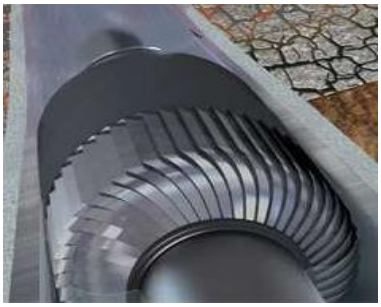

Fig. 3-14 TAM plug with slat type element [27]

This kind of Inflatable packers can accidentally slip down in the hole if the pressure inside the piston decreases and pressure applied against the top of the packer cannot be maintained. This is how Oilfield Innovation Limited will use this packer to push tubing [27, 45].

The previously mentioned challenges of using hydraulic packers will force to think out of the box to find other alternatives with different mechanism like heavy duty mechanical jars or electro- hydro pistons which also will have a lot of challenges not the least the time and cost consuming, these alternatives have never been addressed. As an example of these tools is Well stocker from Welltec.

3.3.2.3. Well stocker (Welltec)

A hydraulic stroking tool that can produce 100,000 lbs impact force shown in Fig. 3-15 and run by electrical line, and is field proved with many succeeded jobs. Tools and adapters can be attached to the actuator piston, and operations can be controlled from the surface after the stroking tool has anchored itself in the hole [23].

Fig. 3-15 Hydraulic stroking tool [23]

The tool is designed to push or pull a number of times during the same run regardless of well depth or deviation. The stroke length of the tool is 14in. Accordingly for 50m compaction of tubing, up to 150 strokes are required [46].

3.4. Oilfield Innovations models

Oilfield Innovations has performed a test in 2013 and will perform another one with real scale pipes in 2017. An essential aim of the modelling attempts is to answer the following question:

- How will the longitudinal and transverse cuts effect the crushing ratio?[17]

3.4.1. Performed Horizontal Crushing of 2 3/8" Tubing within 5 ½" Casing

This model has been performed by Clint Smith[1] and Bruce Tunget[2], and the data cited in this paragraph are based on a report issued by "Oilfield Innovations"[17].

6 runs have been performed using 2 3/8" 4.7 lbs/ft tubing within 5 ½" 20 lbs/ft. casing. In some of the tests, achieved a "dry" compaction reached to 46% compression ratio, where friction factors are at their highest levels.

On the other hand, several failed model runs were confronted because of "various modelling difficulties resulted from the use of minimalistic (hardware store) equipment and short or weak pistons. Accordingly, model runs [1] to [6] suffered from an inability to displace significant volumes at higher pressures, which prevented continuous crushing. Continuous crushing could have been achieved using oilfield specification pumps that can displace significant volumes at high pressures" [17].

[1] *Clint Smith, Houston, Texas, USA; Mobile Tel: =+1 713 204-1878; E-mail: clint@oilfieldinnovations.com*

[2] *Bruce Tunget, Aberdeen, Scotland; Tel: +44 1224 746697; Mobile: +44-7543-641408, E-mail: bruce@oilfieldinnovations.com*

3.4.1.1. Modelling in Details

The test process, briefly, starts with pumping the water into the CSG that push a piston inside the casing to crushed tubing within the CSG. Fig. 3-16, Fig. 3-18 and Fig. 3-17 show some of the used equipment in Boneyard. The constructions of the runs are as the following:

Fig. 3-17 pressurized wet piston end [17]

Fig. 3-16 water pump[17]

Fig. 3-18 test location [17]

- Run (1): Approximately 348 ft. of 2 3/8" TBG was placed inside 380 ft. of 5 ½" CSG to study the friction losses due to buckling (Fig. 3-19).

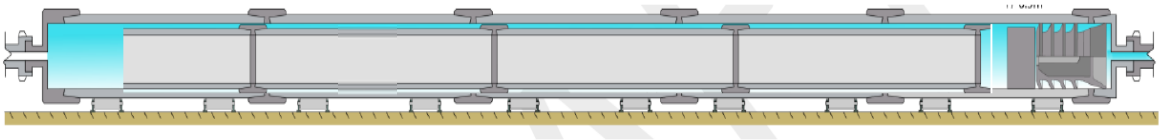

Fig. 3-19 Run 1 Sketch

- Run (2): Approximately 63.5 ft. of TBG with 3 longitudinal slots was placed within the CSG and compacted (Fig. 3-20).

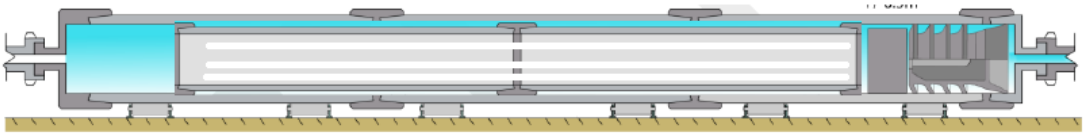

Fig. 3-20 Run 2 Sketch

- Run (3): Approximately 32 ft. of TBG with 6 longitudinal slots was placed inside the CSG and crushed (Fig. 3-21).

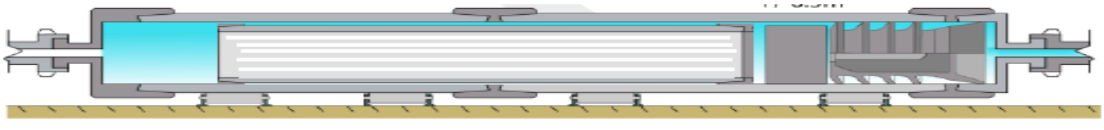

Fig. 3-21 Run 3 Sketch

- Run (4): Approximately 95 ft. of TBG, comprising 31.5 ft. with “6 longitudinal cuts”, 31.7 ft. of TBG with “3 longitudinal cuts” and 31.6 ft of un-slotted TBG, was placed inside the CSG and crushed (Fig. 3-22).
- Run (5): Approximately 31.6 ft. of TBG with 3 longitudinal slots was placed inside the above CSG and crushed (Fig. 3-23).
- Run (6): Approximately 31.6 ft. of TBG with 6 longitudinal slots laterally cut into three

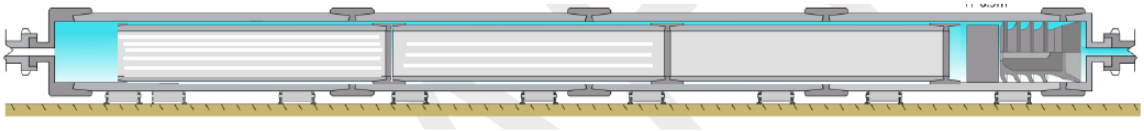

Fig. 3-22 Run 4 Sketch

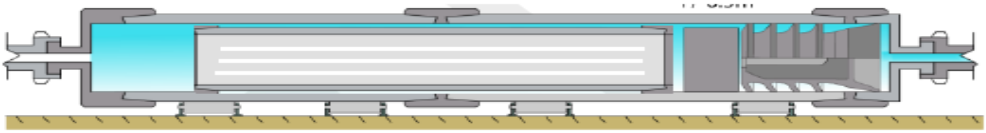

Fig. 3-23 Run 5 Sketch

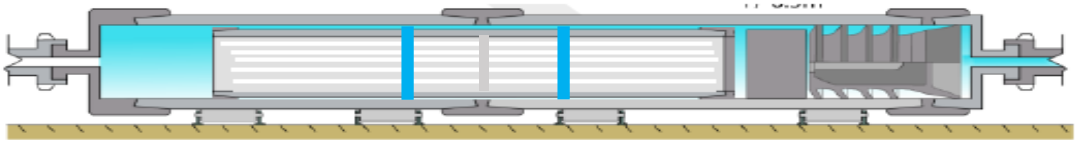

Fig. 3-24 Run 6 Sketch

(3) equal portions was placed inside the above CSG and crushed (Fig. 3-24).

3.4.1.2. Results

This Modelling proved the fundamental principles and feasibility of DHTD idea.

The modelling roughly found that transverse cuts lead to side-by-side compaction of tubing while longitudinal cuts resulted in a common crushing pattern and/or side-by-side compaction. The compaction operation was effected directly by point force of the crushing piston and friction inside a horizontal casing. In this section, the pictures are compounded from different pictures to show a relevant tubing length.

Table 3-2 shows the main parameters and results of each run, also here are some of the comments and observation related to each run [17]:

Fig. 3-25 Run 1- plastic buckling deformation [17]

- Run (2): In this run, a 1in plate was placed at the end of the tubing to centralize the tubing during crushing, which twisted and caused the piston to fail after the tubing parted and compressed into a (side-by-side) type. The twisting of the plate also prevented the axial force to transfer to the rest of the pipe, which resulted in approximately a 15.5% compression ratio (Fig. 3-26).
- Run (3): As shown in Fig. 3-27, a wooden plug, which was stronger than the elastomer ones, also failed under point loading, which ultimately caused the piston and wiper plugs to fail.
- Run (4): Using a 20-in. length improved piston which had plates welded on both ends allowed to continue crushing to 5800 psi and resulted in a compression ratio of 46%. The tubing compacted in a side-by-side shape shown in Fig. 3-28, where the uncut tubing was compacted through the tubing with 3 slots, which in turn compressed the tubing with 6 slots into a shape like that seen in the previous model runs.
- Run (5): A window was cut in the casing to observe the in-place compacted tubing, as shown in Fig. 3-29.

- Run (6): Designed to combine the effect of transverse and longitudinal cutting by splitting one joint of tubing with 6 slots into nearly equal 3 axial parts, the run resulted to combined types of compaction as shown in Fig. 3-30.

Table 3-2 Boneyard crushing modelling results

Run # /Tubing Joints #/ slots #	Max Achievable Pressure	Cause of Ending the test	Compaction Ratio %	Type of compaction
Run#1/3 Joints/Non	2400 psi	failure of the wiper plug	-	helical buckling
Run #2/2 joints/3 slots	4000 psi	Water pump seals failure	15.5% due to plate piston twisting	side-by-side and local buckling (tubing parted)
Run# 3/1 Joint/6 Slots	1800 psi	leakage through the wood piston	11.8%	local buckling
Run# 4/3Joints /Non-3-6 slots	5800 psi		46%	side-by-side and local buckling
Run# 5/1 Joint/3 Slots	4200 psi	cement wiper plug seal failure	45.6%	local buckling
Run# 6/1 Joint/6 Slots	3000 psi		45.6%	side-by-side and local buckling

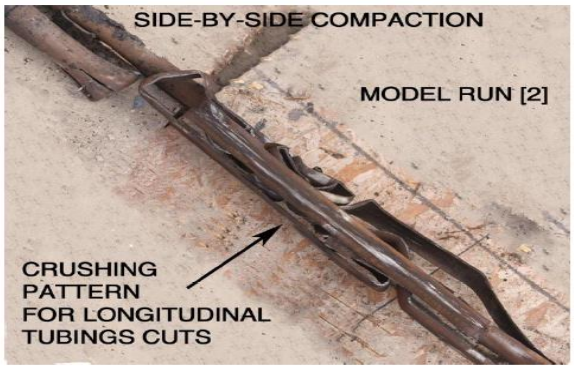

Fig. 3-26 Run-2 compaction shape [17]

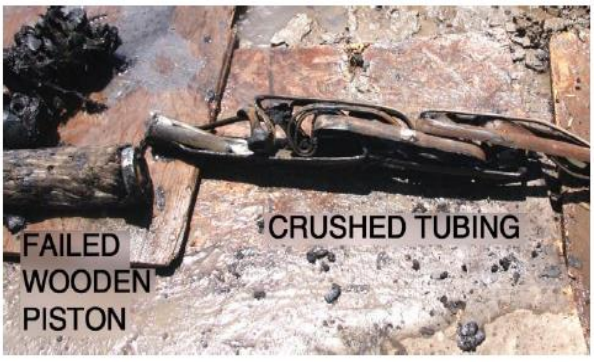

Fig. 3-27 Run-3 compaction shape [17]

Fig. 3-28 Run-4 compaction shape [17]

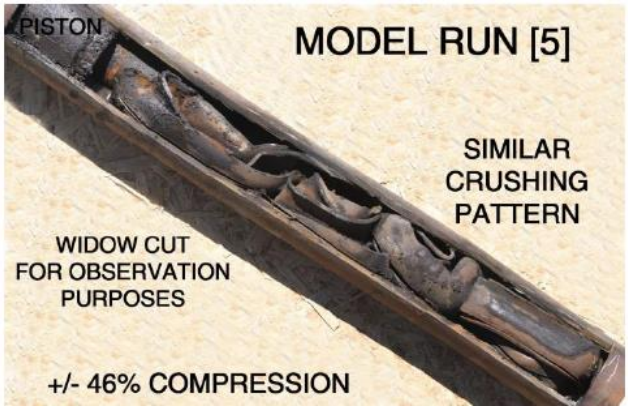

Fig. 3-29 Run-5 compaction shape [17]

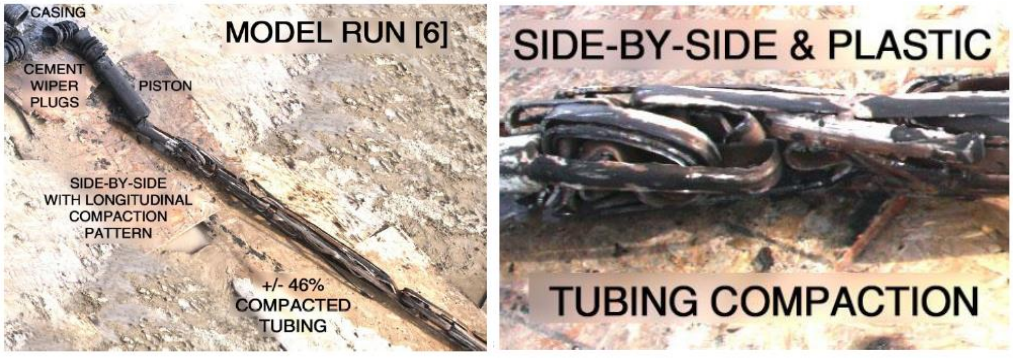

Fig. 3-30 Run-6 compaction shape [17]

3.4.2. Proposed Large Real Scale Tubing Compaction

The results that have been shown in the previous modelling were not convincing enough to the operators to go ahead and apply such a method in their wells, since the model results lack the necessary engineering data in which the method can be implemented in practice. So Oilfield Innovation coordinating with Conoco Philips-Norway have arranged to perform a large

real scale modelling in 2017, which is simulate Scenario 1 of compaction. This section is based on a report delivered by Oilfield Innovation [13].

3.4.2.1. Simulation objectives

The main aims of the modelling are to demonstrate the compaction on a real scale and collect data for numerical modelling of the process. Back to Fig. 3-4, some of the variables can be determined by this simulation, like:

- Friction f_P for either an inflatable or solid piston will be measured by pumping the piston through water filled casing.
- Pumping pressure changes ΔP_S and associated volume changes ΔV_S will be measured and recorded during compaction while return volumes ΔV_{OFL} and pressure P_{OF} will be measured
- Piston lost volume ΔV_{iPL} will be calculated based upon the difference between pumped volumes and return volumes while the associated pressure loss will be valued using available friction values for the simulation pipework.
- The above measured and calculated variables will then be used to estimate the combined yield (Fz_W) and frictional (Fz_S) forces resisting compaction.

To get a rational analysis of these collected data, they must be linked to the simulation arrangement details, like (just to name but a few):

- Casing and Tubing specifications, condition and lengths.
- Tubing plasma cut dimensions, alignment and placement.
- Piston, pump and other rig-up equipment details.
- Visual documentation of the simulation arrangement and the compaction results.

3.4.2.2. Overview of simulation rig-up and procedure

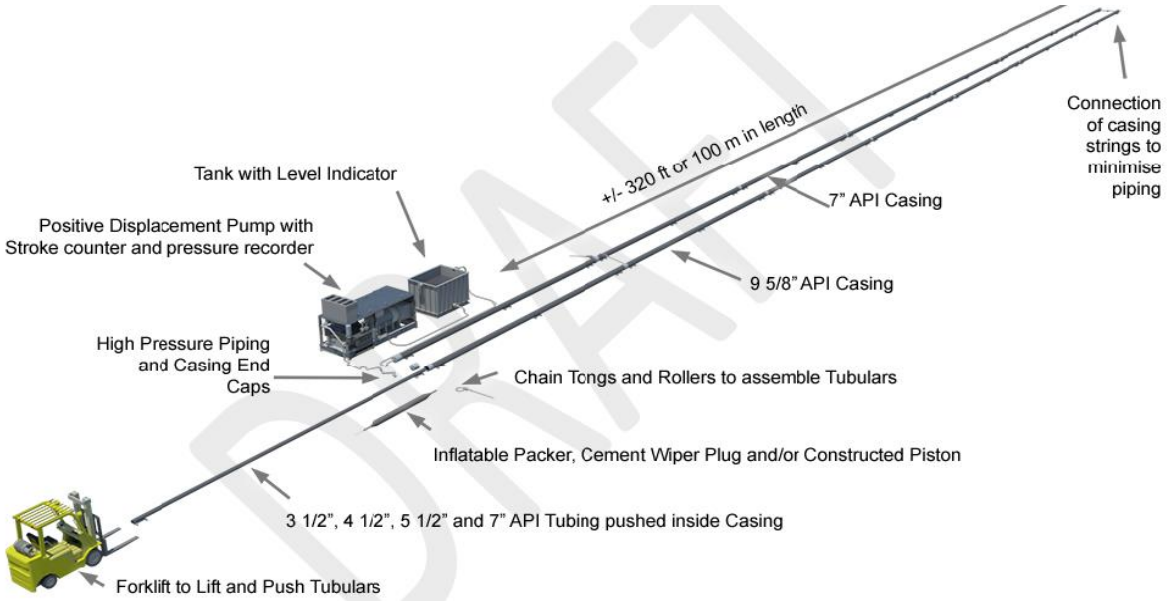

Fig. 3-31 schematic of large scale test rig-up [13]

As shown in Fig. 3-31, the large real scale rig-up for the proposed simulation mainly comprises of:

- 122 m of 9.625" Casing (FF-A1-02),
- 122 m of 7.625" Casing (FF-A1-02)
- 4x100 of 4.5" Tubing (TC-**C1**-(01, 02) and TC-**C2**-(01, 02)).
- 2 Piston (inflatable packers or cement wiper plugs)
- Data recorder, water tank, positive pump and other pipework including valves.

It is clear from Fig. 3-31 that the rig up is designed to be horizontal, because it is the easier and safer as an "up-ground" simulation. Even though it is not applicable (it is difficult to set a cement plug in a horizontal section), but it includes the worst-case condition, and this will give the results a range of tolerance when it comes to using them.

Plasma cutting will be used to create tubing slots which will simulate the downhole longitudinal slicing and perforation, whereas the simulation proposes that in the real case, the upper part of the tubing will be perforated (to prevent its helical bulking) with Gator perforating tool described in Section 3.3.1.1, and the lower part will be cut using Pipe Wheel Cutters described in Section 3.3.1.2.

As shown in Fig. 3-32, to simulate long longitudinal cut along the lower part of the tubing a consecutive set of 1m plasma cuts separated from each other by (1 inch) length spaces will be created in 50m of tubing. This (1 inch) spaces are to enable transferring the tubular and inserting in the casing.

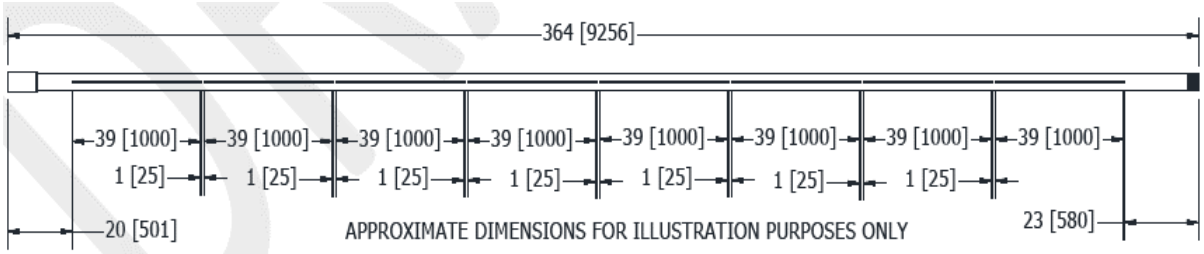

Fig. 3-32 plasma cutting dimensions tubing lower part [13]

To simulate the upper perforated part of the tubing, a consecutive set of 0.1 m plasma cuts separated from each other by 1m length spaces will be created in 50m of tubing as shown in Fig. 3-33.

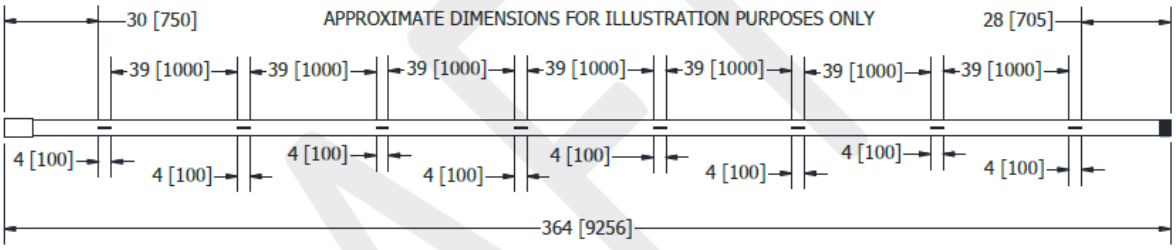

Fig. 3-33 plasma cutting dimensions tubing upper part [13]

As a lesson learned from the previous simulation, to protect the inflatable piston or cement wiper from damaging during crushing, a half meter “push” plug will be used between the inflatable packer or wiper plug and the tubing.

More data about the required equipment and its description are shown in Appendix B, whereas each item has a number related to P&ID schematic shown in Fig. 3-34.

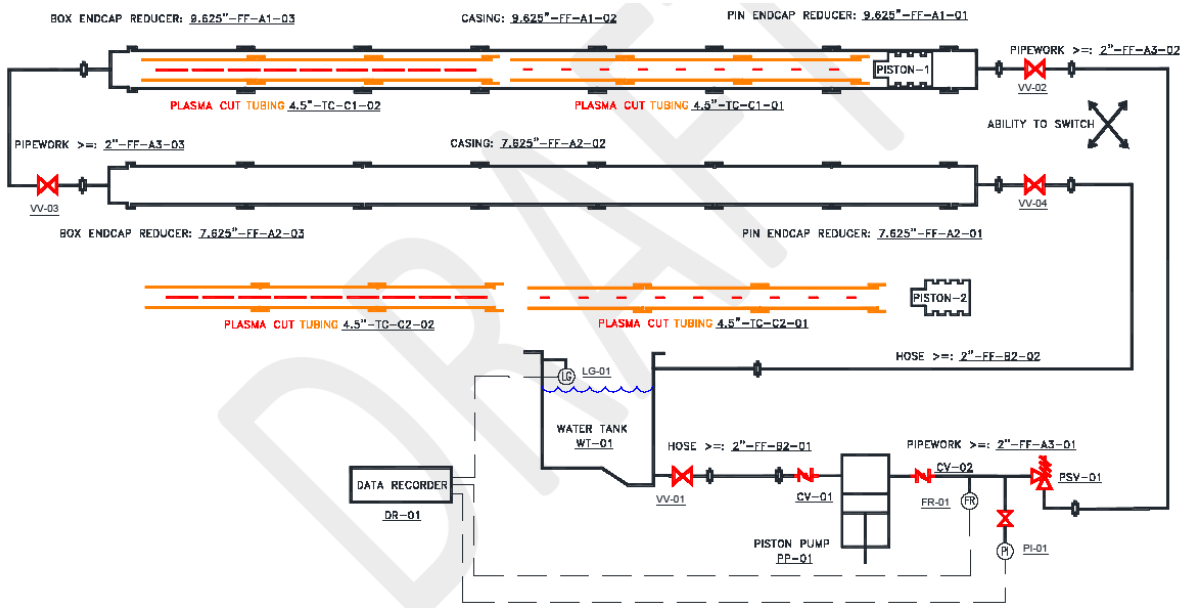

Fig. 3-34 Large Real Scale P&ID Schematic [13]

As a simplified explanation of the simulation, the water will be pumped into one end of the casing to drive a piston that pushes the dashed part of tubing into the sliced one, and a choke valve will be hooked up at the other end the casing to simulate injection pressure into a formation. Fig. 3-35 illustrates the two main stages of the simulation, whereas index 1 represents the starting stage, and index 2 represents the ending stage.

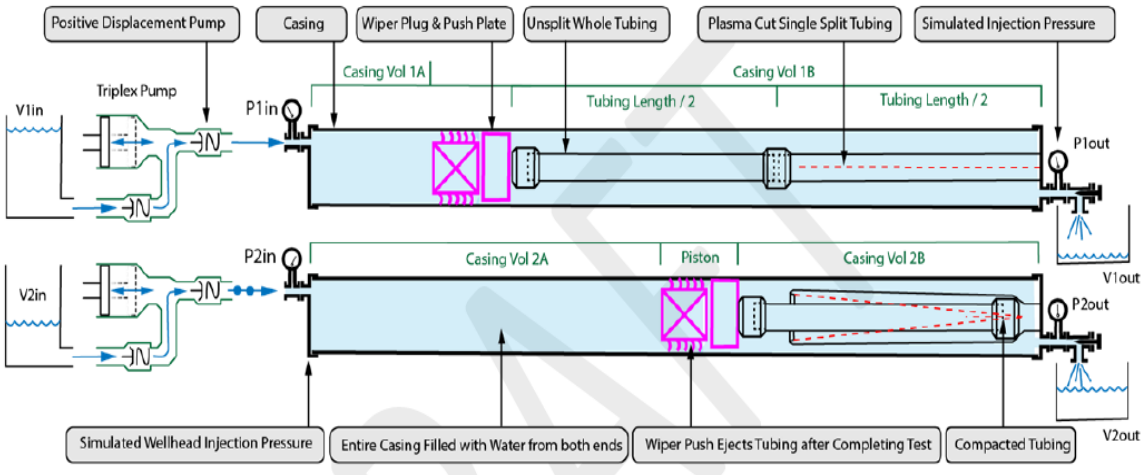

Fig. 3-35 simulation two stages [13]

3.5. Advantages of DHTD method

This method will enable to eliminate some real problematic issues encountered during conventional methods of well plugging, and thus, saving costs by reducing the using of personal and equipment to its lowest level. Furthermore the benefits will go beyond that to a step change in safety and reducing pollution, since all sources of pollution will stay in the well.

The method advantages can be recognised more by comparing the P&A conventional operation with DHTD method operation, as it will be explained below.

3.5.1. Removing XMT and install BOP

In P&A operation when using the drilling rig, it is obligatory to remove the XMT and install BOP's, this step involves many sub-steps to ensure that the well is safe during the changing operation like killing the well and/or set deep-set plug and tubing hanger plug, but with DHTD method, all these operations are cancelled because well intervention is used to perform the operation knowing that well intervention enables the working through the XT. It needs to be mentioned that this method will not prevent the using of the drilling if it is needed.

3.5.2. Completion, control and gauges lines and the clamps removing

Additionally, the method will cancel all the actions required to retrieve the tubing to surface, there are other benefits related to control line presence and good to be mentioned, like:

- BOP's could not seal completely with the presence of control lines and clamps, and in the case of unexpected flow happens then the pulled tubing should be cut, that can require a fishing operation which makes the process more time-consuming. Of course, this will not be the case with DHTD method, because gauge and control lines are left in place downhole until they are crushed with the tubing.
- The challenge of un-reaching the control line during sever the tubing laterally will also be faced in the tubing disposal method, and a proposed solution is be presented in Section 3.6.3.
- A lot of completion design criterions can be challenging when using rigs for P&A like the presence of trapped annulus between tubing packer and liner or PBR, and many of these problems will be eliminated when using the tubing disposal method.

3.5.3. Cementing behind the production casing

The proposed method will enable performing conventional logging to check the integrity of the cement behind the casing by creating the casing window. The compaction piston can rub the casing during compaction to provide a clean casing surface for better logging and placement of a cement plug.

Section 2.3.3 discussed the methods for repairing the bad cement behind production casing like casing milling, which is the undesirable conventional way, or PWC method. Both methods can be used with DHTD method, but in addition to that and as an alternative to perforation, the casing could longitudinally be sliced by the pipe wheel cutter tool, and after cementing, the casing with cement will form a plug like a concrete as shown in Fig. 3-36, and the innovation company has expanded further in offering the advantages of this alternative and can follow through reviewing the company website.

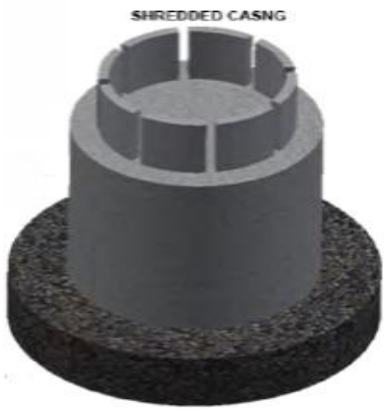

Fig. 3-36 longitudinally slicing casing solution [19]

3.5.4. HSE and Cost Efficiency

The method will minimize the cost and the risks related to P&A operations, since:

- The daily and mobilizing cost will be less, with using the slick line and/or coiled tubing.
- No need to remove the existing well control barriers, since well intervention methods are designed for such case.
- With barriers already in place, testing those barriers in the beginning of the operation is less time -consuming.
- Usually, installations require a refurbishment for Rig P&A operations hence, adding significant cost that can be as expensive as using a mobile offshore drilling unit

- Compared to a rig operation, CT and WL involve fewer people and fewer man-hours, hence, less risk to personnel.
- During rig operations, the exposure to NORM is higher when handling the back brought downhole equipment. Conversely, this method will keep the NORM equipment in the hole and, therefore, has less impact.
- Eliminate the hazardous associated with waste disposal, since the downhole equipment stay in place.
- In a rough cost estimation performed by Oilfield Innovation [19], this method can save at least two-thirds of the cost comparing to using drilling rig method for P&A. And any new cost estimation will be in favour of developing this method since it uses field proven technology with a lower operating cost. It is believed that the cost of verifying this method, can be recovered within the first well P&A operation

3.6. Technology challenges

As any technology, DHTD has its own technical and operational challenges, or even principal ones. In this section, some of these challenges will be presented with some suggestions to skip them.

3.6.1. Field evidence deficiency

The technology is new and unproved and this is the main concern about the method. And this is the case for most of the new ideas. To overcome this issue, Oilfield Innovations with ConocoPhillips-Norway are going to perform tests to qualify the method before performing an actual well abandonment. The method casts a lot of uncertainties about the compaction ratio, the detailed working mechanism and other issues that require more studying efforts.

3.6.2. Undesirable stop of the operation during executing

During operation, the piston could stop due to many reasons, some of these reasons are:

- Large leakage around the piston, this point is discussed in Section 3.6.6.
- Reaching the maximum allowable pressure.
- Rising of enormous frictional forces at piston or over the compacted tubing and producing mechanical lock up.

If this occurs, a drift run will be made to see if the compaction stopped before reaching the required depth, in this case, some of the available options include:

- Place a lubricant above the piston, this option should be performed before running the piston.
- Displace the well with heavier fluid.
- If the maximum allowable pressure was reached with a heavy fluid, then a heavy duty slick line jarring string with a long length of the stem could be used to jar down on top of the piston to add a jarring force [19].
- If the planned depth of the casing window is not critical, then another section of tubing will be cut and compacted above the existing one.

3.6.3. Tubing severing and control-lines

In DHTD, presence of control and gauge lines and their clamps will be also a real challenge. In additional to the probability that the control line could not be cut laterally with the tubing, slicing the tubing longitudinally could not reach the clamps and connectors, and this will harden the compaction and produce high friction forces.

The method gives a suitable solution to deal with control lines, wherein during the compaction process, by positioning a viscous polymers pill above the piston to provide sufficient sealing around an intact control line, and while compacting the tubing the control line will break, thus, allow the broken control line to coil into the bottom of the well [19].

3.6.4. Leak development around the piston

From Table 3-2 which shows the results of tubing crushing experimental model, one can see that the failure in many test runs was the piston failure, where the piston could be exposed to different kinds of stresses and pressures that could result in its failures, and growing leakage around the piston will prevent achieving the maximum pressure. One of the solutions to overcome this problem is to pump viscous pills or a cross-linked polymer above the piston, or run another piston.

3.6.5. Previously collapsed tubing

In some wells and during their production periods, a collapse or deformation can be developed in the tubing because of the different loads and stresses that the tubing is exposed to. Any deformed tubing need to be enlarged to have an internal diameter of at least the outer diameter of the uninflated element. This can be achieved with swaging. If swaging is not able to retrieve the required internal diameter of the tubing to reach the desired depth for the compaction window, then DHTD method cannot be used, so before the proposed method can be used, small diameter tools and/or coiled tubing must pass through any restrictions [19].

3.6.6. Leakage through production casing

Any leakage through the casing above the piston will prevent the required pressure build up, and it should be plugged with lost circulation material or polymers for example.

Contrarily, below the piston or below the required depth of the proposed plug, holes are not necessarily a problem, because planned tubing perforating is a key operation within the proposed method as mentioned before.

4. Theoretical Overview

Tubing crushing for P&A proposes is an innovative approach in the oil industry, so we tried to approximate between different concepts from different industries to come up with some theoretical basics that can be used to design a modelling for crushing method (especially for scenario 2) . This chapter will discuss:

- Some of the principles used to calculate the required and encountered forces during the operation like buckling and friction forces for different cases.
- Other studies covering tube crushing issue.

4.1. Oil wells pipe buckling

The general definition of buckling is “A mode of failure under compression of a structural component that is thin or much longer than wide” [47]. The resultant deformation may be elastic or permanent. In some cases, it may even lead to the structure collapse [48]. The elements that are only exposed to axial compressive loads through the centroid are called *columns*.

In general, loaded columns above their buckling critical load fail disastrously. For short columns (comparing to long well pipe strings), the well-known Euler equation managed to determine this load, but this equation cannot be used in oil wells with the long pipe string.

The Pipe string buckling in wellbores was and is still a challenge for engineering investigation and this includes both types of buckling which are: the lateral or sinusoidal buckling and the helical buckling. At the beginning, the pipe starts to buckle in a sinusoidal way, then with increasing the load it transfers to helical shape, the incremental load above the helical buckling limit will lead to a situation where the pipe cannot be pushed anymore into the well because of increasing the contact force between tubing and casing, and this phenomenon is called (lock-up).

Note that other shapes of buckling may take place depending on the hole geometry [49].

Dawson and Paslay [1, 50] studied the stability of a constrained string in an inclined wellbore and obtained Eq. 4.1 for the sinusoidal buckling load F_{sin} which is widely used:

$$F_{sin} = 2\left(\frac{EIwsin\alpha}{r}\right)^{0.5} \qquad 4.1$$

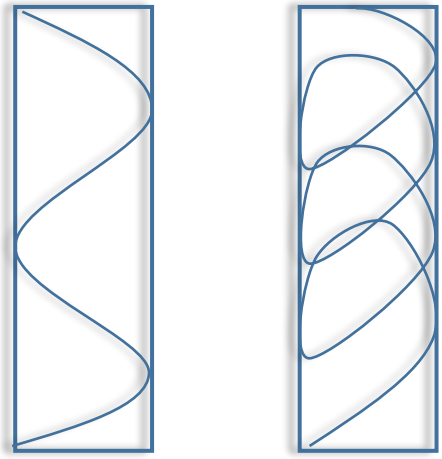

Fig. 4-1 Type of Tubing Buckling in oil wells

Where,

- E *Young's elastic modulus*
- w *Buoyant weight unit of the pipe*
- α *Wellbore trajectory inclination angle*
- I Moment of inertia is calculated by:

$$I = \frac{\pi}{4}(r_o{}^4 - r_i{}^4) \qquad 4.2$$

And r is the radial clearance between the casing inner diameter (Di) and the outer diameter of the tubing (do). This is given as:

$$r = 0.5(D_i - d_o) \qquad 4.3$$

Some modification in Eq. 4.1 is done to include the friction factor in the previous equation to become:

$$F_{sinf} = 2\left(\frac{EIw_{cf}}{r}\right)^{0.5} \qquad 4.4$$

The modified contact force w_{Cf}, in Eq. 4.2 is defined as:

$$w_{Cf} = \frac{w\sin\alpha}{\sqrt{1+\mu^2}} \qquad 4.5$$

where μ is the dynamic friction coefficient for sliding of the tube on the casing wall [1].

4.1.1. Helical buckling

4.1.1.1. Derivation of Helical buckling using energy method

Several researchers derived equations for helical buckling loads. In this work, the helical critical load will be considered as the criterion for any further solution since it generates numerous contact forces with the increased compressive load.

The easier way to calculate the helical buckling force could be using the energy method which is often used due to the complexity of the forces involved when using the differential equations solution [1, 51].

The total energy is obtained by the sum of the bending strain energy and the work done by the gravity. The conservation of mechanical energy states that the total energy of the system is given by the work done by the external axial load required for tube buckling and is given as:

$$\Delta U = \sum \Delta W \qquad 4.6$$

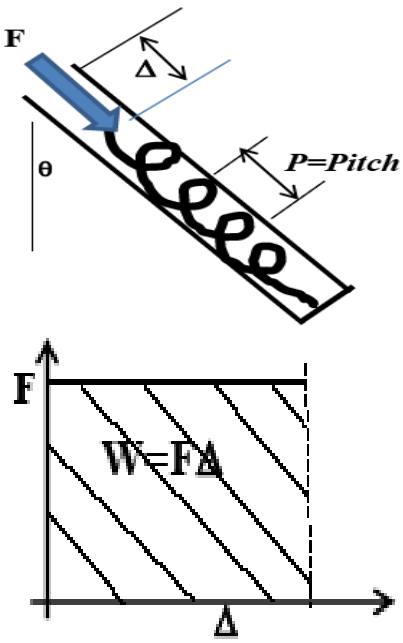

Fig. 4-2 Load- displacement relation [1]

Where ΔW is the sum of work done by the external loads and force. ΔU is the stored energy and potential energy due to gravity [51].

The work done by the applied load is Fig. 4-2 is given as:

$$W = F * \Delta \qquad 4.7$$

Where F is external axial load, (wall friction forces are ignored in this analysis) and Δ is the displacement which is given by [15]:

$$\Delta = \frac{2\pi^2 r^2 L}{p^2} \qquad 4.8$$

Where, L is the length of the string, p is the pitch length.

As the pipe starts to buckle, the bending strain energy is stored in the pipe and it is given by Miska [51], assuming the average pitch to be constant:

$$U = \frac{8\pi^4 r^2 EIL}{p^4} \qquad 4.9$$

In an inclined borehole, the component of the string of a tube also does work against gravity.

The magnitude of the work is given as:

$$W_g = wrL\sin\alpha \qquad 4.10$$

Substitution of Eq. 4.6 in Eq. 4.5, and then Eq. 4.5, Eq. 4.8 and Eq. 4.10 in Eq. 4.4 and fixing for F, one gets:

$$F = \frac{4\pi^2 EI}{p^2} + \frac{p^2 w \sin\alpha}{2\pi^2 r} \qquad 4.11$$

Eq. 4.11 can be graphically depicted in Fig. 4-3, and the smallest (critical) value for F in this equation is given by:

$$\frac{dF}{dp} \cong 0 \qquad 4.12$$

By solving this equation, one can obtain the pitch length:

$$p^4 = \frac{8\pi^4 EIr}{w \sin\alpha} \qquad 4.13$$

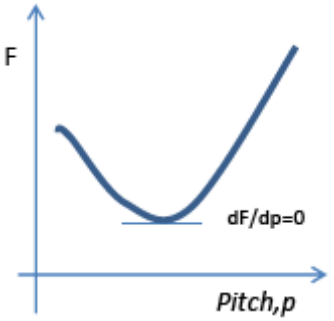

Fig. 4-3 Force-Pitch relation [1]

Substituting Eq. 4.13 back in Eq. 4.11 yields the critical helical buckling force as:

$$F_{hel} = 2\left(\frac{2EIwsin\alpha}{r}\right)^{0.5} \qquad 4.14$$

Or, compared with Eq. 4.1:

$$F_{hel} = \sqrt{2} F_{sin} \qquad 4.15$$

4.1.1.2. Helical buckling models

Mitchell [52] developed a different helical buckling critical (HBC) load:

$$F_{hel} = 2\sqrt{2} F_{sin} \qquad 4.16$$

The region between the two values in Eq.'s 4.15 and 4.16 is believed to be either helical or lateral, and there are many HBC equations developed by other authors but their results are in-between the last two values. However, Eq. 4.16 is believed to be the sinusoidal buckling limit on loading to create the helix, and this equation will be used in this work, while Eq. 4.15 is the helical buckling limit on unloading from a helical buckled condition [53].

It is important to mention that using the buckling criteria represented by Eq.'s 4.1 and 4.16 may give conservative results because numerical modelling and experimental tests have

shown that even if the compressive load is greater than the conventional helical critical load, the axial force is still able to be transferred [49].

4.1.1.3. The compression ratio of a whole tubing due to helical buckling load only

By substituting Eq. 4.13 in Eq. 4.6, one can get the helical compressing distance (Fig. 4-2) for the whole pipe without any weakening when applying an axial force (F):

$$\Delta = \frac{Fr^2 L}{2EI} \qquad 4.17$$

For example, for 4.5" 12.6 lbs/ft API steel tubing inside 9 5/8" 53.5lbs/ft casing, this distance will be only 1.5ft when applying 60400lbs (which is the critical helical load using Eq. 4.) on 100m of nearly vertical (10 deg incl.) tubing.

Note that, this value is not accurate because it is calculated under specific limitations set by the publishers who modified the previous equations and did not mention these restrictions is due to the lack of importance here.

4.1.1.4. Effect of the packer and the tool joint on buckling loads

In DHTD method, if the handled tubing is the part of tubing which connected to the packer and with the relatively short length of this tubing (around 200m) so the effect of packer should be considered.

Mitchel [24] showed that when tubing attached to a packer (as shown in Fig. 4-4) is exposed to an axial compressive load the helix will start at a distance from the packer (L_1) which can be expressed by (assuming weightless pipe):

$$L_1 = 4.5\left(\frac{EI}{F}\right)^{0.5} \qquad 4.18$$

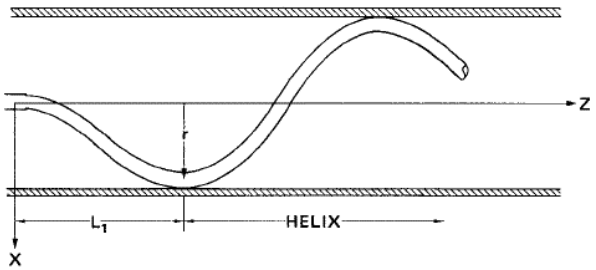

Fig. 4-4 tubing buckling above the packer [24]

Also, he showed decreasing by (40%) in the contact force formed due to helical buckling and increasing in the helical critical load 2.8 times to give the same pitch length [24].

As an example for the problem, assuming 4.5" 12.6 lbs/ft. N80 tubing in 9 5/8" 53.5 lb/ft. casing, the relation between the packer-to-helix length, $L_1$and the axial load F is showed in Fig. 4-5, it is clear that inducing an axial load reduces the packer-to-helix length rapidly from 600ft to 83ft at 5000lbs, and with increasing the load, the decreasing ratio of this length will be lower to be 29 ft. at 20000lbs, it is important to know that even this part of the tubing will not be a straight pipe but it has a resistance to buckle, which will be so useful for crushing scenarios where inducing buckling - and in turn mechanical lock up - could be a real problem. On the other hand, if Scenario 1 is to be performed, it should be considered that keeping the tubing connected to packer can reduce compaction ratio because the lower sliced part of the tubing will be centralized by the packer.

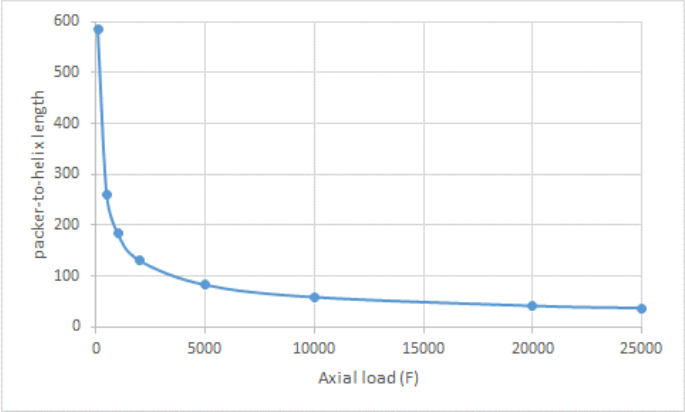

Fig. 4-5 the packer-to-helix length vs axial force

The Buckling behaviour of the pipes has usually been studied with an assumption of continuous configuration, ignoring the effect of pipe joints. Duman et. al., [54] performed an experimental study to investigate the effect of tool joints on the buckling, they found that:

- The tool joints do not affect the sinusoidal buckling critical load that much, but it increases the helical critical load approximately by 20%.
- The axial load transfer increases by approximately 40% in the presence of tool joints.

4.2. Column Buckling

4.2.1. Elastic and inelastic buckling

When a column (cylinder in this work) is exposed to an axial compression load, it could buckle, and this buckling may be elastic or inelastic (permanent). Buckling could also happen in the case of cylinders subjected to axial compression, torsion, external pressure or these loads together. For example, buried pipelines used to transport fluids can experience high compressive axial loads leading to axial buckling.

In the elastic buckling, the section buckles under a critical load given by Euler's equation (Eq.4.19) when the material of section is still in its elastic region.

$$F_{cr} = \frac{\pi^2 EI}{(KL)^2} \qquad 4.19$$

K, effective length factor which differs based on the boundary conditions, Fig. 4-6 illustrates the proposed values of this factor.

Buckled shape of column is shown by dashed line	(a)	(b)	(c)	(d)	(e)	(f)
Theoretical K Value	0.5	0.7	1.0	1.0	2.0	2.0
Recommended design value when ideal condition are approximated	0.65	0.80	1.2	1.0	2.10	2.0
End Condition code	Rotation fixed and translation fixed Rotation free and translation fixed Rotation fixed and translation free Rotation free and translation free					

Fig. 4-6 Effective length factors for columns [12]

While in inelastic buckling, parts of the section yield before buckling occurs due to residual compression stresses in the section, and the previous equation is not valid to determine the inelastic buckling limit. In general, the numerical investigation of plastic buckling needs to determine the nonlinear stress-strain path in the stress-strain curve (Fig. 4-7).

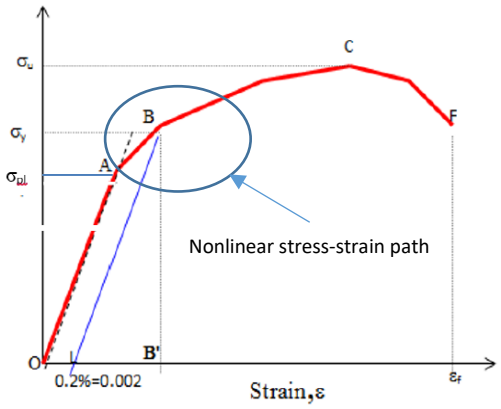

Fig. 4-7 stress-strain for alloyed steel

AISC specifications discriminate between the two types of buckling (elastic and inelastic) and the one occurring with the least compressive forces must be determined by comparing the column slenderness ratio to the effective (Euler) slenderness ratio [8].

The column slenderness ratio (C_c) is defined as:

$$C_c = \pi(2E\sigma_y)^{0,5} \qquad 4.20$$

The effective slenderness ratio (SR) is defined:

$$SR = KL_u\sqrt{A_s/I} \qquad 4.21$$

If SR<Cc, inelastic buckling is critical and the critical load (F_{Cr}) is given by:

$$F_{cr} = \sigma_y A_s\left(1 - \frac{SR^2}{2C_c^2}\right) \qquad 4.22$$

Or according to AISC specifications:

$$F_{cr(AISC)} = \sigma_y A_s\left(0.685^{\frac{2SR^2}{C_c^2}}\right) \qquad 4.23$$

Where, A_s Cross-sectional area of the pipe, $L_u$unsupported length of the pipe, σ_yYield strength of pipe.

If SR>C_c, then the elastic buckling is critical and the critical load is given by Euler Eq. 4.19.

In AICS specifications, Euler equation involves the value (0.877) as a factor for initial crookedness and by substituting Eq. 4.21 in Eq.4.19, one can get:

$$F_{cr(AISC)} = 0.877\left(\frac{\pi^2 EI}{(KL_u)^2}\right) = 0.877A_s\left(\frac{\pi^2 E}{SR^2}\right) \qquad 4.24$$

The previous AISC specifications for column design includes all issues related to crookedness, residual stresses, accidental eccentricity [55], and it is abdicable under two conditions:

- The effective slenderness ratio, preferably should not exceed 200.
- The column should be non-slender element compression members.

The calculated loads by Eq.'s 4.19 and 4.22 are theoretical loads assuming that the string is new and it has no initial wear, crookedness, corrosion or any type of damage.

As an example, to compare between the AISC and the theoretical equations results, Fig. 4-8 illustrates the relation between the unsupported length and the critical buckling loads for 4.5" 12.6 lbs/ft. N80 fixed ends tubing. AISC underestimates the loads since it is preferable for design engineers as a safety factor. In this work, the theoretical equations will be used since it represents the worst case during crushing.

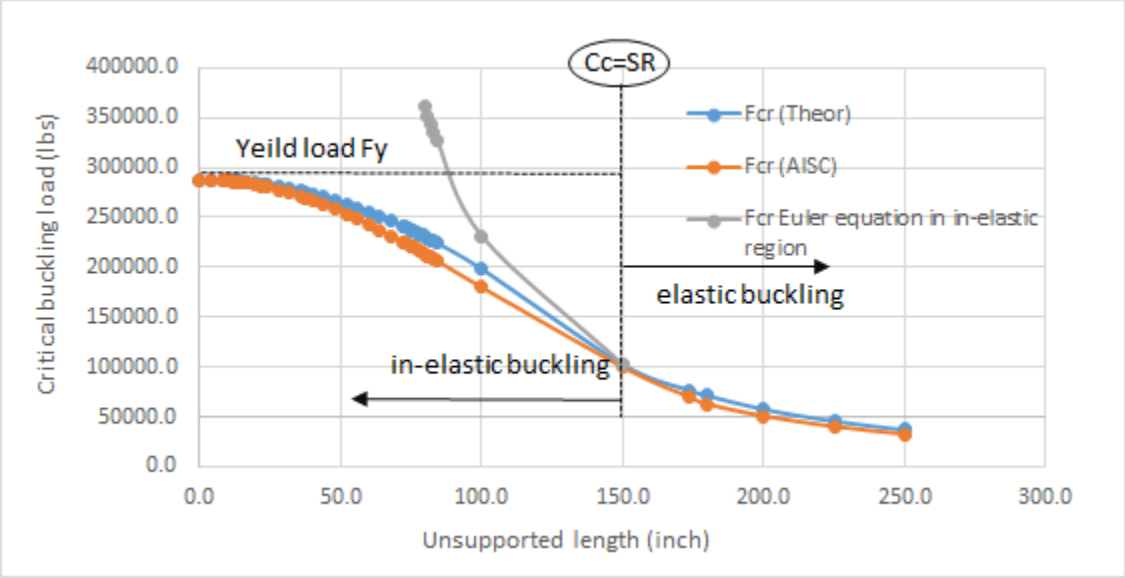

Fig. 4-8 Critical buckling load (Theoretical vs AISC)

It is clear from Eq's 4.22, 4.23 and 4.24 that the slenderness ratio affects on the strength of the columns, and lower strength can be achieved by increasing the slenderness ration, which in turn can be result of:

- Reducing the moment of inertia of the cross-section.
- And for a fixed cross section area, increasing the unsupported length.

4.2.2. Buckling of curved plates

After slicing the tubing, it will form a bunch of connected curved plates, and during compaction process, the axial compressive load will act on these curved plates. So, estimating the required load to initiate a column buckling in the slotted tubing body could be related to that required to buckle a group of connected, fixed and symmetrical curved plates.

It is expected that the behaviour of curved plates under compressive load would be similar in many respects to that of a cylinder since a curved plate is basically a piece of a cylinder.

NACA [56] stated that "the large curvature plates buckles in the same manner as a cylinder and the small curvature plates buckles basically as a flat plate." Also, it stated that "the buckling stress values for the plates depend on the geometry of the plate and on the boundary conditions. Predicting the plate-buckling behaviour require additional parameters to describe, which increases the difficulty of predicting".

The previous section explains how to calculate column buckling limit loads for any type of sections. So, one can calculate the critical buckling loads for one curved plate, if the moment of inertia is calculated (or the radius of gyration) of such section. Through the assistance rendered by Mr. Giorgio Pattarini (PhD student in the mathematic department at UIS), a relation to calculate the moment of inertia for thick wall curved plate (I_{cp}) was derived and the result was:

$$I_{cp} = 2\left(\frac{1}{16}(r_o^4 - r_i^4)(\theta + sin(\theta)) - \frac{\left(\frac{1}{3}(r_o^3 - r_i^3)\,sin\left(\frac{\theta}{2}\right)\right)^2}{\frac{1}{4}(r_o^2 - r_i^2)\theta}\right) \qquad 4.25$$

Derivation of this equation can be found in Appendix C.

The radius of gyration, r_g is given by

$$r_g = \sqrt{\frac{I}{A_{cp}}} \qquad 4.26$$

Where A_{cp} is the cross-section area of the curved plate:

$$A_{cp} = \frac{1}{2}(r_o^2 - r_i^2)\theta \qquad 4.27$$

Where, θ is plate curvature angle, r_i pipe inside radius, r_o pipe outside radius.

As an example, if a cylinder is split into two halves then, there are two curved plates with plate curvature angle (θ =π) angle, and so on. Table 4-1 shows the value of moment of inertia and radius of gyration for sliced 4.5” 12.6lbs/ft. n80 API tubing.

Table 4-1 moment of inertia and radius of gyration for different tubing curved plate angle

plate curvature angle (θ)	Corresponding cuts or curved plates number in cylinder	radius of gyration	moment of inertia	Corresponding yield force for each curved plate
360	0	1.503	3.432	288036
180	2	0.656	1.716	144018
120	3	0.327	1.144	96012.01
90	4	0.199	0.858	72009.01
72	5	0.140	0.686	57607.21
60	6	0.111	0.572	48006.01
45	8	0.087	0.429	36004.51

Fig. 4-9 shows the relation between number of the cuts (or curved plates) in a cylinder and the moment of inertia value. It is clear how creating cuts in a cylinder can reduce the moment of inertia sharply, and it is the same for the radius of gyration as Fig. 4-10 shows.

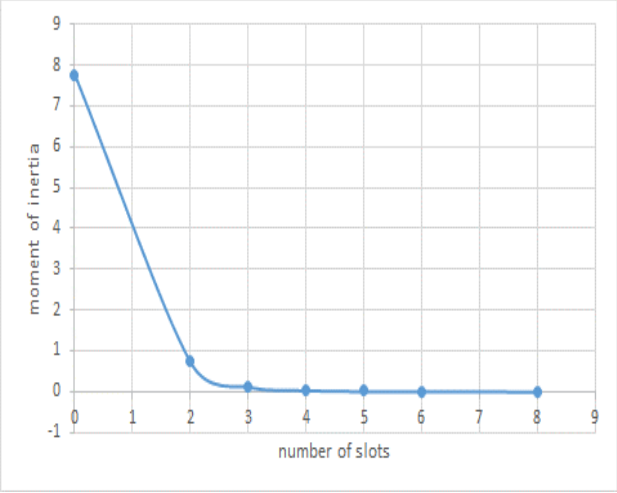

Fig. 4-9 effect of slicing on I value

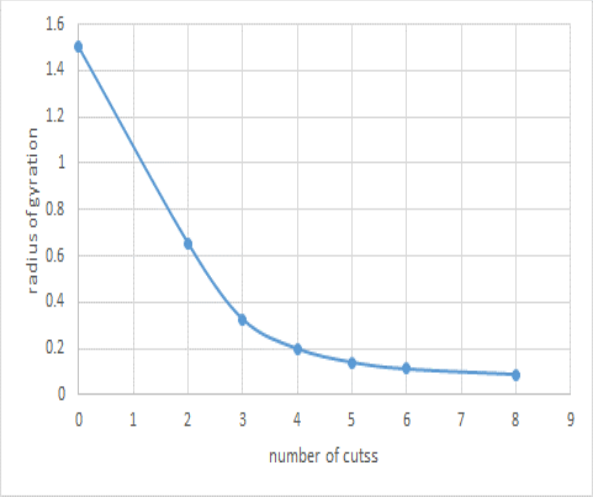

Fig. 4-10 number of cuts vs radius of gyration

Back to the slotted tubing (where the slices of the tubing are still connected at the bottom and at the top as Fig. 4-11 shows) and to calculate the critical load for such structure using Eq. 4.19 or 4.21, a suitable value for "K" factor should be defined, and the experiments will be the only way to validate this idea.

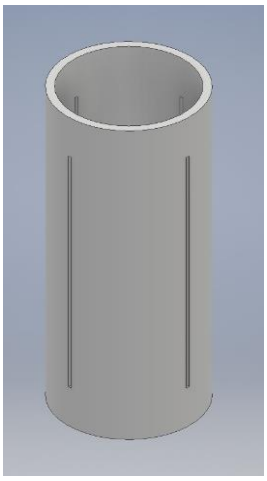

Fig. 4-11 example of the sliced pipe

4.2.3. The inelastic local buckling and crushing analysis for whole thin-wall cylinders

Buckling of the columns under compression may take place within a cross section before the overall column buckling or overall failure by lateral buckling or yielding. This phenomenon is called *local buckling* and usually occurs when the thin plates are slender. For cylinders, the local buckling will be developed under compression if diameter-to-thickness ratio, λ, greater than limiting width-to-thickness ratio for a non-compact cylinder, $\lambda_r = 0.11\frac{E}{\sigma_y}$. [55].

As an example, for N80 API 4.5" tubing 12.6 lbs/ft.

$$\lambda = \frac{4.5}{0.271} = 16.6 < \lambda_r = 0.11 \times \frac{30\times10^6}{80\times10^3} = 41.25$$

So, this tubing is non-slender compression members and un-subjected to local buckling.

The local buckling has the effect of reducing the load carrying capacity of the structure due to the reduction in stiffness and strength of the locally buckled plate element, and if local buckling occurs, then the column may not be able to develop its buckling strength.

Many fields of science and industry have been studying the local buckling and crushing for the thin-wall cylinder to prevent the collapse under compressive loads or to design the energy absorbers.

Andrews et al., [22] performed an experimental investigation to classify the axial crushing modes of quasi-statically compressed aluminium alloy whole tubes and presented the influence of tube geometry on the crushing mode in a classification chart (Fig. 4-12).

The experiments covered a wide range of:

- Length to internal diameter ratio (L/D) [between 0.174 and 8.754]
- Thickness to internal diameter (t/D) ratio [between 0.0165 and 0.25].

Thus, the tubes they used could not be considered very thin.

In general, they found 7 modes of local buckling, the modes that the tube dimensional ratios correspond with API tubing (t/D between 0.08 and 0.14) and in some way, more practical (for example L/D>0.5) are:

- Concertina: (for t/D<0.1) axisymmetric and successive folding
- Diamond: successive folding associated with a change in the cross-section shape of the pipe.
- Euler for L/D>5: Bending of tube as a strut.
- Concertina and 2-lobe and/or 3-lobe diamond: Folding first in the concertina mode changing to the diamond configuration; 2 lobe: square cross-section pattern; 3 lobe: hexagonal cross-section pattern.

All modes together with experimental examples and load-displacement curves for each mode and the absolute size of the tubes are shown in (Appendix D).

Andrews et al., [22] reached the conclusion that “the collapse mode of a cylindrical tube of ductile material is not influenced by the absolute size but by the slenderness” .

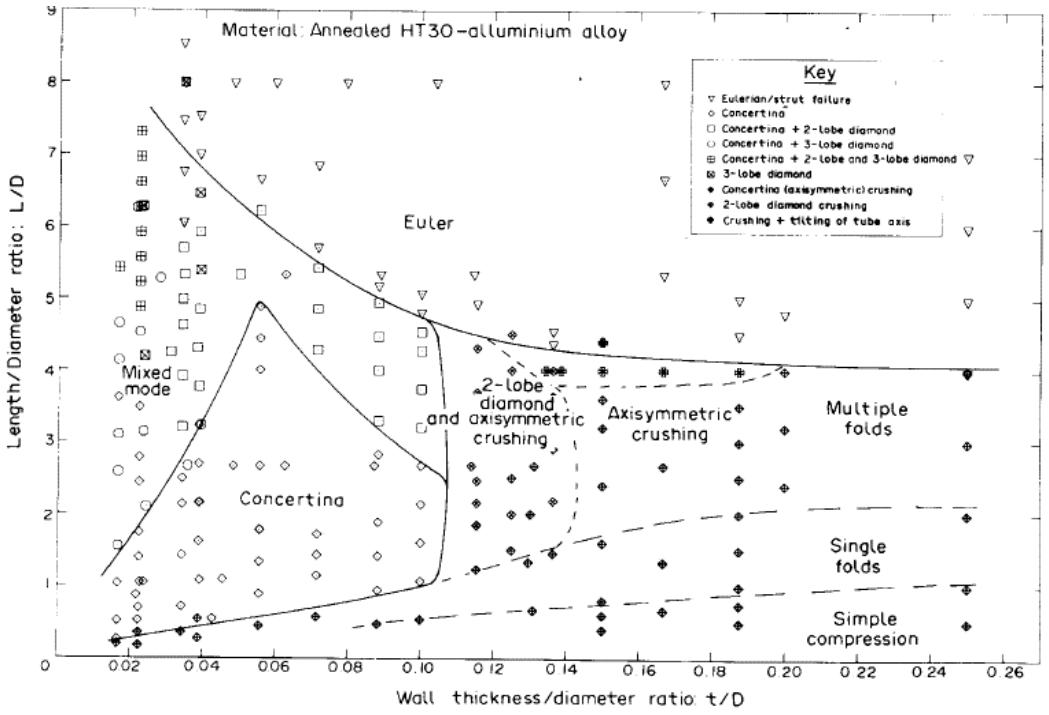

Fig. 4-12 classification chart for crushing modes of AL alloy tubes [22]

Fig. 4-13 illustrates an example of the concertina case from an experimental work performed by Alexander [18], and Fig. 4-14 illustrates the relation between the crushing force and displacement, he also derived an approximation relation to calculate the mean (average) crushing force for thin cylindrical shells under axial loading:

$$Favg = C\sigma_y t^{1.5}\sqrt{d} \qquad 4.28$$

Where C is a constant, can be determined by few experiments, *d: mean diameter, t: thickness.*

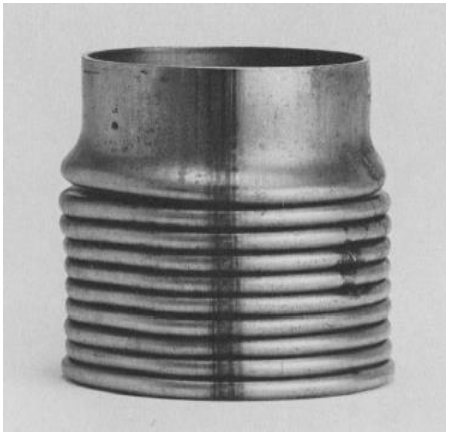

Fig. 4-13 Example of the concertina case [18]

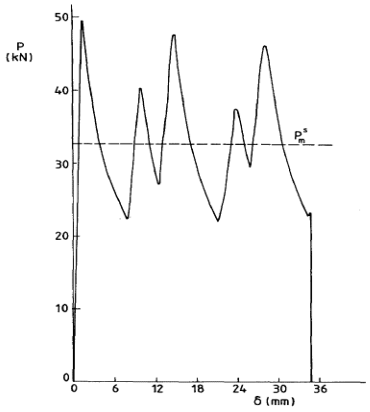

Fig. 4-14 Example of static axial load vs crushing distance for the concertina case [18]

The mean (average) crushing force, can be calculated by dividing the absorbed energy by the total displacement, where the absorbed energy can be obtained by integrating the area under the axial load-displacement curve [57].

It is clear from Eq. 4.28 that the mean crushing force is determined in terms of the material properties and the geometry. It should be noted that this relation cannot be used when a large deformation or buckling occurs [18].

4.3. Loads acting on the piston (pressures and forces)

At the outset talk about this topic, it should be noted that since the length of the handled tubing length regarding TDHD method is relatively short (up to 200m), so it will be assumed that the well is inclined only and any further calculations will be based on this assumption, ignoring by this way the curved pipe case.

The applied pressure above the piston calculated by Eq. 4.29 will be affected by the wellbore fluids properties and restricted with the maximum allowable differential pressure across the piston and the well construction like the casing rating and condition.

$$P_{piston} = P_{surf} + \sum_{i=1}^{n} g_i h_i - \Delta P_{fluid\ friction} \qquad 4.29$$

Where; P_{piston} : Pressure above Piston, P_{surf} : Surface presuure, g_i : Pressure gradient of well bore Fluid (i) above the piston, h_i Height of well bore Fluid column (i) above the piston, $\Delta P_{fluid\ friction}$: pressure drop due to well fluids (above the piston) friction.

Throughout the compaction process, the piston should overcome a bunch of forces and pressures which are generated from the first moment of the process. In Section 3.2.3, it is discussed that one of the main aims of any modelling is to estimate these forces and pressures, which include, but are not limited to, the following:

- Piston friction and weight.
- The required force to splay and compact the tubing (Fcr).
- Tubing weight and its drag force.
- Friction force due to lateral or helical buckling of the tubing
- Friction force due to splaying the tubing
- The expected formation injection pressure below and above the piston.
- The thixotropic fluid friction force above the piston.

Each one of these loads will be discussed more in detail except the second item which is covered in Section 4.2.1.

4.3.1. The Piston and the thixotropic fluid friction

The piston should hold the pressure above it, and then transfers it as a force to the tubing, this means that the piston will be in contact with casing all the time with the minimum allowable leakage, thus a friction force will be produced between the piston and the casing and it can be estimated by:

$$F_{fric\ p} = \mu_p . P_{p\ in} A_{pc} \qquad 4.30$$

Where; $F_{fric\ p}$: friction force between the casing and the piston, μ_p: dynamic friction coefficient of the piston, $P_{p\ in}$: applied pressure inside the piston to inflate A_{pc}: contact area between the piston and the casing. This force should be reduced as much as possible, and for

this purpose, it is proposed to displace the well to a lubricant liquid before the compaction process.

On the other hand, a thixotropic fluid (cross linked polymer) should be placed above the piston to reduce the leakage around the piston. For laminar flow and in single phase, the pressure loss due to friction for constant flow velocity and tubular diameter is given by [58]:

$$\frac{dp}{dx} = \frac{4}{D_i}\frac{16}{Re}\frac{1}{2}\rho.U^2 \qquad 4.31$$

Where; U is flow velocity, ρ fluid density and Re Reynolds number is given by

$$Re = \frac{\rho.U.D_i}{\mu_f} \qquad 4.32$$

Where μ_f fluid viscosity. Using the last two equations, the pressure drop due to well fluids (above the piston) friction can be written by:

$$\Delta P_{fluid\ friction} = 40.76\frac{Q}{{D_i}^4}.\sum_{i=1}^{n}{\mu_f}_i h_i \qquad 4.33$$

Where Q is the pump flow rate during the progression, assuming to be constant.

Since the weight of the piston is relatively small then it can be neglected.

4.3.2. The required force to splay and compact the tubing (F_{splay})

In Section 3.2, two scenarios of compacting have been presented, each scenario has a different approach to estimate the required splaying and compacting force.

For Scenario 1, it will be difficult to find a proper analytical estimation for the required force and experimental or numerical modelling is essential to solve this problem, and this work does not present any proposal for that.

This work is more focused in Scenario 2, so an analytical estimation, numerical modelling and in a small part experimental work have been performed to estimate the splaying and compacting force and it will be presented more in details in Chapter 6.

4.3.3. Tubing weight and its friction forces throughout the compaction

Tubing friction forces are the additional loads generated by tubing contact with the casing due to the weight of tubing, lateral buckling and splaying during compaction. In general, the friction force equal to the friction coefficient multiplied by the normal force (N). Fig. 4-15

illustrates a simple schematic of a pipe mass element and its mass components on an inclined plane.

As a straight section is proposed for the tubing, and using Coulomb friction model, the differential equation for static axial force balance (as depicted in Fig. 4-15) is given by [59]:

$$\frac{dF_z}{dz} = w.cos\alpha - \mu N \qquad 4.34$$

The first term defines the weight unit of the pipe axial component and for the piston downward movement, this pipe weight component will be an auxiliary force. The second term is the friction or drag component and it is subjected to N: The total normal force per length unit and friction coefficient, and one can notice that the effect of lubrication is rising again here to reduce the friction force by reducing friction coefficient.

Within inclined straight well arrangement, the total normal force will be equal to the tubing unit weight radial component plus the forces induced through buckling and tubing splaying,

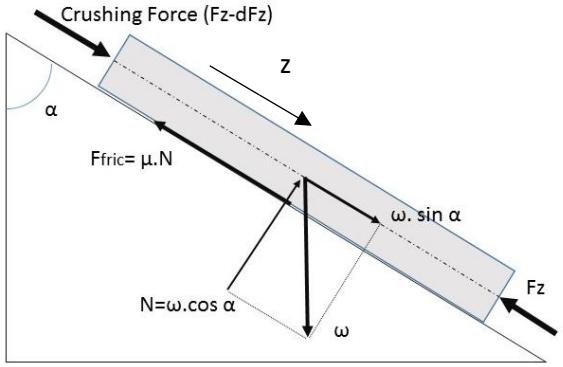

Fig. 4-15 Tubing weight components

which increased with downward axial movement and associated tubing crushing, and it can be expressed by:

$$N = N_W + N_{Splay} \qquad 4.35$$

Where $\boldsymbol{N_W}$: the contact force due to tubing weight and buckling which depends on the tubing configuration and calculated by Eq.'s 4.36, 4.37 and 4.38, for straight, sinusoidal and helical configurations, respectively [60]:

$$N_{Wst} = w.sin\alpha \qquad 4.36$$

$$N_{Wsin} = EIr\left(\frac{2\pi}{P_{sin}}\right)^4 [3A^2 - (A^2 - \theta_c^2)(7 + A^2 - \theta_c^2)] + rF\left(\frac{2\pi}{P_{sin}}\right)^2 (A^2 - \theta_c^2) + w.sin\alpha.cos\theta_c \qquad 4.37$$

$$N_{Whel} = \frac{F^2 r}{4EI} + w.sin\alpha.cos(\frac{2\pi z}{P}) \qquad 4.38$$

Where; P is the pitch of the helix, and θ_c, the angle between the pipe centre and the coordinate axis.

$$\theta c = A.sin\left(\frac{2\pi z}{P_{sin}}\right) \qquad 4.39$$

Where P_{sin} is the length of the sinusoidal buckling pitch which in equilibrium condition is be given according to Miska [60] by:

$$P_{sin} = 2\pi.\sqrt[4]{\frac{EIr(\frac{3}{2}A^2+1)}{wsin\alpha(1-\frac{A^2}{8})}} \qquad 4.40$$

And A, the amplitude of a pipe sine curve.

Calculating N_W starts with assuming the initial axial force, then the shape (straight, sinusoidal, helical) can be determined. Next, the matching calculated contact force N_W is substituted in Eq. 4.35, then N is substituted in Eq. 4.34, and the resultant non-linear ODE can be solved numerically. For helical case, solutions of Eq. 4.34 are presented in details by Wu and Juvkam -Wold [61]. Where Miska [60] improved a mathematical model that includes stable sinusoidal post-buckling configuration.

It is important to note that these set of equations are designed for a whole coiled tubing case, so the effect of the tool joints and/or the slots in the tubing body are not included.

A study by Mitchell [62] about the effect of friction on initiating buckling in tubing covered one case of a slotted pipe (scenario one in crushing method). The study has shown that If the pipe is slotted, then the initial buckling critical load will be less due to the lower polar moment of inertia, which in turn will produce the contact force due to buckling faster. As a part of the study, it is important to mention that Mitchell state: “the sliding friction does not allow buckling for a perfectly straight pipe, unless the pipe is allowed to roll”.

In Chapter 6, a comparison is held to show the effect of the inclination, magnitude of the inducing force by the piston, and the friction on the transferred force along the handled tubing assuming the worst case which is transferring the force with a helical configuration of the tubing.

N_{Splay}: is the normal force created by splaying the tubing. When the tubing is splayed, it will expand until it becomes in contact with the casing, and that will create additional contact force between the tubing parts, on the one hand, and, on the other hand, between the tubing with casing. There is no analytical estimation for this force in any of the scenarios, so the numerical and/or experimental modelling is required to estimate these forces. Logically these forces increase gradually during compaction process until a part of compacted tubing forms a rigid solid body which cannot be compacted any more, at this level the contact force will be maximum and this part will be in full contact with the casing and the whole applied axial force will transfer to a normal force (as it will be seen in the results section (6.2.2.1)) and the compacting process will create a mechanical lock up, and this condition should be avoided in any compaction designing before reaching the required casing window length.

In this work, it is assumed that this force could be estimated by per the length unit, since there are a consequent segments of compacted tubing and each segment produces its one normal force

4.3.4. The expected formation injection pressure below and above the piston

It has been mentioned before that perforation for tubing and casing below the piston is an essential operation before starting compaction to prevent hydraulic lock up.

After setting the piston and starting pumping at surface, the piston will start to move downward and the pressure will build up below the piston until it reaches the pressure

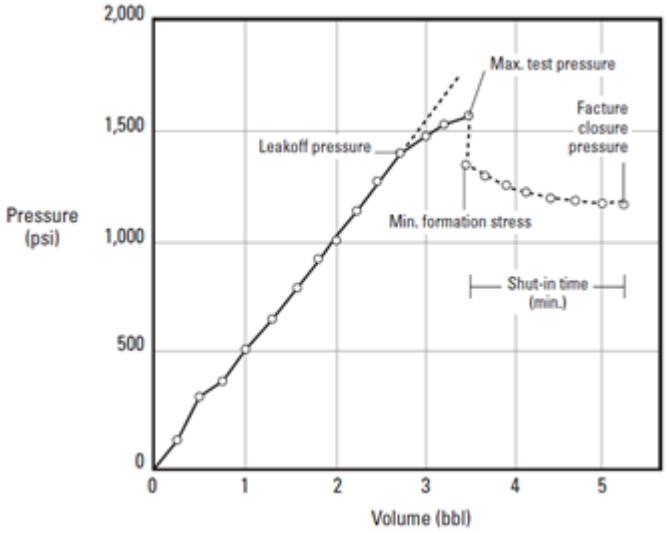

Fig. 4-16 formation pressure test [3]

required to initiate a fracture in the formation behind the perforated casing and tubing below the piston, then the pressure will drop slightly as shown in Fig. 4-16 to the fracture closure pressure. The values of this pressure can be collected from well data. If the fluid below the piston has pressure gradient g_b and the height of this fluid column between the piston and perforation point h_b then the pressure that the piston should overcome from below during compaction:

$$P_i = P_{closure} - g_b . h_b \qquad 4.41$$

Where $P_{closure}$ is fracture closure pressure. Controlling the crushing process with this pressure gives a safety factor to the operation whereas the piston will not move until this pressure is build up below it.

This pressure will be as a cushion working on mitigating the high sudden movement of the piston during the crushing because the numerical results showed that the changes of the tubing reaction force with the crushing displacement are irregularly oscillated (Fig. 6-14 as an example), these oscillations may cause some problems during the process, to name a few piston failure and contamination of the fluids with each other above the piston, not to mention the surface pressure fluctuation and its consequences, beside that it will help to prevent a premature mechanical lock up by giving the tubing the time to distribute the applied load in a more balanced way.

On the other hand, the casing above the piston may be deteriorated and it has been mentioned that a leak point to the formation behind the casing in a case like this should be fixed, but if it is not, the initiation fracture pressure of this formation and/or the intermediate casing rating should be considered in the design process, thus, this pressure will be an additional limitation of the maximum applied pressure, and it may be acceptable if the applied pressure causes a limited leakage to the formation.

5. FEM Model Building and the Experimental Validation Test

Numerical approaches are now widely used in engineering due to the advancing step in computational resources. Among the numerical methods, FEM is the most popular convenient approach, because it is easy to implement for all kinds of boundary and loading conditions and it can be used for analysing large complex structures. However, experimental measurements are still considered a powerful data required to approve most of those models.

The aims of this chapter are to introduce this method (FEM) and its computational commercial tools and to obtain numerical data about tubing crushing to predict its necessary parameters. The chapter also includes the details about the experimental test which was performed to validate the FEM modelling and the analytical estimation.

When having a look over numerical simulation and buckling behaviour, one can find numerous studies about this topic, but tubing crushing and numerical modelling is a real new approach, therefore what will be presented in this work about it is a step of the novice, and a try to step forward into this area.

5.1. FEM Modelling

5.1.1. Introduction to FEM

FEM starts with discretizing the structure over a mesh of elements which are simpler to be analysed using equations. Thus, more number of elements leads to more exact solution to the problem.

Solving the problem will go through sequent steps shown in Fig. 5-1, starting with defining the physical system and trying to build a numerical model for it, to pass through analysing stage and improve the model, then to end with setting the criteria for optimum design for the system parameters which in turn leads to solving the problem [25].

In FEM, each stage of this process involves different issues should be considered, as it follows [25]:

- Defining the physical system:
  - Structure dimensions and symmetry.

- Load magnitude, type and its variation with time
- Constrains on the structure.

- Building the numerical model:
  - Structure material properties and geometry
  - Loads applied on the structure and boundary conditions
  - Environment interaction with the structure
- Meshing the structure:
  - Element type and type of formulation
  - Meshing quality and fineness of meshing for stress concentrations.
  - The transition between elements types.
- Type of analysis:
  - Static analysis: the basic type, no dynamic effects on the system.
  - Harmonic analysis: used to predict the response of an assembly to continuous cyclic loads.
  - Transient dynamic analysis: used to measure the dynamic response of an assembly when dynamic loads are applied.
  - Dynamic analysis: used for complex dynamic systems that transient analysis cannot solve. In Abaqus, two kind of dynamic simulation are available (explicit and implicit).
- Model verification and validation
  - Check the acceptability of the solution
  - Requirements for any modifications on the model
  - The accuracy of the solution by comparing the results with real case results.

During building the model, load category can be chosen according to what the physical system is exposed to. The FEM tools involve these categories:

- Body loads: where the load acts on the whole body (weight of the body as an example) and the load is distributed on the nodes (that make up the elements).
- Surface loads: where the load acts on one of the body surface or edge (internal pressure as an example) and the load is also transferred onto the nodes.
- Pointed loads: where the load acts on an exact point in the body
- Dynamic loads: the previous loads are static loads, and if a dynamic analysis is to be chosen, then the load will be changing with time.

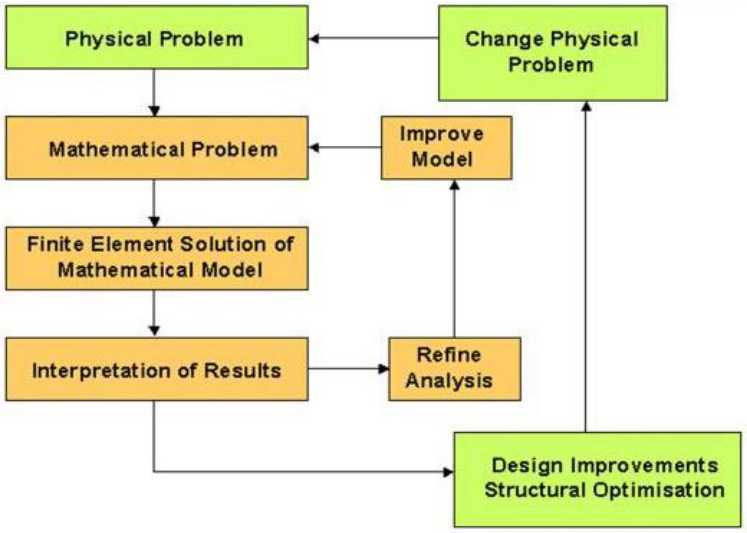

Fig. 5-1 steps of problem solving using FEM numerical solution [25]

5.1.2. Overview of ABAQUS/CAE 6.14-2 and Autodesk Inventor workbench 17.0

ABAQUS/CAE is one of the commercial tools that uses FEA technique for simulations purposes. This tool is mostly used by structural and mechanical engineers to simulate real-life models and test its compatibility and material performance under different conditions. In this work, both ABAQUS/Standard and ABAQUS/Explicit are used.

Autodesk Inventor workbench 17.0 is another tool used in this work to build the proposed assemblies, and then they are transferred to ABAQUS to be modelled.

5.1.3. Geometry Building using Autodesk Inventor

The geometrical pipe models were built based on the following tubular dimensions:

- 5.5” 17lb/ft (ID=4.77”) with 10” slots length used for experimental validation.

- 4.5” 12.6 lb/ft (ID=3.96”) with (39.37” =1m) slots length to simulate the length of slots in the lower part of tubing in in the large real scale test [13].
- 9 5/8” 53.5 lb/ft (ID=8.535”) for the casing that will case the tubing during crushing simulation.

The number of slots in the experimental and tubing pipes will be 4 centrally faced slots.

The rest of dimensions like the total length of each tubular and the un-slotted separator parts length in the tubular will be mentioned Table 5-1, and the figures from Fig. 5-2 to Fig. 5-4 (created by Auto Inventor workbench 17.0) show these models.

Table 5-1 geometry of the simulated assemblies

Model number	**Details**	**Remarks**
Model#1 (a slotted piece of tubing with one set of slots) Fig. 5-2.	13.4 “length 5.5” Pipe with 10” length and unslotted top and bottom bases 1.7 in length for each	The aim is to compare with analytical estimation and experimental results
Model#2 (a slotted piece of tubing with one set of slots within 9 5/8” casing) Fig. 5-3.	44 “length 4.5” tubing with 40” length and unslotted top and bottom bases 2” length for each	Simulate the proposed large real scale experiment
Model#3 (one whole joint of tubing slotted with same set of slots in model#2 within 95/8” casing) Fig. 5-4.	396” length 4.5” tubing with repeated set of (4x40”) slots separated by 4” uncut tubing part and unslotted top and bottom bases 2 in length for each	Simulate the proposed large real scale experiment

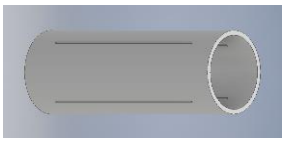

Fig. 5-2 Model 1

Fig. 5-3 Model 4

Fig. 5-4 Model 5

The sketches of the assemblies are created in 2D first then extruded to 3D when the length of each sketch is added in the second step. Creating the slots was a challenge but it became easier with the help from Mr. Adugna Akessa (senior engineer - structural engineering

department in UIS). The tubular centre is the centre of the coordinate system (x, y) = (0, 0) and the diameters are inserted regarding this point.

5.1.4. ABAQUS models building

In ABAQUS software, different modules are used to design the required model like (Part, Interaction, Assembly and so on). The following steps are performed by using those modules:

- Creating pipe parts: the parts are imported from Autodesk Inventor as step files and set as deformable parts for tubing and experimental pipes and as discrete rigid part for casing pipe. All pipes have a "solid shape" base feature but the casing is converted from solid to shell afterwards to ease creating the inner casing rigid surface which will be used later. In this stage a reference point for casing pipe is created too.
- Inserting pipe properties: two sets of material data are created:
  - Material 1 (N80): referring to the data in Table 5-2 which are used to simulate slotted tubing placed inside casing and based on API L80 material.
  - Material 2 (S110): referring to the data in Table 5-3 which are used to simulate the experimental pipe and based on API S110 material.

  The plastic deformation data for the corresponding tubular grade are taken from graphs shown in Fig. 5-5, and no shear failure is involved, so the pipe will not fail whatever the stress and strain are.

  After choosing the proposed material for each pipe, a section is created for the tested pipes under "solid" category and "homogenous" type and the pipes is assigned to that section, but for the casing pipe since it is rigid part so it cannot be assigned section.

Table 5-2 API 4.5" 12.6 lb/ft L80 tubing properties

Material 1 (tubing joints) properties		**Plastic properties:**		
OD	4.5in	**Stress psi**		**Strain**
ID	3.96in	96000		0.5%
Wall thickness	0.27in	**Tension**	97000	1%
Material yield strength	80000 psi		85000	1.5%
Young's modulus	29.10^6 psi		64000	2%
Ultimate yield strength	97000 psi	**Compression**	108000	1%
Poisson's ratio	0.3		140000	1.5%
linear hardening modulus	14470psi		172000	2%

Table 5-3 API 5.5" 17lb/ft P110 casing properties

Material 2 (Experimental pipes) properties		**Plastic properties:**		
OD	5.53in	**Stress psi**		**Strain**
ID	4.77in	140000		0.5%
Wall thickness	0.38in	**Tension**	130000	1%
Material yield strength	110000 psi		105000	1.5%
Young's modulus	29.10^6 psi		84000	2%
Ultimate yield strength	140500 psi	**Compression**	166000	1%
Poisson's ratio	0.3		198000	1.5%
linear hardening modulus	27778psi		-	2%

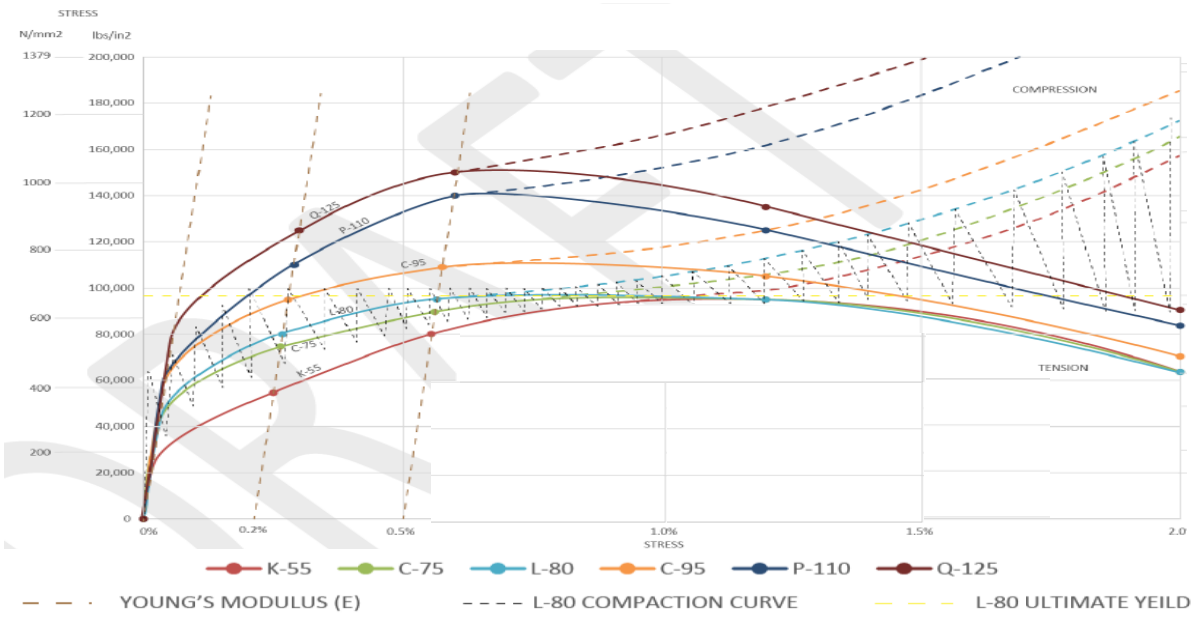

Fig. 5-5 API tubular steel stress- strain relation [13]

- Creating Assemblies: for models 2&3 the casing and tubing pipes should be assembled, in this stage many sets are created for different reasons explained later.
- Creating steps: for this modelling, different jobs are created with different kinds of steps in order to compare and verify the effectiveness of the FEM in estimating a correct forces values in additional to the unique features that each step has. In all jobs, an initial step is created by default to define the initial boundary condition for each job, then each job can have its own steps.

  The steps used in the modelling are:

- Buckling (Abaqus/Standard): this step simulates the modes of the linear buckling that can be generated due to an axial compression force and predicts the equivalent Eigen values. Two jobs are created and associated with this step for models 1 and 2. As inputs for this step: the requested number of eigenvalues was 5, and the maximum number of iteration was 300, where vectors used per iteration were 100.
- Static-Riks (Abaqus/Standard): this step is useful for problems that has low speed nonlinear dynamic, but this tool cannot be used for material local crumpling cases or to estimate the post-buckling behaviour also it overestimates the buckling force, since it calculates a linear buckling. But comparing to the previous step, it gives an estimation for the reaction force after buckling. Two jobs are created and associated with this step for models 1&2.
- Dynamic-Explicit: this kind of step is effective to study the performance of any mechanical system and it contain all nonlinearities like large deformation, nonlinear material response and self-contact because this technique includes the dynamic force in the motion equations sets and integrates these equations with time. Also, it is so useful for crushing tests and post-buckling simulations. 3 jobs are created and associated with this step for models 1, 2 and 3, the time period is 1 second, and to obtain the large deformation and the nonlinear material response (NLEGEOM) is activated.

- Creating Interaction: in Dynamic-Explicit step, contact force between surfaces or the tested body with itself can be assigned, so for models 2&3 two types of interactions are created:
  - Surface to surface contact: where the master surface was the inside casing surface, and the slave one was all tubing nodes.
  - General contact: to create a contact domain for the tubing pipe with itself.
  - For both assigned interactions, one interaction property is used which is mechanical tangential behaviour with friction coefficient = 0.3.
- Defining constraint: which can be found in Interaction module. A rigid body constraint is chosen to constrain motion of the top cross-section surface of the tubing (or the

experimental pipe) to the motion of a reference point chosen to be at the top of the pipe, and this will enable to apply a concentrated force at the top surface of the pipe.

- Meshing: the proper element shape for slotted pipe is tetrahedral and for casing pipe is Quad-dominated and a default algorithm is used, the approximate global size is 0.3 for tubing and experimental pipes and 1.4 for casing pipe and an example is shown in Fig. 5-6.

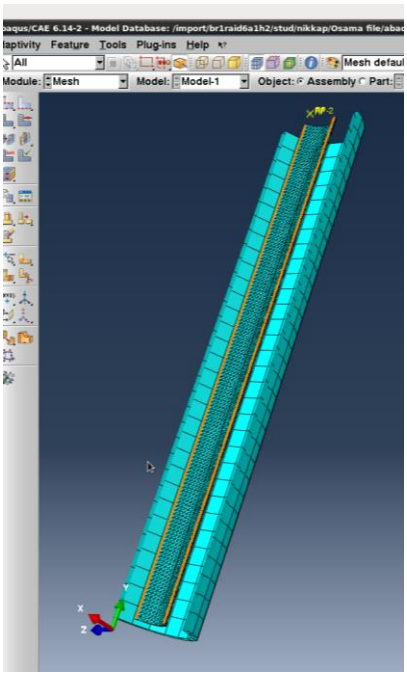

Fig. 5-6 meshed experimental pipe (model 2)

The number and type of elements presented in Table 5-4 along the side of each part in the models are selected based on the mesh analysis scope.

Table 5-4 Element types in the created models

Model	Part	Element type
Model 1	Experimental Pipe	C3D10M
Model 2& 3	Tubing	C3D10M
	Casing	R3D4
		R3D3

- Boundary Conditions setup: the following boundary conditions are assigned with the initial step:

  - Bottom cross-section surface of the tested pipe is assigned to a symmetry (Encastre) boundary condition which prevents the surface motion in any direction.

- The top reference point of the tested pipe is assigned to a Displacement/Rotation boundary condition to allow this point to move only in the direction of the applied axial force, by this way and with the assigned constraint between this point and the top cross section surface, the later will has the same restricted motion.
- The casing pipe is assigned to a symmetry (Encastre) boundary condition too.

Creating load: for each step, different load is assigned:

- For buckling step, a concentrated force is assigned to the top reference point of the tested pipe, which means applying this force on the top cross section surface, and the inserted value for this force is (-1) in the direction of the axial load, so the resulted Eigen value will be the critical buckling load.
- For Static-Riks step, a concentrated force is assigned to the top reference point too, and the magnitude of the compression force is (-10^6 lbs) in the axial direction of the pipe.
- For explicit step, no load condition is required to be assigned, only an additional (Displacement/Rotation) boundary condition should be defined for the moving surface (the top surface in this work) after creating this step. In this BC, the required crushing distance should be defined, for example: the crushing distance in the axial direction for the tubing in (model 2) is (-40 inches) as shown in Fig. 5-7.

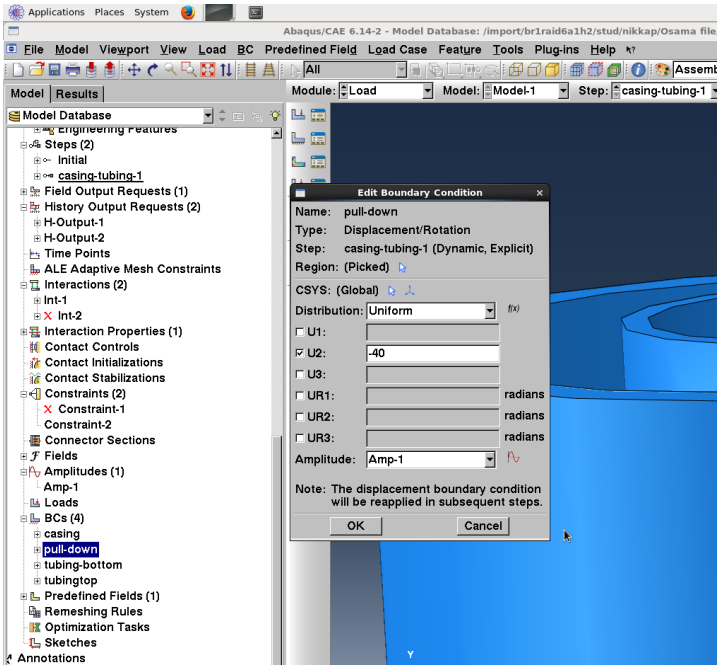

Fig. 5-7 define the BC for the explicit step in model 2

- Creating job: once all tasks involved in defining the model have been finished, the job is created to start the analysing the model. It is preferred to perform data check before submitting the job to change any errors in the model inputs.

5.2. Experimental work tools and execution

The aim of the experimental work was to verify the numerical simulation and compare the achieved initial buckling force with the analytically calculated one.

5.2.1. The used pipe specifications

The use pipe is supposed to be used previously to perform experiments related to a master thesis [63], and some of the pipe properties are taken from that work, while the rest of the mechanical properties of the pipe are taken from graphs shown in Fig. 5-5 on the ground that the pipe is API standard 5.5" casing. The measured size was used in calculation for both the analytical estimation and numerical solution.

The pipe was available pipe in UIS Drilling Engineering store, and it has the specifications presented in Table 5-3, based on an assumption that it is the same pipe in Giskemo's experiments.

5.2.2. The apparatus (the hydraulic press)

Located in (Ivar Langens hus) building in UIS and belong to civil engineering laboratory, (Toni Technik) hydraulic press is used to apply the required forces (Fig. 5-8), and the press is calibrated and tested in 2015 up to 3000KN. The press has position sensor, pressure sensor and proper data acquisition tools.

5.2.3. Other tools

Many tools (located in IKM workshop, Kjølv Egeland hus, UIS campus) have been used to complete the experiment like:

- Cutting machine to cut the pipe Fig. 5-9.
- Grinder to make the longitudinal slots.
- Measuring tools.

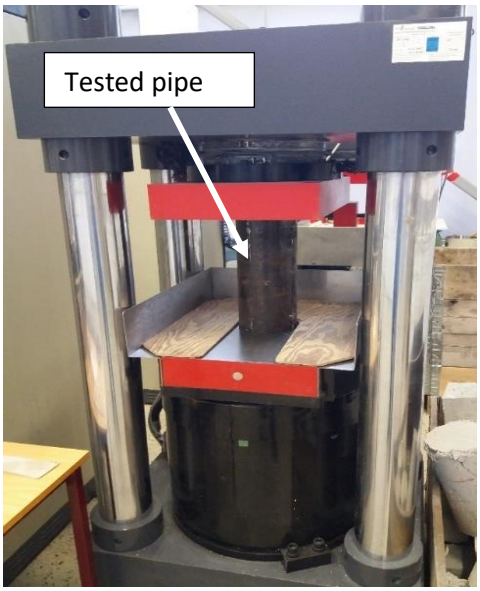

Fig. 5-8 Hydraulic press used to perform Test 1

Fig. 5-9 pipe sawing machine

5.2.4. Test steps

It is important to mention that, it was proposed to perform more than one experiment to cover more details, but the shortage in the time, available equipment capabilities and a proper pipe availability reduced the planned tests to one.

All other testing details used in the experimental work were necessarily simulated in finite element model.

- **Pipe preparation**

To perform the test, a 13.4in (34cm) pipe with properties presented in Table 5-3 was cut longitudinally to create four symmetric equal in length (10in) slots, and the slots were created using grinder in a way that the pipe is still whole at the top and the bottom.

- **Test performance**

The pipe is subjected to axial compression force using the hydraulic force, the speed of testing was 0.1mm/s and the load- displacement curve was obtained on the computer attached to the machine. The stages of the collapsing are shown in Fig. 5-10.

For safety reasons, the collapsing operation is stopped without reaching the total deformation of the pipe, and the last reached level is shown in the last picture to the right in Fig. 5-10.

Fig. 5-10 pipe collapse stages

5.2.5. Other experimental work

Another and (similar in principle) experimental work was performed by "Andreas Holsen[3]" as a part of his master thesis and the test results were not published at the time of writing this thesis, some of these results were used to validate the analytical estimation, so it had to mention the data and conditions about those experiments:

The tests were revolved applying compression axial force against a 1in steel pipe placed in to bigger pipe using a hydraulic press.

The pipe properties are presented in Fig. 5-11, Andreas performed different test with or without slots, the slots number varied between 1 to 5. And the results and their comparison with other data are presented in the next chapter.

L=40cm

l_{slot}= 38cm

do= 2,5 cm

di= 2.1 cm

Di= 4.93

σy= 265MPa

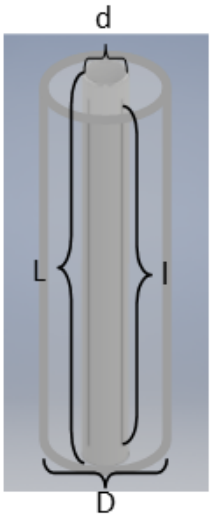

Fig. 5-11 experiment pipe figuration

[3] Andreas Holsen: Master student in drilling engineering (2015-2017), University of Stavanger

6. Results and Discussion

6.1. Analytical estimation of the initial crushing force results

In DHTD method, applying a pressure above the piston during crushing will produce a force acting on the top of the handled tubing. To bring the idea closer to the mind, the graph in Fig. 6-1 illustrates an example for the relation between the pressure and its produced force, the example is based on an assumption that the piston is placed in 95/8" 53.5 lb/ft casing and applies the force in the cross section of 4.5" 12.6 lb/ft L80 tubing. In this context, Table 6-1 shows some other examples of the force magnitude that will be delivered by applying certain pressures using water or dense fluid, and one can see clearly that using heavier fluids increase the pressure applied to the piston thus, the force for crushing.

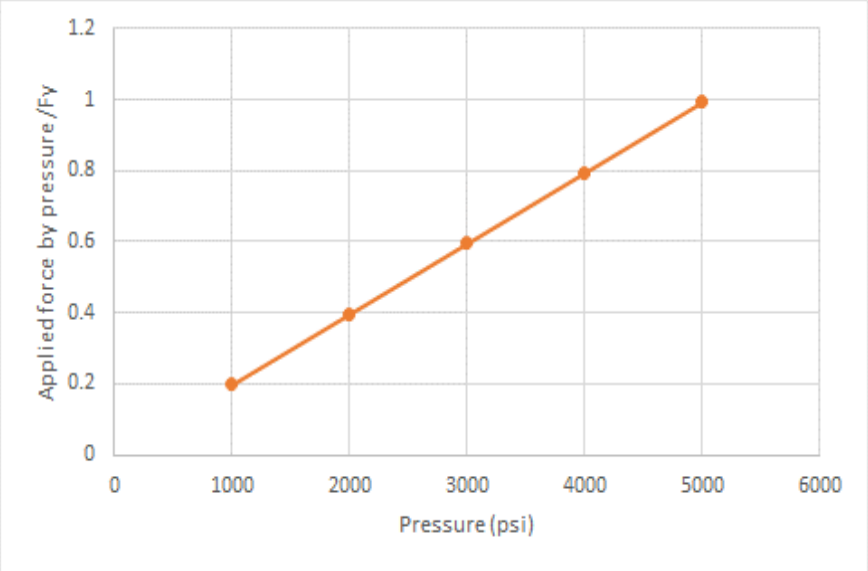

Fig. 6-1 produced force due to applied pressure

Table 6-1 example compaction loads

Casing/Tubing	13.375 in.	9.625 in.	7 in	5.5 in
Weight	72 ppf	53.5 ppf	29 ppf	23 ppf
Internal Diameter	12.347 in	8.535 in	6.184 in	4.67 in
Piston Area	119.7 in2	57.2 in2	30 in2	17.1 in2
Force per 1000psi with H20	54.4 tons	26 tons	13 tons	7.8 tons
w/ 3,000 psi w/ 10ppg (1.2sg) compaction fluid @ 9,843 ft/3,000 m	209.5 tons	100.1 tons	52.6 tons	30 tons

In Chapter 4, an estimation of the initial "Euler type" buckling force was presented in Section 4.2.1, and based on Eq's 4.19, 4.22 and 4.25, some calculations were performed to see the effect of slots number and length on the initial buckling strength, while keeping the many rest parameters unchanged.

It is important to be mentioned that this estimation is a rough estimation and it is just an idea which needs a lot of extra studying and experimental work and it only covers one set of slots (Fig. 5-11). On the ground, a lot of other issues should be considered and this estimation could be totally different specially when it comes to determine (k) value in those equations since the type of plates connection is odd, so it is chosen to be 1 for whole unslotted pipe, and 0.32 for the slotted tubing as an estimated value based on some experiment results shown in the following Section 6.1.1, which is not enough to judge the validity of this estimation.

The following results are based on calculations considering the following data:

- 4.5" 12.6 lb/ft. tubing.
- Young's modulus $30\text{x}10^6$ psi.
- The moment of inertia values are taken from Table 4-1.
- The length of slot varied from 1in to 400in (app. 1 joint of tubing).
- Number of slots varied from 2 to 8 slots.

Presented in Table 6-2, the values of helical and sinusoidal buckling limits at different degrees of inclination are calculated based on Eq's 4.1 and 4.16 assuming the same tubing is placed inside 9 5/8" 53.5 lb/ft. casing, and the helical critical limits are presented in the following figures for the 30deg and the 60 deg. inclination, it is important to mention that helical buckling calculations are based on a whole tubing pipe without slots. Honestly, the effect of slots on lateral and helical buckling is not clear and unknown therefore, more studies should be performed to evaluate this effect.

In the following graphs, the values of critical Euler's buckling loads are divided by the whole un-slotted tubing yield force (288000lbs in this example) for better understanding.

Table 6-2 Sinusoidal and helical limits (95/8"53.5lb/ft. CSG x4.5" 12.6lb/ft. TBG)

Section	Inclination angle (Degrees)	Sinusoidal limit	Helical limit	F_{crhel}/ F_y
vertical	0	1076.967	2250.861	0.007815
inclined	15	10223.1	28931.37	0.100444
	30	14209.2	40212.02	0.139608
	60	18700.35	52922	0.183734
	75	19749.51	55891.12	0.194042

Fig. 6-2 shows that for 8 slots case regardless of the slot length and for 60deg inclination, the required force to start the slotted tubing crushing will not produce any helical buckling, and It is shown that for 3 slots -and more- with slot length more than 100in, the required crushing force will be less than the helical critical limit too.

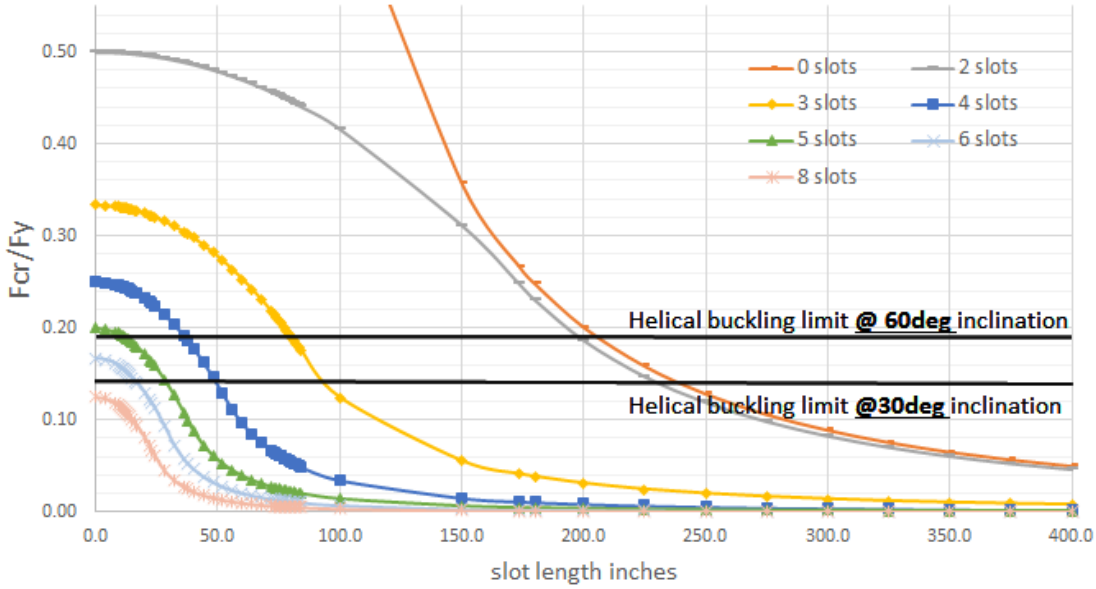

Fig. 6-2 slot length effect on the critical Euler's buckling limit ratio

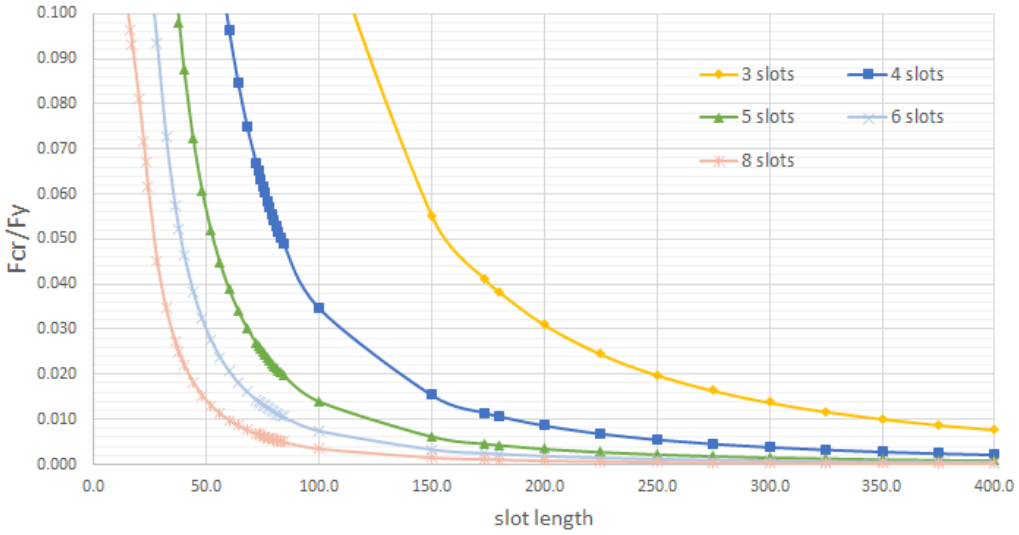

Fig. 6-3 effect of slot length on the buckling strength ratio (for ratio< 10%)

By Comparing Fig. 6-1 and Fig. 6-2, one can see that any applied pressure can produce Euler buckling for this example.

The effect of increasing the slot length on the relative buckling strength ratio, for which the number of slots is more than 2 slots and buckling strength ratio is less than 10%, is shown in Fig. 6-3, and one can notice the following points:

- The longer the slot, the lower the buckling strength ratio.
- Neglecting the region with slot length less than 100in, generally, with increasing the length of slot, the weakening effect of that on the buckling strength ratio is decreased, to appear as if the ratio does not change with the increasing of the slot length.
- Within the region where the slot length less than 100in and with increasing the number of slots, the relative buckling strength ratio gets a higher descending trend versus the length parameter and the descending rate of the curve is much higher when the length is lower.
- The effect of slots number -higher than 3 – seems to be less on the buckling strength ratio with increasing the length of the slots over 200in.

For further understanding, Fig. 6-4 and Fig. 6-5 show the relation between the slots number and the buckling strength ratio for different slot lengths. One can notice the following points:

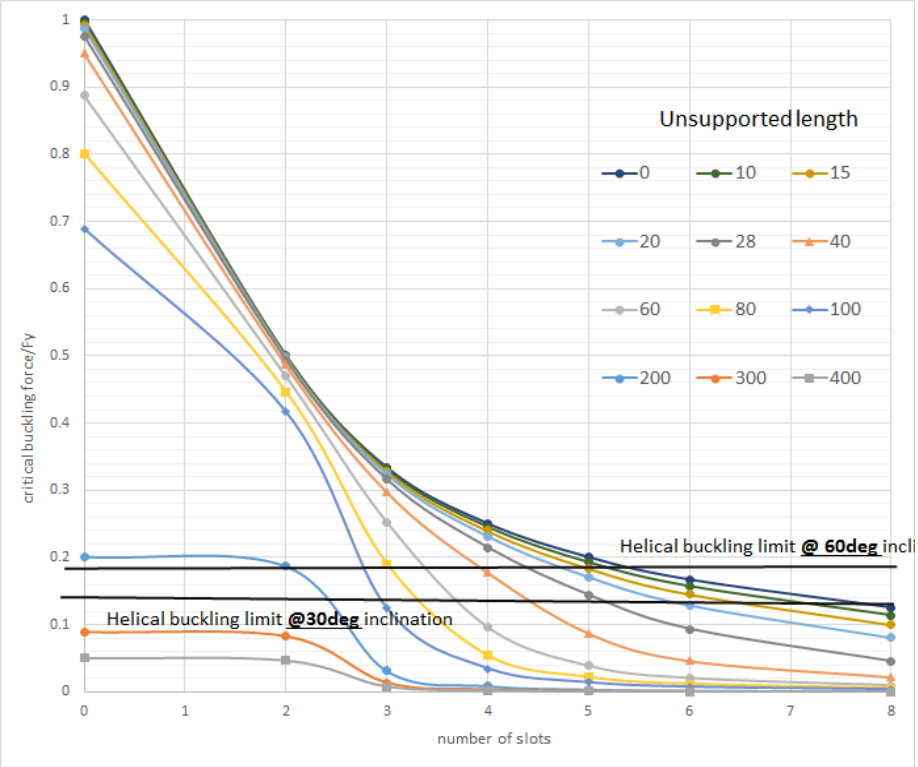

Fig. 6-4 slots number vs buckling strength ratio

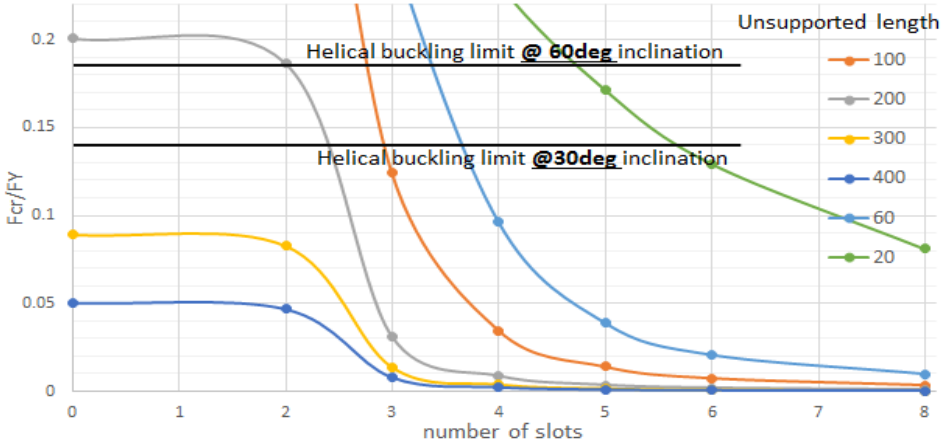

Fig. 6-5 effect of slots number on the buckling strength ratio for ratio< 20%

- With the length of slot lower than 100in, the relative buckling strength ratio gets a rapid descending trend versus number of slots. The ascending rate of the curve is much higher when number of the slots is lower than 4 slots, while 3 & 4 slots numbers are an articulated points for the most of the cases (L>60in), while after this number, neither the length of the slots nor the number of them has significant effect on the buckling strength ratio.

Fig. 6-6 shows the critical force divided by the corresponding curved plate yield force vs the length of the slot, the curves are raised to value 1 at 0 length which represents the yield force for each plate (check Table 4-1). One can notice in this figure that the whole cylinder curve is below the 2 slots cylinder curve, also one can see the high effect of the plate curvature on the buckling strength, whereas, the smaller curvature the higher effect on buckling strength at lower plate length .

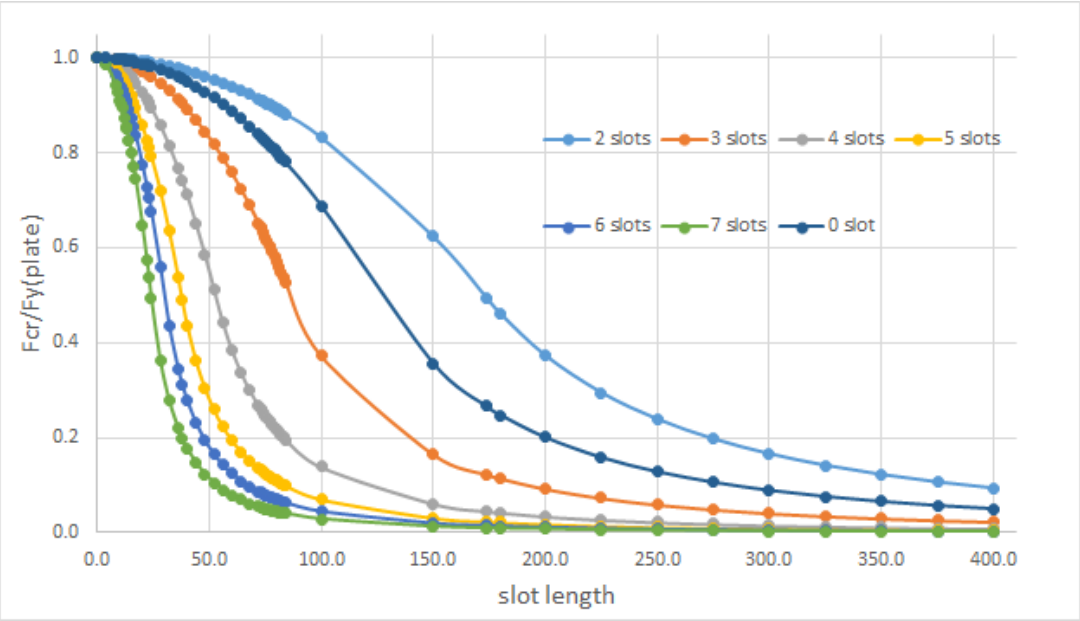

Fig. 6-6 the critical buckling load to yield force of curve plate vs the slot length

6.1.1. Comparing Analytical estimation with experimental results and the numerical solution

The initial buckling force achieved by the first experiment (explained in details in Section 5.2) was (2775.25 kN = 623901lbs) which is close to the yield force of the pipe. This result could be represented by one point in the previous curves as shown in Fig. 6-7. The shown curve is drawn by using identical data to the experimental pipe data shown in Table 5-3 but with different numbers of slots.

Comparing the predicted load that obtained by calculations with the experimental result revealed a miscorrelation between the two values which can be attributed to the high hardness of the used pipe and to strain hardening and geometry of the tube [64].

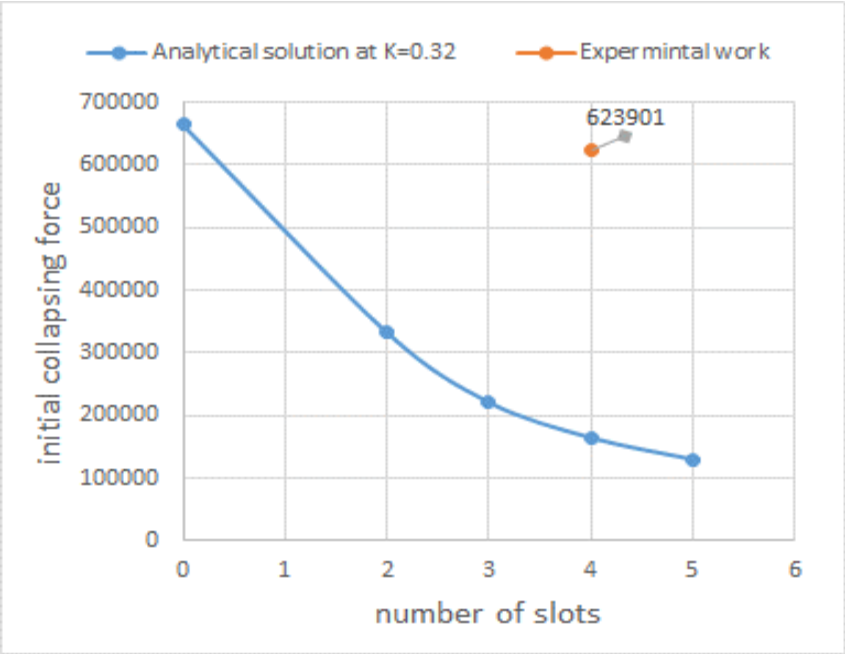

Fig. 6-7 comparison between the experimental work and analytical solution

The second experiment was not published at the time of writing this thesis, but the results were obtained by verbal communication with the student who performed the tests, the setup data and condition of experiments were presented in the previous chapter.

Within the framework of the analytical estimation outlined above, the important part from Andreas's results is the first peak of each test which represents the initial buckling force, here the K value for non-slotted pipe was chosen to be 1 and for the slotted pipe was 0.32 those

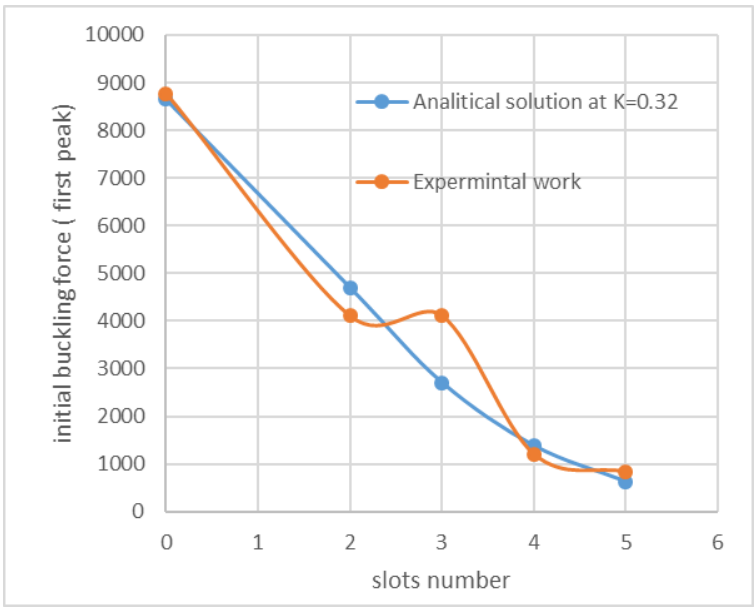

Fig. 6-8 comparison between the experimental work and analytical solution

values gave fair agreement between the analytical and the experimental results as shown in Table 6-3 and Fig. 6-8.

Table 6-3 comparison between experimental results and analytical estimation

Slots number	Analytical estimation Lbs	Experimental results Lbs	Remarks
0	9013.134	8769.799	Based on 44ksi as a yield strength
2	4698.183	4105	Based on average of two values
3	2705.805	4111.757	
4	1378.298	1209.472	
5	624.5704	845.2818	

Another comparison is illustrated in Fig. 6-9. It can be seen that the predicted values are within (-16%) and (+50%) of the measured results. The over and under estimation reasons are not clear, and more experimental work is required to verify such estimation, but one can say that at higher number of slots the analytical estimation gives good agreement with the experimental work.

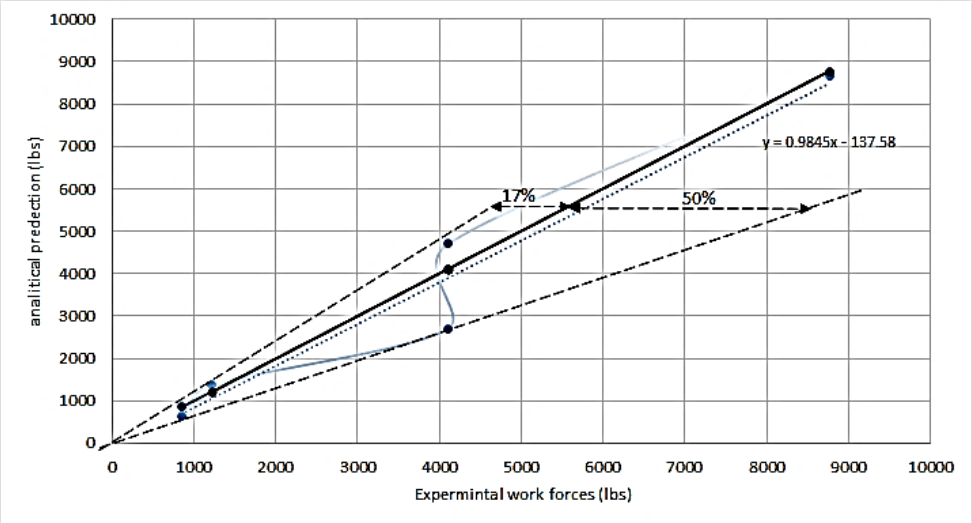

Fig. 6-9 comparison between experimental and analytical prediction

6.2. FEM simulation results and analysis

The main target of the numerical study is to figure out the FEM ability in modelling the downhole tubing disposal. It is important to mention that several attempts were made to achieve this target, but the limited time of the thesis work since the tool consumed a considerable time, in addition, to the lack of knowledge and experience in using such tool without any kind of help, with the exception of the help from Dr. Mesfin Belayneh, all of that

did not allow to achieve the required target, this however does not mean that the technique is not a powerful method to solve these kind of problems.

6.2.1. Validation FEM results with experiment

Fig. 6-10 shows a comparison between Abaqus Model#1 results (using the static step and the explicit one) and the experiment results (explained in Section 5.2), and Fig. 6-11 shows a

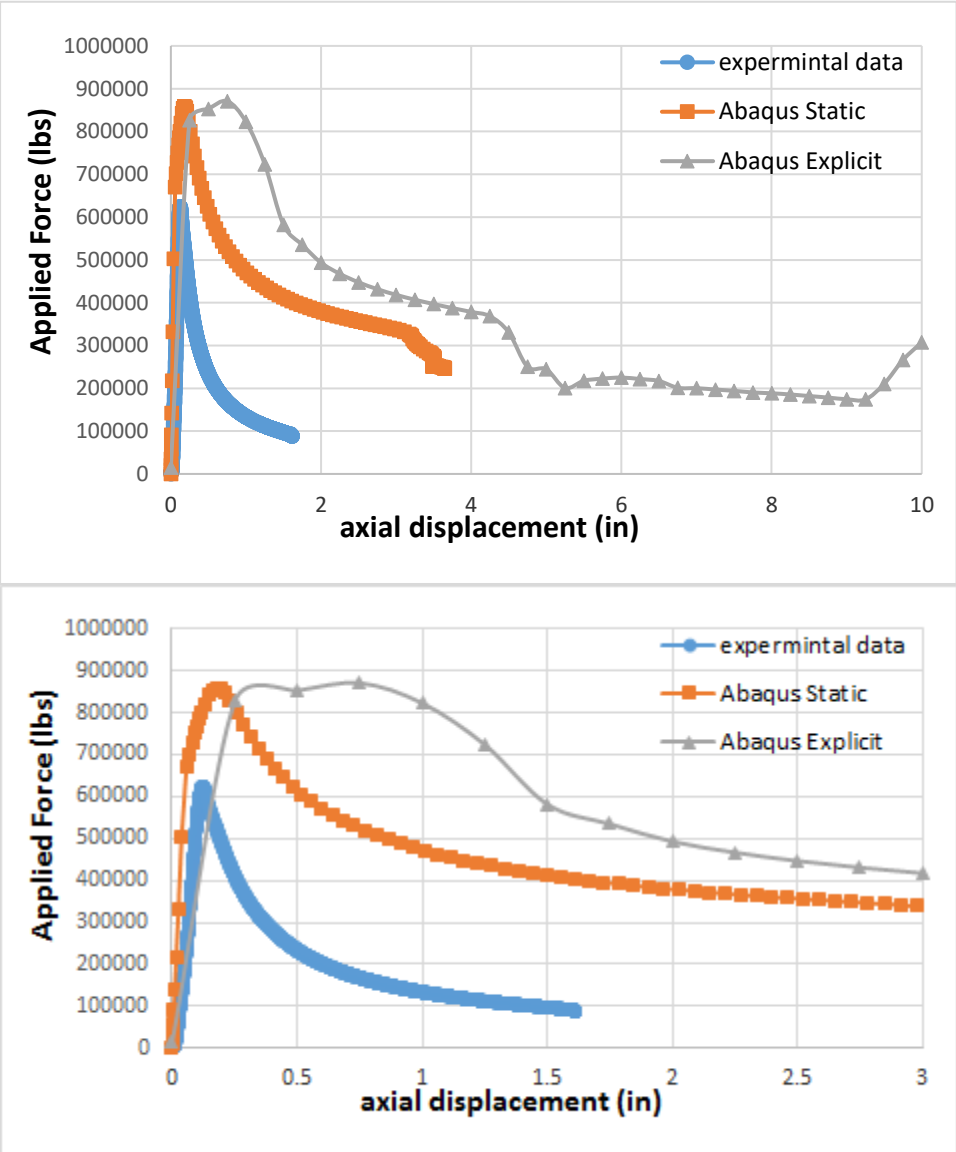

Fig. 6-10 crushing curves comparion

comparison of the way the pipe collapsed. When the buckling step is applied in model 1 in Abaqus, different shapes of collapsing are obtained and the one shown in Fig. 6-11 is the most close one to the expermint result.

The load-displacement graph starts with a rapid increase of the force due to the elastic compression, followed by a rapid drop (but slower than the previous raising), and then a slight

drop in the force start with increasing the displacement. The predicted post-buckling is only shown in the Abaqus/explicit graph and shows a steep rising of the force when the parted walls come into contact at the end of the crushing operation.

The shape of the graphs in the experimental test and the Abaqus/Static-Riks step are similar, but it is clear that the FEM method overestimates the crushing load, and this is due above all to the way that the load and the constraint are defined in the model, because the force could have been less if the load was assigned to the top surface directly where each node of the surface share the same applied load, but in this model, the load is assigned to one reference point and then distributed to the whole top surface, and this highlights the importance of the role that experiments play to figure out the ideal type of model inputs.

The seeming hump in the Abaqus explicit curve is a result of the self-contact of the pipe and that can be noticed in the video of the pipe crushing shown in Appendix E.

By comparing the results of Explicit step and Static-Riks step, one can see that inducing the contact force increases the crushing force in Explicit step, this is also due to the simple difference between the two techniques, whereas in the static technique “the time increment size is limited only by the desired accuracy of the solution” [65], so the large time period (1second) used in explicit step reduce the accuracy of the solution and to get better results this time period should be optimized.

For this special combination of slots number and length, the visual examination of the pictures in Fig. 6-11 showed:

- Good agreements between the numerical simulations and the experimental outcomes (this is one of the shapes obtained by buckling step).
- The pipe buckling starts at the middle, and the maximum lateral displacement is also noticed at the middle of the pipe.
- The direction of the pipe part movement could be inward or outward, in the experiment one part moved inward and the rest moved outward, while in the simulation it gives different shapes.

- The pipe buckling shape is an “Euler” mode that is mentioned in Section 4.2.3.

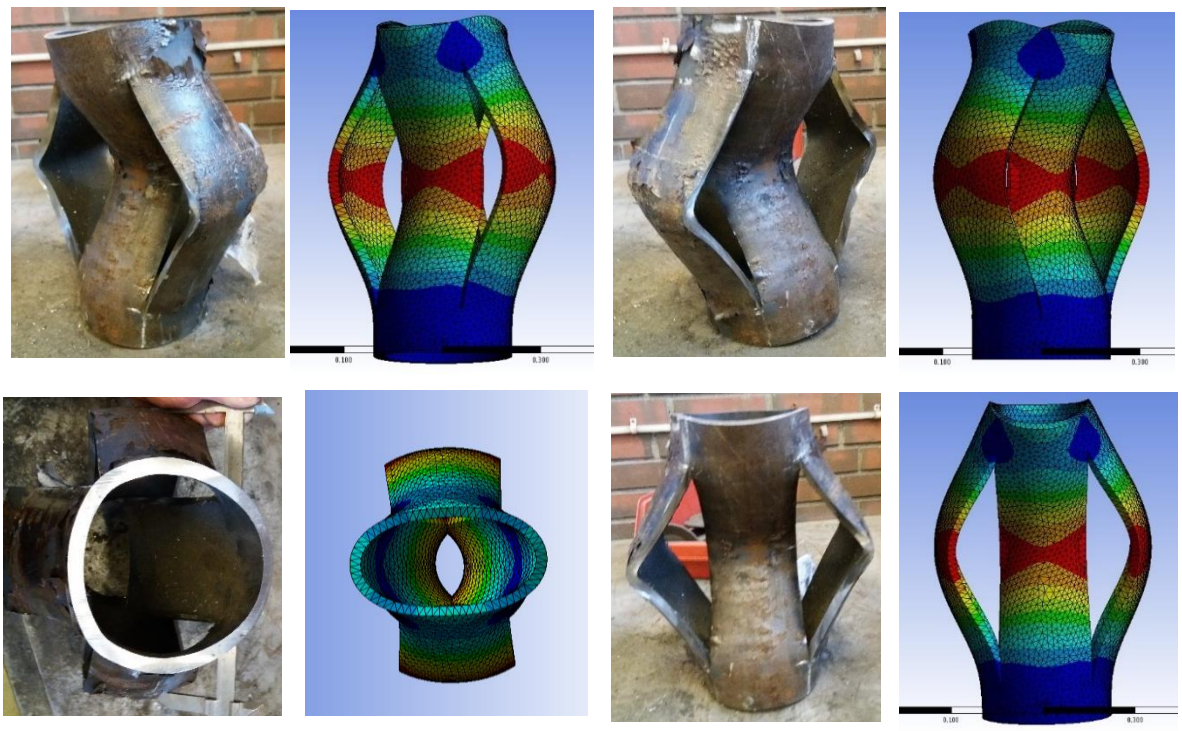

Fig. 6-11 the manner of collapsing using ANSYS workbench

6.2.2. Results from ABAQUS simulation and analysis:

6.2.2.1. Model #2 results:

Three jobs are created for this model each job is associated with different step (Buckling, Static-Riks and Explicit).

The buckling step results show different way of pipe buckling with rough estimation for the critical (linear) buckling force (Eigen value) as Fig. 6-12 shows.

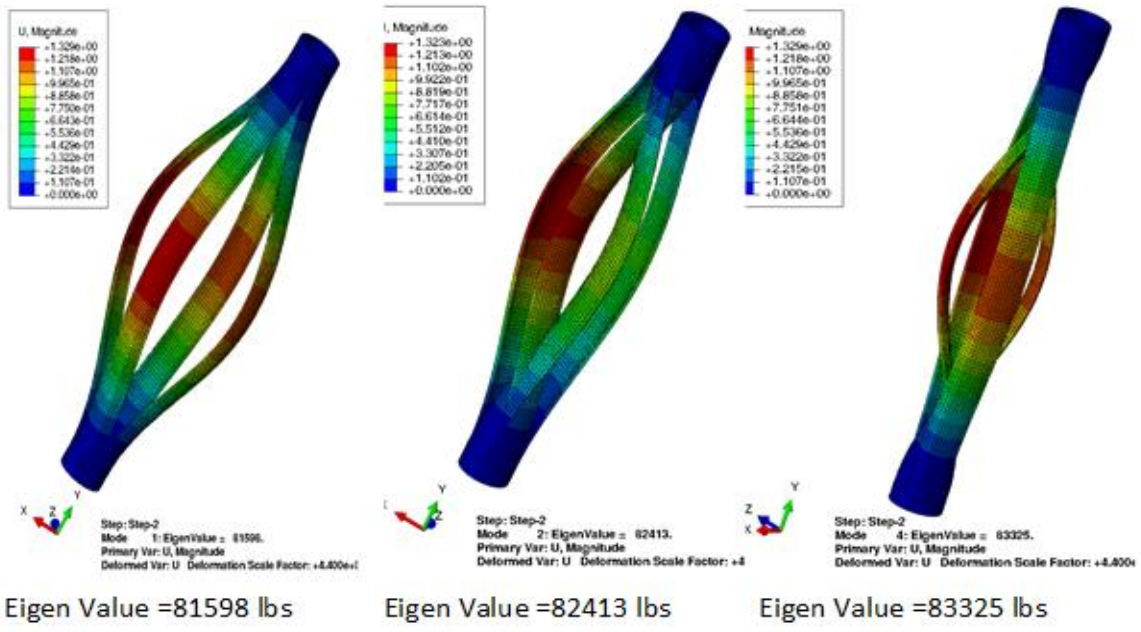

Fig. 6-12 Examples of Model#2 buckling

While Fig. 6-13 and Fig. 6-14 show the force-displacement relation for both Explicit and static. Once again, it should be recalled that the crushing load results could be overestimate due to the reasons mentioned above.

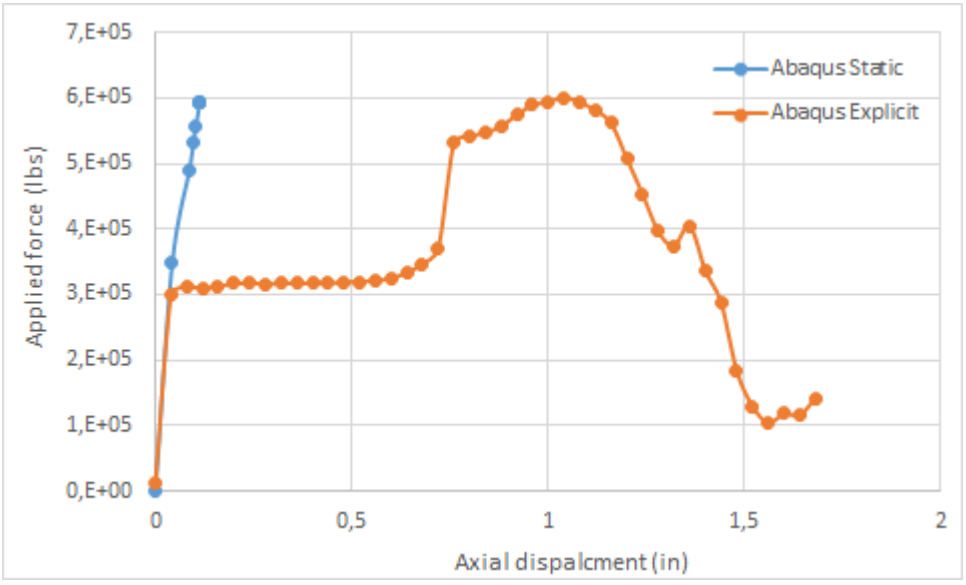

Fig. 6-13 Model#2 initial buckling force vs displacement

In Fig. 6-13, one can see that the maximum crushing force in both steps is the same but it has been reached at different displacement and this could be due to the contact definition of the tubing with itself and with the casing and the post buckling behaviour in the explicit step [66],

which is also the reason behind seeing the hump in the Abaqus explicit curve and that can be noticed in the video picture of the pipe crushing shown in Appendix E.

From Fig. 6-14 which shows the whole crushing process, it can be observed that, when compaction start, a load peak is produced and it is higher than any other peaks, and it is clear how the applied force fallen sharply after the first peak and then it started increasing gradually until the two pipes contact restrict any additional movement when the reaction forces start to increase rapidly as one can see from Fig. 6-15. This job did not complete due to an error but it was close to the required displacement input (40in).

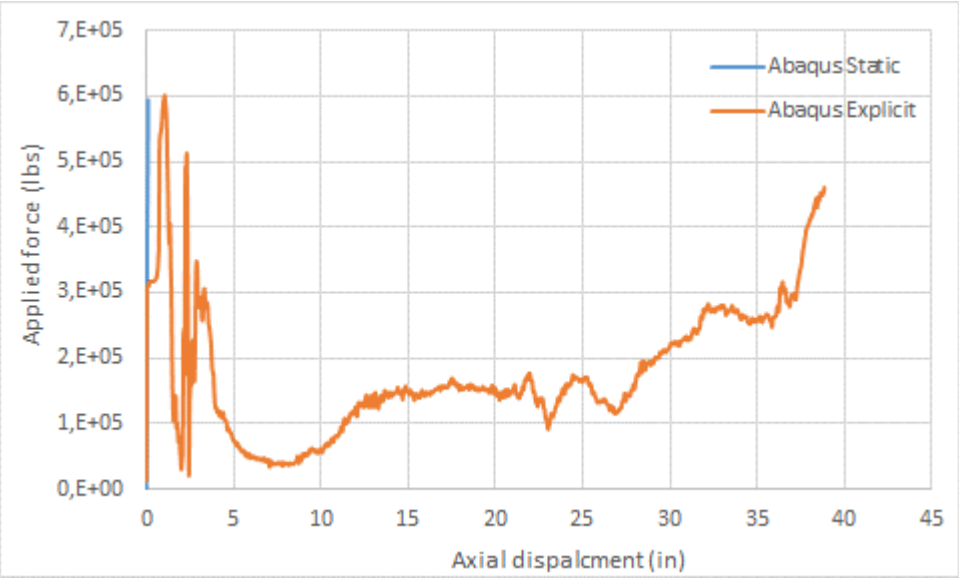

Fig. 6-14 Model#2 crushing force vs displacement including post-buckling

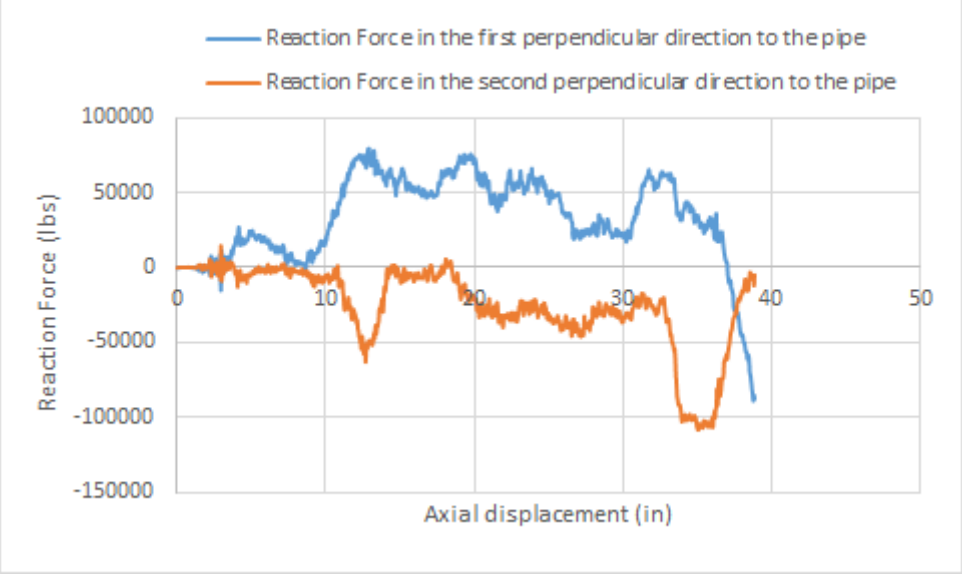

Fig. 6-15 Reaction Force in the perpendicular directions to the pipe Model#2

Some images of crushing process are shown in Fig. 6-16.

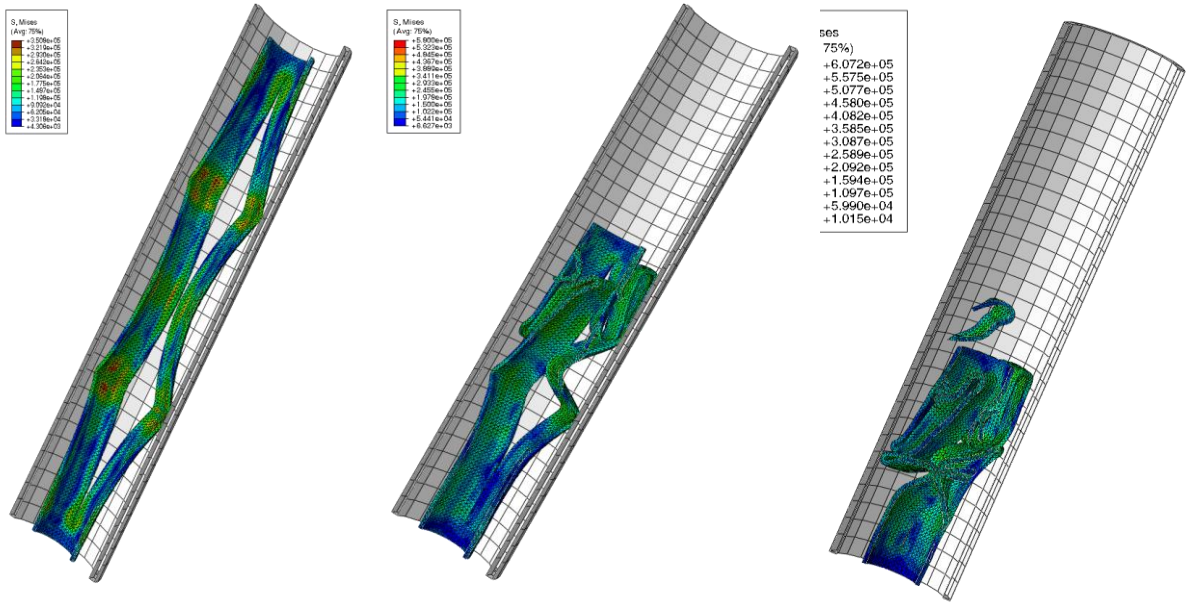

Fig. 6-16 tubing inside casing crushing process example

6.2.2.2. Model #3 results:

This model was the most time-consuming model, each one run took several days especially when assigning a long time period (1sec for example), since the number of elements and nodes was incredibly high (around 410000 element). The model simulated one slotted joint of tubing (many segments of slots as shown in Fig. 5-4) placed inside a casing pipe. None of the pipe inclination, the oil well buckling or initial casing/tubing contact is involved in the model.

The results shown in this section are the "last moment" results - just before submitting this work - and the Abaqus job was not completed yet. Only one step was used for this model, which is explicit step, the time period was 1sec, whereas with lower period, the jobs was aborted due to errors.

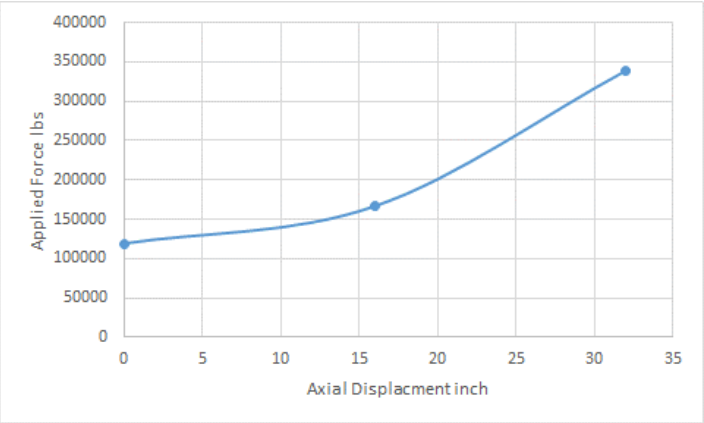

Fig. 6-17 Model#3 Load-Displacement after 0.1 sec

Fig. 6-17 shows the axial applied load at the top reference point of the crushed pipe vs the axial displacement until the moment the result was taken (t=0.1sec) when it was supposed to be 1sec.

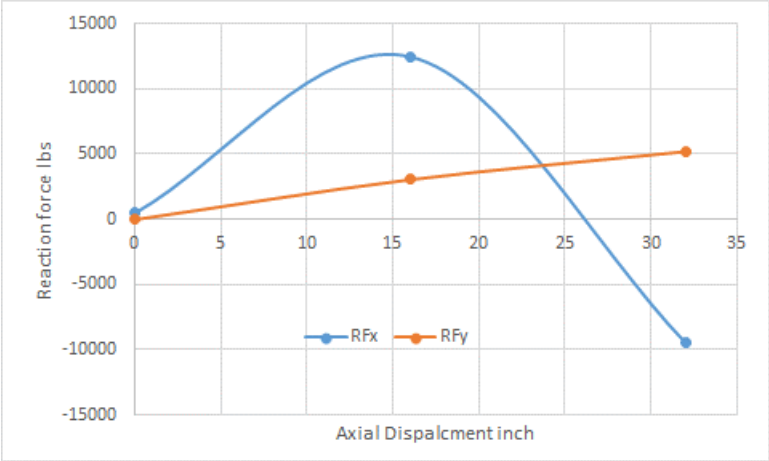

Fig. 6-18 Reaction Force in the perpendicular directions to the pipe Model#3

Fig. 6-18 shows the reaction forces in the perpendicular directions to the pipe at time 0.1sec too, and it is difficult to comment about these data because of its inadequacy.

On the other hand, and by visual inspection of the deformed tubing shown in Fig. 6-19, Fig. 6-20 and Fig. 6-21 at 0.1 second, one can see that after the upper two segments are totally compressed, the deformation starts at the bottom segments and not at the middle segments. This kind of optimum condition is a result of the initial force impact at the top, while the pipe weight contribution and presence of the bottom boundary condition initiate the splaying at the bottom segments and that occurs when the contact force between tubing and casing resulted from crushing the upper segments mitigate the transferred force through the tubing (check videos in Appendix E for more clarification).

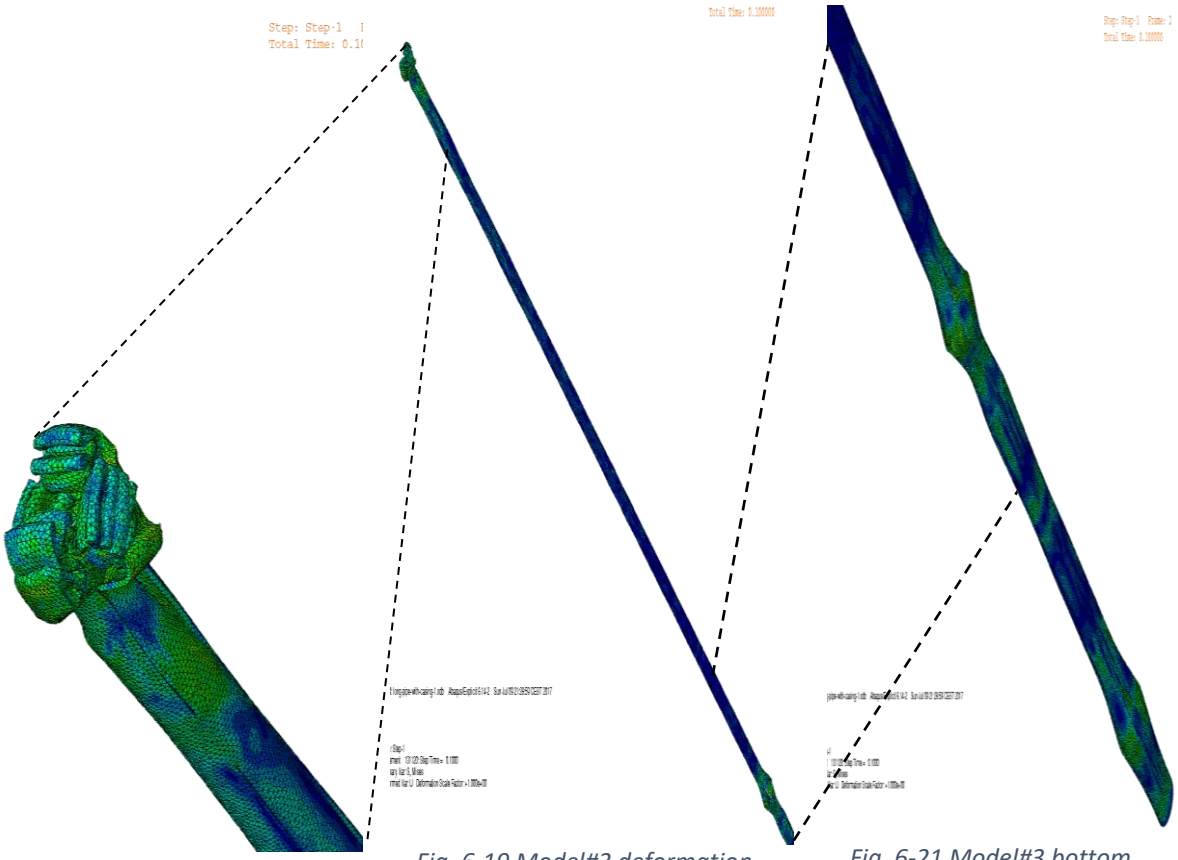

Fig. 6-20 Model#3 top deformation after 0.1 sec

Fig. 6-19 Model#3 deformation after 0.1 sec

Fig. 6-21 Model#3 bottom deformation after 0.1 sec

6.3. Analysis of transferred axial force along the tubing

The enormous frictional forces over the compacted tubing due to splaying and wedging could stop the operation, and a better design of the operation could mitigate producing this kind of forces, and with no unavoidable occurrence of that, the effect of these forces on the transferred axial force along the pipe should be estimated for better understanding the course of things. But the associated chaos with compaction operation will make it difficult to find convincing solutions for that.

In Chapter 4, Section 4.3.3 showed a set of equations to calculate the transferred axial force using Coulomb friction model presented in Eq. 4.34. In this section, an example will show the transferred axial force in helically buckled pipe case (the case that consumes the greatest amount of the transferred force compared to the straight or sinusoidal buckled pipe). The importance of this example is to show how the contact force per length unit can change with the presence of external force and bending moment acting on the pipe since there is no model can predict this force for the splaying slotted tubing. So the point is to see the effect of different parameters on the normal force and hence the axial transferred force.

The example will show the effects of the following parameters on the transferred force:

- Inducing force by the piston
- The friction coefficient
- Wellbore inclination.
- Different set-up's of the tubing and casing combinations

The transferred force is calculated using Microsoft Excel tool. At the first step, the value of inducing force is assumed and then the contact force due to tubing weight and buckling is calculated using Eq. 4.37 and 4.38, then the change in the transferred force after a distance step (assuming to be 1m) is calculated using the model in Eq. 4.34 after discretizing it to be in the shape:

$$\Delta F = (w.cos\alpha - \mu N)\Delta x \qquad 6.1$$

At each step, the resultant value from this equation will be added to the force in the previous step until the end of the pipe.

The tubing and casing combination used for the first three following sections is 4.5" 12.6lbs/ft. tubing in 95/8" 53.5 lb/ft. casing and the effect of buoyancy is ignored.

6.3.1. Influence of the inducing force

Fig. 6-22 shows the transferred force as a function of the length of the parted tubing (assuming whole un-slotted tubing) at different inducing force magnitudes, the inclination is assumed to be 30 deg., and the friction coefficient is 0.3.

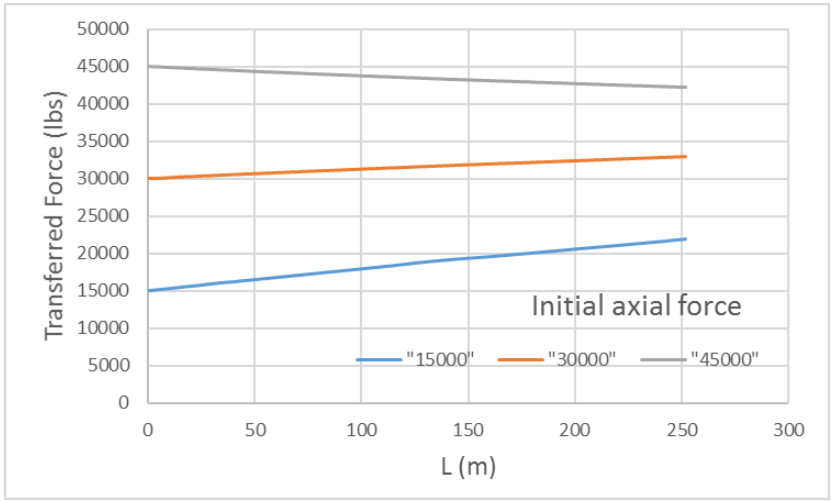

Fig. 6-22 effect of inducing force on the transferred force

One can see from the figure that increasing the inducing force above a certain limit will reduce the transferred axial force with increasing the pipe length which will make the later values of the transferred force close to each other regardless of the initial applied force.

6.3.2. Influence of the friction coefficient

Fig. 6-23 shows the transferred force as a function of the length of the parted tubing (assuming whole un-slotted tubing) at different friction coefficient, the inclination is assumed to be 30 deg., and the inducing force is 30000lbs.

In general, one can say that the effect of reducing the friction coefficient will increase the transferred axial force, and vice versa, but for this special case with these specific input data, the unexpected result is that with lower friction coefficient the increasing effect on the axial force is higher than the reducing effect with higher friction coefficient, and of course there is a value where the friction is not affecting.

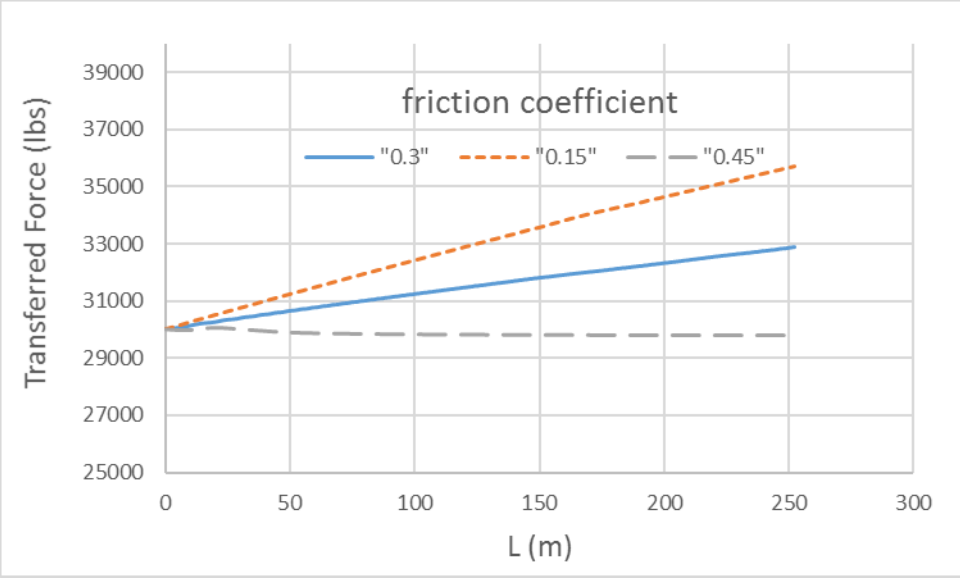

Fig. 6-23 effect of friction coefficient on the transferred force

6.3.3. Influence of the inclination angle

Fig. 6-24 shows the transferred force as a function of the length of the parted tubing (assuming whole un-slotted tubing) at different inclination angles, the friction coefficient is assumed to be 0.3, and the inducing force is 30000lbs.

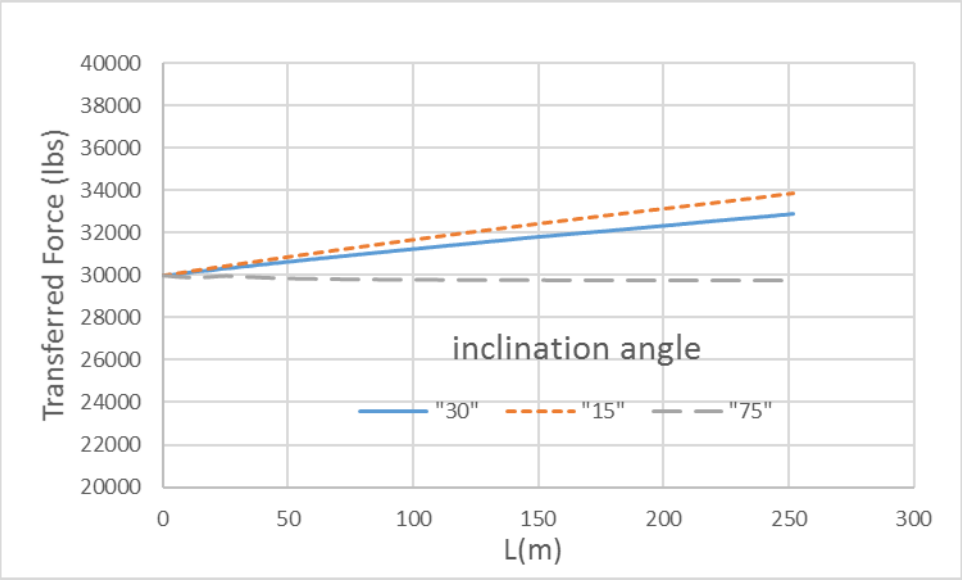

Fig. 6-24 effect of inclination angle on the transferred force

Fig. 6-24 tells that the effect of reducing the inclination angle will increase the transferred axial force, and vice versa, it has been noticed that the magnitude of inclination effect is changed with changing other parameters.

6.3.4. Influence of the casing and tubing combination sizes

6.3.4.1. Effect of tubing size

For a better understanding of the tubing size effect on the axial transferred force, a constant (assumed) value of the radial clearance is assumed in order to neutralize the role of this parameter in the used equation, and this value is not available on the ground for all used tubing sizes in this example. The assumed radial clearance is 1.4in and it is selected depending on the average of the radial clearances of different tubular combinations. The rest of the assumptions are the same in the previous sections: (inclination angle 30deg, friction coefficient 0.3, inducing force 30000lbs).

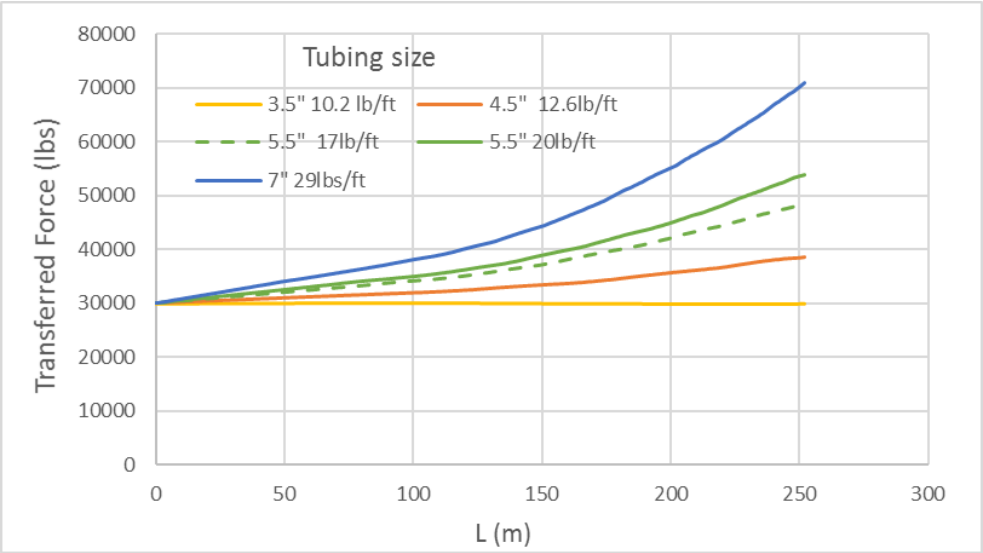

Fig. 6-25 tubing size effect on the axial transferred force

Fig. 6-25 shows the transferred force as a function of the length of the parted tubing at different tubing size and weight units, and it is noticeable from the figure that the tubing size and weight unit has a great effect in the transferred force, the bigger tubing - and its weight unit- the higher transferred force especially with pipe length increasing.

It is very necessary to recall here again that this example does not express a tubing crushing case but a pipe under helical buckling and the effect of the tubing size could be totally different, and more experimental studies are required to check the validity of this statement.

6.3.4.2. Effect of casing size

In Eq. 4.38, the casing size effect appeared in the radial clearance. So, to estimate this effect, different values of the radial clearance is assumed (0.8, 1.2, 1.6, 2 in) which are not available on the ground for the tubing size (4.5”), the higher radial clearance the bigger casing. These values are chosen to be in a range of the radial clearances of different tubular combinations. The rest of the assumptions are the same: (inclination angle 30deg, friction coefficient 0.3, inducing force 30000lbs).

Fig. 6-26 shows the transferred force as a function of the length of the parted tubing at different radial clearance values, and the effect of decreasing the radial clearance is clear in increasing the transferred force, and the effect of the radial clearance is much lower compared to the tubing size effect. But here again, it should be recalled that this example does not express a tubing crushing case but a pipe under helical buckling and the effect of the radial clearance could be totally different.

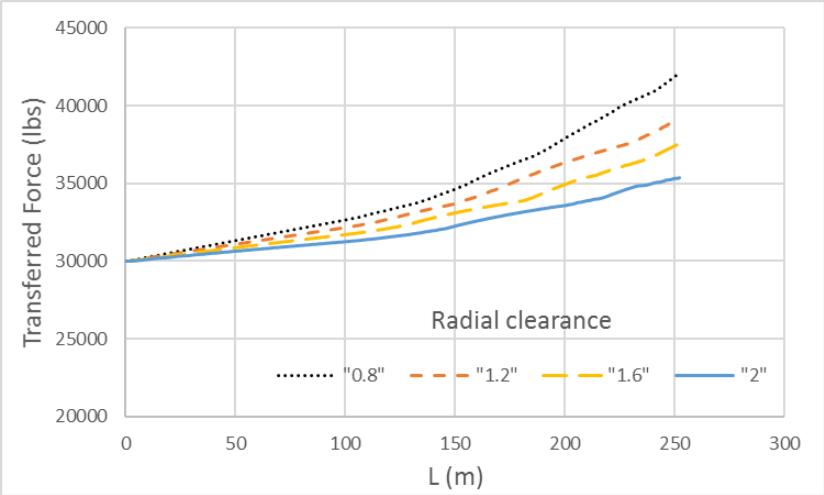

Fig. 6-26 effect of radial clearance on the transferred axial force

7. Summary, Conclusion and Recommendation

7.1. Summary

Conventionally, P&A operations use large expensive drilling rigs to pull the tubing to provide an open casing window to set a full cross section cement plug barrier.

The presence of tubing in the area where the permanent plug should be set is still a thorny issue for P&A rig-less operation for many reasons. Recently there are many approaches for removing tubing in place without pulling it to surface, and Oilfield Innovation has taken a patent on one of these new ideas. The idea can be titled as downhole tubing disposal (DHTD) on a rig-less concept, the method can be summarized as follows:

Compacting a part of weakened tubing instead of pulling the whole tubing out of the hole. The weakening can be achieved by slicing the tubing longitudinally and two scenarios for the weakening are presented to perform the method in a well with an explanation for the necessary tools. The required compacting force on the tubing can be a hydraulic force achieved using a piston positioned above the parted tubing, thus a casing window will be created and it will enable to log cement behind casing and set the barrier, and Oilfield Innovation performed many physical tests on the idea achieving compression ratios up to 46%.

The method has worth considering advantages starting with saving costs by reducing the usage of personal and equipment to its lowest level, passing through reducing the pollution and increasing the safety. On the other hand, the technology has its own challenges, particularly the field evidence deficiency, as well as some technical issues.

Studying the topic in theory is a real hard work because it is not only related to crushing a piece of pipe but also related to the oil well condition, which has different theoretical principles when it comes to apply a compression load on top of long string of pipes. Therefore, in this work, one of the tubing wreaking scenarios is chosen to simplify the study.

This scenario proposes to crush the tubing by locally deforming slotted segments, and from this perspective, an analytical idea is presented and it is based on treating each slotted segment as a bunch of connected curved plates and then defining the required force to initiate buckling on these plates. This work also involved a study to determine the loads acting on the crushing piston.

In chapter 5, FEM is introduced to use this method in building models that simulate the tubing crushing, and ABAQUS tool is used since it is as powerful tool to solve this kind of problems. In addition, experimental work is performed to check the results from both analytical estimation and numerical analysis.

7.2. Conclusion

This section addresses the findings of the numerical analysis and the analytical estimation and their validations, whereas three buckling strength histories for a slotted API piece of pipe were obtained by three different ways (analytical, numerical and experimental) and comparing the results show that:

- Miscorrelation is reported between the analytical initial bucking force of the pipe with that obtained experimentally. On the other hand, another experiment work shows a fair agreement between the two studies. It is believed that for small “length/diameter” ratio, the analytical estimation could not be applicable. Anyhow, more experimental studies are still required to validate the whole analytical estimation idea, and on the ground, a lot of other issues should be considered.
- Overestimation is reported between the FEM force history with that obtained experimentally, but this is due to the lack of experience in using a complicated tool such Abaqus, which required considerable expertise to approximate the FEM solution to the experimental one in such problems. On the other hand, the shifting values can be attributed to the post buckling behaviour of the pipe. Even though, the visual inspection shows good similarity between the shape of the experimentally crushed pipe and the one obtained by FEM model.
- In the analytical estimation, two main parameters were changed (the length of slot and slots number) while keeping the rest of the parameters unchanged, and the effects due to their variation on the buckling strength were studied.
- If it is recognized that the analytical estimation gives a rough idea about the required initial splaying force, then the results can tell:
  - Slicing has significant weaken effect on the buckling strength, and the magnitudes of such effects are dependent on both length and number of slots.

- The effects of slots number (more than 2 slots) on the relative buckling strength ratio of curved plates, for which (Length of slot <150”) is much higher than that in higher lengths.
- The shorter slot (L<150”), the greater the effects of slot length on their buckling strength.
- Neglecting a range of short slots, generally with the increase of the slot length, the weakening effect of it on the buckling strength of is decreased.
- With increasing the number of slots, the relative buckling strength ratio gets a rapid descending trend versus the length parameter.
- With increasing the length of slot, the relative buckling strength ratio gets a rapid descending trend versus number of slots. The descending rate of the curve is much higher when the number is in the middle (2,3 or 4 slots).

- The results from FEM were very useful since the Abaqus can provide different kinds of data, including the reaction forces between the tubing and the casing with a visualization features that can give a better understanding of the whole process, and it is recommended to use this tool as a guide when planning any similar process.

7.3. Recommendation

This section summarizes some - but not all - points related to DHTD method including its proposal test and links the obtained findings to this method on the ground to produce the most desirable results.

- It is recommend to perform any proposed test with similar couplings, cable and gauge clamps to prove the theory.
- It may not be useful to induce a high force above the piston because this could accelerate crushing the top part of the handled tubing and not the lower one. In addition, above certain inducing force, the transferred axial force can be reduced with increasing the pipe length.
- Reducing the friction in the handled tubing area is highly vital issue at all levels, the less friction the higher efficiency of the process.

- Tubing size and its weight per length unit could be the most influential – but uncontrolled - parameter that affects the whole process.
- The pressure applied above the piston can produce a significant force on top of the handled tubing, which can reach to the pipe yield force, but the formation fracture pressure will narrow the range of the applicable effective pressure.
- Regarding to the two scenarios issue, it is believed that the outcomes from Scenario 1 are relatively difficult to be guaranteed with presence of tool joints, clumps and control lines, though, comparing to Scenario 2 the required force in Scenario 1 could be less and the compaction ration could be higher.
- If Scenario 2 is to be adapted, then the length of the slots at each segment should be optimized in a way that the axial force can still be transferred to the following segment and the compacted steel will not produce a rigid body preventing any farther compaction. Within this context, it might be also preferable to leave an adequate length of the unslotted segment of the tubing between the slotted ones, since the numerical simulation showed that the compressed parts will go up and down.

References

1. AGONAFIR, M., *Advanced Drilling Engineering and Technology, Ch #2*. 2016, University of Stavanger.
2. Baker Hughes. *Pipe Recovery Tools*. 2017; Available from: https://www.bakerhughes.com/products-and-services/evaluation/cased-hole-wireline-services/pipe-recovery/mechanical-pipe-cutter-mpc.
3. Khalifeh, M., *Casing Removal*. 2016, University of Stavanger: Stavanger, Norway.
4. Gadrilling. *Plasmabit technology PLASMABIT Milling*. 2017 2017 [cited 2017; Available from: http://www.gadrilling.com/applications/.
5. Welltec, *RLWI Solutions*, w. Cutter, Editor. 2014, Welltec: http://www.welltec.com.
6. Norsok, D., *010. Well integrity in drilling and well operations.* Standards Norway, Rev, 2013. **4**.
7. World Oil Tools. *Thru-Tubing Inflatable Packer*. 2010 [cited 2017; Available from: http://www.worldoiltools.com/thru-tubing-packer.htm.
8. Abel, L.W.F., Robert *Safer Snubbing Depends on Proper Pre-job Calculations.* World Oil,, 1988: p. 85-91.
9. GE Oil&Gas. *Wireline Technology*. 2017 [cited 2017; Available from: https://www.geoilandgas.com/oilfield/wireline-technology/downhole-electric-cutting-tool-dect.
10. Halliburton, *Jet Cutters*, P.R.S. Reducing Nonproductive Time, Editor. 2011, halliburton.
11. Halliburton, *Control Line Clamp*, C.L.C.a. Protectors, Editor. 2013, Halliburton.
12. Wikipedia. *Euler's critical load*. 2017 2017, May 19 17:53, June 5, 2017]; Available from: https://en.wikipedia.org/w/index.php?title=Euler%27s_critical_load&oldid=781148479.
13. Oilfield Innovations Limited, *Large Real Scale Tubing Compaction Simulation* C. Smith, Editor. 2017: USA. p. 48.
14. Valdal, M.B.L., *Plug and abandonment operations performed riserless using a light well intervention vessel*, in *Petroleum engineering*. 2013, University of Stavanger: Stavanger, Norway.
15. Lubinski, A. and W.S. Althouse, *Helical Buckling of Tubing Sealed in Packers.* 1962.
16. Oil and U.K. Gas, *Guidelines for the suspension and abandonment of wells , Issue 4, July 2012, Guidelines on qualification of materials for the suspension and abandonment of wells, Issue 1, July 2012*. 2012, London: Oil & Gas UK.
17. Smith, C. and B. Tunget, *Crushing of Tubing within Horizontal Casing*. 2013, Oilfield Innovations Limited: Delta Colorado.
18. Alexander, J., *An approximate analysis of the collapse of thin cylindrical shells under axial loading.* The Quarterly Journal of Mechanics and Applied Mathematics, 1960. **13**(1): p. 10-15.
19. Oilfield Innovations Limited, *Tor E18 Well Example Downhole Tubing Disposal*, in *Downhole Tubing Disposal*. 2015, Oilfield Innovations Limited,. p. 48.
20. Statoil, *Subsea well intervention: Learning from the past - planning for the future*. 2010, Statoil. p. 8.
21. Denney, D., *More-Effective Plug-and-Abandonment Cementing Technique.* 2012.
22. Andrews, K.R.F., G.L. England, and E. Ghani, *Classification of the axial collapse of cylindrical tubes under quasi-static loading.* International Journal of Mechanical Sciences, 1983. **25**(9-10): p. 687-696.
23. Buch, J., H. Mourani, and D. Ngo, *New Advances in Mechanical Engineering Enables Pulling Forces of up to 60,000 lbs. – Experience Gained from Offshore Norway Case Stories*. 2015, Society of Petroleum Engineers.
24. Mitchell, R.F., *Buckling Behavior of Well Tubing: The Packer Effect.* Society of Petroleum Engineers Journal, 1982. **22**(05).

25. Saad, I., *Plug and abandonment operations and tool positioning*, in *Petroleum Engineering Department* 2014, University of Stavanger: Stavanger, Norway.
26. Ahmad, A., et al., *Benefits of Cutting Pipe under Compression in Deepwater Rig Operations*. 2017, Society of Petroleum Engineers.
27. Tunget, B. and C. Smith, *Mitigating the high cost of offshore well P and A*, in *Downhole Tubing Disposal*, O.I. Limited, Editor. 2016, Oilfield Innovations Limited Website. p. 93.
28. NPD. *Exploration and Development wellbores - ordered by the year drilling was entered*. 2017 13/2/2017 [cited 2017 13/2/2017]; Available from: http://factpages.npd.no/factpages/.
29. Myrseth, V., et al., *Development of a Norwegian Open-Source Plug-and-Abandonment Database With Applications.* 2017.
30. Halvorsen, C., *Plug and Abandonment Technology Evaluation and Field Case Study*. 2016, University of Stavanger, Norway.
31. Liversidge, D., S. Taoutaou, and S. Agarwal, *Permanent Plug and Abandonment Solution for the North Sea*. 2006, Society of Petroleum Engineers.
32. Oil and Gas UK, *Guidelines on well abandonment : cost estimation*. Issue 2. ed. 2015, London: Oil and Gas UK.
33. OFFSHORE, I. *OPEN WATER COIL TUBING; A GAME CHANGER IN THE OFFSHORE INDUSTRY*. 2012 [cited 2017; Available from: http://www.islandoffshore.com/media/news-archive/2015/open-water-coil-tubing-a-game-changer-in-the-offshore-industry.
34. Varne, T., et al., *Plug and Abandonment Campaigns from a Riserless Light Well Intervention Vessel Provide Cost Savings for Subsea Well Abandonments*, in *SPE Bergen One Day Seminar,*. 2017, Society of Petroleum Engineers: Bergen, Norway.
35. Island Offshore, *Plugging & abandonment of subsea completed wells – can this be done from a mono-hull vessel?*
36. Halliburton. *The abrasive jet cutting system*. 2017; Available from: http://www.halliburton.com/en-US/ps/project-management/well-control-prevention/jet-cutter.page.
37. Baker Hughes. *Radial Analysis Bond Log (RAL)*. 2017; Available from: https://www.bakerhughes.com/news-and-media/resources/brochures/radial-analysis-bond-log-service-o.
38. Schlumberger, *Cement Bond Logging Tools*, Schlumberger, Editor. 2007, Schlumberger,.
39. HydraWell, *HydraWash™*. 2013.
40. Conoco Phillips Norway, *Developments in Non-Traditional Plug and Abandonment Methods*. 2013, norskoljeoggass.no: Stavanger, Norway.
41. Baker Hughes. *Wellhead Abandonment Straddle Packer*. plug and abandonment barrier installation 2017 [cited 2017 05/03/2017]; Available from: https://www.bakerhughes.com/capabilities/well-plug-and-abandonment/plug-and-abandonment-barrier-installation/wellhead-abandonment-straddle-packer.
42. Kvithyll, J.E., *Gator Perforation Tool*. 2017: TOOLSERV, Stavanger , Norway.
43. The engineering toolbox. *Friction and Friction Coefficients*. Available from: http://www.engineeringtoolbox.com/.
44. World Oil Tools. *Thru-Tubing Inflatable Packer*. 2010 [cited 2017; Available from: http://www.worldoiltools.com/thru-tubing-packer.htm.
45. TAM International, *Thru-Tubing Workover Services* in *Inflatable and Swellable Packers* 2008, TAM International,: USA.
46. Larsen, J.O., *Well Stroker Abilities*. 2017: by Email.
47. Britannica, T.E.o.E., *Buckling*, in *Encyclopædia Britannica*. 2011, Encyclopædia Britannica, inc.
48. Kumar, B. and D.M. Marshall, *An illustrated dictionary of aviation*. 2005: McGraw-Hill Professional.
49. Menand, S., *A New Buckling Severity Index to Quantify Failure and Lock-up Risks in Highly Deviated Wells*. 2012, Society of Petroleum Engineers.

50. Dawson, R. and P.R. Paslay, *Drill Pipe Buckling in Inclined Holes.* Journal of Petroleum Technology, 1984. **36**(19).
51. Miska, S. and J.C. Cunha, *An Analysis of Helical Buckling of Tubulars Subjected to Axial and Torsional Loading in Inclined Wellbores*. 1995, January 1, Society of Petroleum Engineers.
52. Mitchell, R.F., *Effects of well deviation on helical buckling.* SPE Drilling and Completion, 1997. **12**(01): p. 63-70.
53. Mitchell, R.F., *Tubing Buckling - The State of the Art*. 2006, Society of Petroleum Engineers.
54. Duman, O.B., S. Miska, and E. Kuru, *Effect of Tool Joints on Contact Force and Axial-Force Transfer in Horizontal Wellbores.* 2003.
55. AISC, A., *Specification for Structural Steel Buildings*, in *DESIGN OF MEMBERS FOR COMPRESSION*. 2016, AMERICAN INSTITUTE OF STEEL CONSTRUCTION: Chicago, Illinois, UIS. p. 33-43.
56. Gerard, G. and H. Becker, *Buckling of curved plates and shells*, in *Handbook of structural stability* 1957, NATIONAL ADVISORY COMMITTEE FOR AERONAUTICS (NACA): USA.
57. Younes, M.M., *Finite element modeling of crushing behavior of thin tubes with various cross-sections*, in *13th International Conference on Aerospace Sciences and Aviation Technology, ASAT-13,*. 2009, Military Technical College: Cairo, Egypt p. 19.
58. Time, R.W., *Definitions and basic quantities*, in *Two Phase Flow in Pipelines*. 2009, University of Stavanger: Stavanger, Norway.
59. Aadnøy, B.S., *Modern well design*. 2nd ed. 2010, Boca Raton: CRC Press/Balkema.
60. Miska, S., et al., *An Improved Analysis of Axial Force Along Coiled Tubing in Inclined/Horizontal Wellbores*. 1996, Society of Petroleum Engineers.
61. Wu, J. and H. Juvkam-Wold, *Helical buckling of pipes in extended reach and horizontal wells--Part 2: Frictional drag analysis.* Journal of Energy Resources Technology;(United States), 1993. **115**(3): p. 6.
62. Mitchell, R.F., *The Effect of Friction on Initial Buckling of Tubing and Flowlines.* SPE Drilling and Completion, 2006. **22**(02).
63. Giskemo, J.T., *Experimental study of expandable tubular*, in *Petroleum Engineering* 2005, UIS: Stavanger.
64. Reid, S.R., *Plastic deformation mechanisms in axially compressed metal tubes used as impact energy absorbers.* International Journal of Mechanical Sciences, 1993. **35**(12): p. 1035-1052.
65. Abaqus, *Abaqus 6.12 /CAE User' s Manual*. 2012, Dassault Systèmes/ Simulia Corp: RI, USA.
66. Aljawi, A., *Numerical simulation of axial crushing of circular tubes.* JKAU: Eng. Sci, 2002. **14**(2): p. 3-17.

Appendix A

Description of Variable associated with Fig. 3-4	Variable
Area associated with Pressure Differential across the Compaction Piston	A_P
Area associated with Pressure Differential across the Travelling Valve	A_T
Force of Circumferentially Split Tubing acting between Whole Tubing and Casing	$F(z_S, t+1)$
Force of mass and gravity of the Piston at time (t+1)	$m_P g$
Force of Whole Tubing between Split Tubing and Casing Resisting the Piston	$F(z_W, t+1)$
Friction Force acting against Piston at time (t+1)	$f_{P(t)} + \Delta f_{P(t+1)}$
Height of Hydrostatic Column at the Top of the Piston at time (t+1)	$h_{P(t+1)}$
Height of Hydrostatic Column at the Point of Injection below the Piston at time (t+1)	$h_{i(t+1)}$
Measured length of Compacted Tubing along well bore axis	z_C
Measured Length of Inflatable Piston along well bore axis	z_P
Measured Length of Initial Circumferentially Split Tubing along well bore axis	z_S
Measured Length of Initial Circumferentially Whole Tubing along well bore axis	z_W
Measured Length of Space Unobstructed by Tubing along axis of well bore	z_U
Measured Length of Tubing to be compacted along well bore axis	$z_{P\&A}$
Normal Force of Piston against Casing at time (t+1)	$N_{P(t)} + \Delta N_{P(t+1)}$
Number of periods (n)	n
Pipe Angular Buckling Deflection	θ
Pressure associated with hydrostatic head of drive fluids (d=1 to e) above the compaction piston at time (t+1)	$P_d = \sum_{d=1}^{e} \rho_{d(t+1)} \cdot h_{(t+1)} \cdot c$
Pressure associated with hydrostatic head of injected fluids (i=1 to j) below the compaction piston at time (t+1)	$P_i = \sum_{i=1}^{j} \rho_{i(t+1)} \cdot h_{(t+1)} \cdot c$
Pressure for Fracture Initiation of leakages above piston at time (t+1)	$P_{FI(t+1)}$
Pressure Loss of lines between pumps and casing at time (t+1)	$PL_{S(n+1)}$
Pressure of Accumulator formed by Initiating Fracture at time (t+1)	$P_{FI(t)} + \Delta P_{FI(t+1)}$
Pressure of Accumulator formed by Opening Fracture at time (t+1)	$P_{OF(t)} + \Delta P_{OF(t+1)}$
Pressure of Drive Fluid above Piston at time (t+1)	$P_{d(t)} + \Delta P_{d(t+1)}$
Pressure of Injection Fluid below Piston at time (t+1)	$P_{i(t)} + \Delta P_{i(t+1)}$
Pressure Opening Fracture below piston at time (t+1)	$P_{OF(t+1)}$
Pressure within Piston's Inflatable Element at times (t) and (t+1)	$P_{P(t)}, P_{P(t)} + \Delta P_{P(t+1)}$
Pump Stroke Pressure Change at time (t+1)	$\Delta P_{S(t+1)}$
Pump Stroke Volume Change at time (t+1)	$\Delta V_{S(t+1)}$
Radial Clearance	r_c
Specific Gravity of well bore Fluids	$\rho_{d(1)}, \rho_{d(2)}, \rho_{d(3)}, \rho_{i(1)}$
Spring force exerted against travelling valve at time (t)	$S_{F(t)}$
Spring force exerted against travelling valve at time (t+1)	$S_{F(t+1)}$
Time period (t)	t
Viscosity of well bore Fluids	$\mu_{d(1)}, \mu_{d(2)}, \mu_{d(3)}, \mu_{i(1)}$
Volume increase of Travelling Valve Stroke added to fluid above piston at time (t)	$\Delta V_{Td(t)}$
Volume increase of Travelling Valve Stroke added to fluid below piston at time (t+1)	$\Delta V_{Ti(t+1)}$
Volume lost from Accumulator formed by Initiating Fracture at time (t+1)	$\Delta V_{FIL(t+1)}$
Volume lost from Accumulator formed by Opening Fracture at time (t+1)	$\Delta V_{OFL(t+1)}$

Description of Variable associated with Fig. 3-4	Variable
Volume of Accumulator formed by Initiating Fracture at time (t+1)	$V_{FI(t)} + \Delta V_{FI(t+1)}$
Volume of Accumulator formed by Opening Fracture at time (t+1)	$V_{OF(t)} + \Delta V_{OF(t+1)}$
Volume of Drive Fluid above Piston at time (t+1)	$V_{d(t)} + \Delta V_{d(t+1)}$
Volume of Driver Fluid Leakage around Piston to Injection Fluid Volume	$\Delta V_{iPL(t+1)}$
Volume of Injection Fluid below Piston at time (t+1)	$V_{i(t)} + \Delta V_{i(t+1)}$
Volume within Piston's Inflatable Element at times (t) and (t+1)	$V_{P(t)}, V_{P(t)} + \Delta V_{P(t+1)}$
Well Bore Coordinate axis approximately parallel to the earth's surface	y
Well Bore Coordinate axis approximately perpendicular to the earth's surface	x
Well bore trajectory azimuth angle	ϑ
Well bore trajectory inclination angle	φ

Appendix B

Defines the P&ID numbers in Large Real Scale P&ID Schematic shown in Fig. 3-34 and its lengths:

#	Figure 2 P&ID Number	Instructions
1.	9.625"-FF-A1-01	As per Figure 18, one (1) API 9 5/8" (244.5 mm) outside diameter casing pin end cap reducer to the diameter of valve (VV-02) and pipework (2"-FF-A3-02 and 2"-FF-B2-02) of sufficient grade and wall thickens to withstand a pressure of greater than or equal to 5,000-psig or 345-barg.
2.	9.625"-FF-A1-02	As per Figure 14, at least 112 metres (368 feet) and preferably 122 metres (400 feet) of coupled API 9 5/8" (244.5 mm) outside diameter casing joints (+/- 12 Range 2) of sufficient grade and wall thickens to withstand a pressure of greater than or equal to 5,000-psig or 345-barg. Preferably premium couplings with flush internal diameter to minimise piston packer damage.
3.	9.625"-FF-A1-03	As per Figure 18, one (1) API 9 5/8" (244.5 mm) outside diameter casing box end cap reducer to the diameter of valve (VV-03) and pipework (2"-FF-A3-03) of sufficient grade and wall thickens to withstand a pressure of greater than or equal to 5,000-psig or 345-barg.
4.	7.625"-FF-A2-01	As per Figure 18, one (1) API 7.625" (193.7 mm) outside diameter casing pin end cap reducer to the diameter of valve (VV-04) and pipework (2"-FF-A3-02 and 2"-FF-B2-02) of sufficient grade and wall thickens to withstand a pressure of greater than or equal to 5,000-psig or 345-barg.
5.	7.626"-FF-A2-02	As per Figure 14, at least 112 metres (368 feet) and preferably 122 metres (400 feet) of coupled API 7.625" (193.7 mm) outside diameter casing joints (+/- 12 Range 2) of sufficient grade and wall thickens to withstand a pressure of greater than or equal to 5,000-psig or 345-barg. Preferably premium couplings with flush internal diameter to minimise piston packer damage.
6.	7.625"-FF-A2-03	As per Figure 18, one (1) API 7.625" (193.7 mm) outside diameter casing box end cap reducer to the diameter of valve (VV-03) and pipework (2"-FF-A3-03) of sufficient grade and wall thickens to withstand a pressure of greater than or equal to 5,000-psig or 345-barg.
7.	4.5"-TC-C1-01	At least 50 metres (164 feet) of coupled API 4.5" (114.3 mm) outside diameter tubing of any condition (e.g. used), any grade, any wall thickness and any connection plasma cut (see Table 9 Step 4 Figure 20). See Table 6 for total amount of tubulars this size.
8.	4.5"-TC-C1-02	At least 50 metres (164 feet) of coupled API 4.5" (114.3 mm) outside diameter tubing of any condition (e.g. used), any grade, any wall thickness and any connection plasma cut (see Table 9 Step 3 Figure 19). See Table 6 for total amount of tubulars this size.
9.	4.5"-TC-C2-01	Same as Step 7 above, wherein the difference in labelling is used to differentiate between the larger and smaller casing string compactions.
10.	4.5"-TC-C2-02	Same as Step 8 above, wherein the difference in labelling is used to differentiate between the larger and smaller casing string compactions.
11.	PP-01, CV-01, CV-02, FR-01, PI-01, PSV-01 and associate pipework 2"-FF-A3-01	One (1) Positive Piston Pump (PP-01) and associated pipework (2"-FF-A3-01) capable of 100 litres (0.6 bbls) per minute at a pressure of at least 345 bar (5,000-psi) with associated pump valves (CV-01 and CV-02). The pump must be equipped with a flow rate stroke counter (FR-01), pressure gauge (PI-01) and pressure safety valve (PSV-01) or pressure relief valve settable to prevent over-pressuring of pipework.
12.	WT-01. LG-01 and VV-01	One (1) valve (VV-01) usable to contain water within one (1) open water tank (WT-01) equipped with one (1) level indicator (LG-01) when connecting pipework (2"-FF-B2-01) to the pump (PP-01) suction inlet.
13.	2"-FF-A3-02	One (1) series of pipework compatible with the high pressure side of the pump (notionally at least 2" or 50.8 mm outside diameter) capable of withstanding at least 5,000-psig (345 barg) to connect from the pump (PP-01) to the casing end cap (9.625"-FF-A1-01 and 7.625"-FF-A2-01) valves (VV-02 and VV-04).
14.	2"-FF-A3-02 and VV-03	One (1) each series of pipework (2"-FF-A3-02) and valve (VV-03) capable of withstanding at least 5,000-psig (345 barg) to connect casing pin endcap (9.625"-FF-A1-03) to the corresponding casing pin end cap (7.625"-FF-A1-03). Please note that high pressure piping is used between the two casing strings to allow pressure testing of both casing strings at the same time.
15.	2"-FF-B2-01	One (1) series of hoses and/or pipework compatible with the low pressure side of the pump PP-01 (notionally at least 2" or 50.8 mm outside diameter) capable of withstanding at least 100-psi (7 bar) to connect the water tank (WT-01) to the pump (PP-01).
16.	2"-FF-B2-02	One series of hoses and/or pipework capable of transporting water between casing box end caps (9.625"-FF-A1-01 and 7.625"-FF-A2-01) valves (VV-02 and VV-04) to the open water tank without significant leakages.
17.	DR-01	One (1) data recorder capable of recording flow rate (FR-01), pressure (PI-01) and tank level (LG-01) digital measurements at least every second.
18.	PISTON-1	A machined piston with seals, cement wiper plug or an inflatable packer sized for 9 5/8" API casing.
19.	PISTON-2	A machined piston with seals, cement wiper plug or an inflatable packer sized for 7 5/8" API casing, depending upon which is used.

Appendix C

Derivation of the moment of inertia for thick wall curved plate presented in Eq. 4.25

- General formula

$$I_x = \iint_{Area} y^2 . dx. dy$$

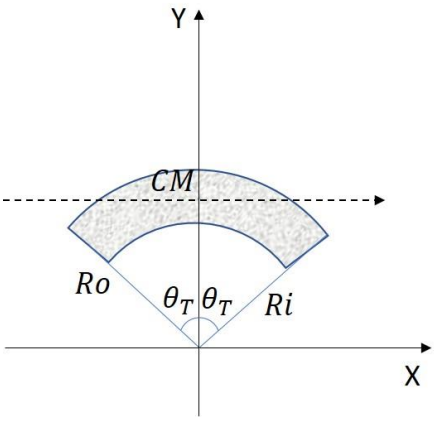

Polar coordinates:

x= r.sin θ

y= r.cos θ

Area inertia around the X-axis (for half section):

$$I_x = \int_{Ri}^{Ro} dr \int_0^{\theta_T} r. d\theta. y^2$$

$$= \int_{Ri}^{Ro} dr \int_0^{\theta_T} r. d\theta. (r. cos\theta)^2$$

$$= \int_{Ri}^{Ro} r^3. dr \int_0^{\theta_T} cos^2\theta$$

$$= \frac{1}{4} (Ro^4 - Ri^4). (\frac{\theta_T}{2} + \frac{sin(2\theta)}{4})$$

- We want the moment of inertia around the axis passing through the centre of mass (CM) at Y coordinate:

$$CM_y = \frac{\iint_{Area} y.dx.dy}{Area}$$

$$= \frac{\int_{Ri}^{Ro} dr. \int_0^{\theta_T} r.d\theta.y}{\int_{Ri}^{Ro} dr. \int_0^{\theta T} r.d\theta}$$

$$= \frac{\int_{Ri}^{Ro} dr. \int_0^{\theta_T} r.d\theta.rcos\theta}{\int_{Ri}^{Ro} rdr. \int_0^{\theta T} d\theta}$$

$$= \frac{\int_{Ri}^{Ro} r^2 dr. \int_0^{\theta_T} cos\theta.d\theta}{\frac{1}{2}(Ro^2 - Ri^2).\theta}$$

$$CM_y = \frac{\int_{Ri}^{Ro} r^2.dr. \int_0^{\theta_T} cos\theta.d\theta}{\frac{1}{2}(Ro^2 - Ri^2).\theta}$$

$$= \frac{\frac{1}{3}(Ro^3 - Ri^3).sin\theta_T}{\frac{1}{2}(Ro^2 - Ri^2).\theta}$$

- We move the axis from the x-Axis to the CM – Axis

$$I_{X_{CM_{1/2}}} = I_x - Area.CM_y^2$$

$$= I_x - \frac{1}{2}(Ro^2 - Ri^2).\theta_T.\left(\frac{\frac{1}{3}(Ro^3 - Ri^3).sin\theta_T}{\frac{1}{2}(Ro^2 - Ri^2).\theta_T}\right)^2$$

$$= I_x - \frac{(\frac{1}{3}(Ro^3 - Ri^3).sin\theta_T)^2}{\frac{1}{2}(Ro^2 - Ri^2).\theta_T}$$

$$= \frac{1}{4}(Ro^4 - Ri^4).\left(\frac{\theta_T}{2} + \frac{sin(2\theta_T)}{4}\right) - \frac{(\frac{1}{3}(Ro^3 - Ri^3)sin\theta_T)^2}{\frac{1}{2}(Ro^2 - Ri^2)\theta_T}$$

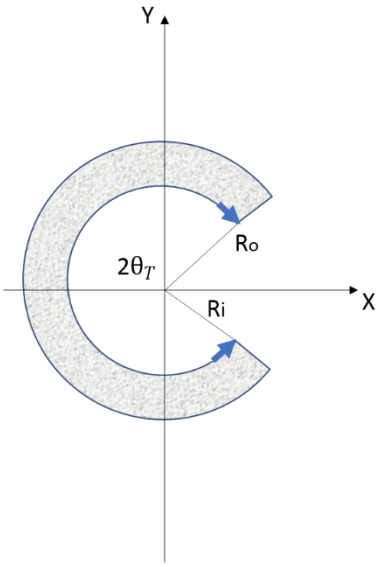

This is for one half, for all, it is double:

$$I_{x_{CM}} = 2.I_{X_{CM_{1/2}}}$$

- Check that works:

For θ = π and Ri=0 we should get a full circle:

Put it into the $I_{x_{CM}}$ formula:

$$I_{x_{CM\,(\theta=\pi, R_i=0)}} = 2.\frac{1}{4}\left(R_o{}^4\right).\left(\frac{\pi}{2} + \frac{sin(2\pi)}{4}\right) - (0)$$

$$= \frac{1}{4}\pi R_0{}^4 \quad \textit{Correct!!}$$

Appendix D

The experimental examples and load-displacement curves for collapsing modes and the absolute size of the tubes used in “Classification of the axial collapse of cylindrical tubes under quasi-static loading “ study performed by Andrews et. al.,[22]:

COLLAPSE MODES

From the axial crushing of 189 tubes, the following modes of collapse were identified[1]:

(a) *Concertina*
Axisymmetric and sequential folding starting at one end of the tube.

(b) *Diamond*
Non-axisymmetric but sequential folding accompanying a change in the cross-section shape of the tube.

(c) *Euler*
Bending of tube as a strut.

(d) *Concertina and 2-lobe and/or 3-lobe diamond*
Folding first in the concertina mode changing to diamond configuration; 2 lobe: square cross-section pattern; 3 lobe: hexagonal cross-section pattern.

(e) *Axisymmetric/concertina*
Simultaneous collapse along the length of the tube, axisymmetric single or multiple barrelling of tube.

(f) *2-Lobe diamond*
Simultaneous collapse along length of tube in the form of the 2-lobe diamond configuration.

(g) *Tilting of tube axis*
Shearing of tube on the platen surface in the form of transverse displacement at one end.

Examples of some of these modes together with diagrams of the appropriate load-displacement curves are shown in Figs. 1–5. Table 1 gives the dimensions of each of the specimens shown in these figures. It can be seen that although none of the curves exhibits a smooth displacement response, the concertina mode presents a regular fluctuation of load about a mean value in a controlled manner. Full details of all tests carried out can be found in [1].

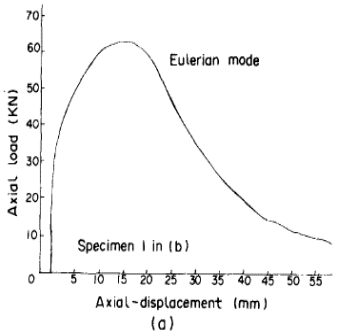

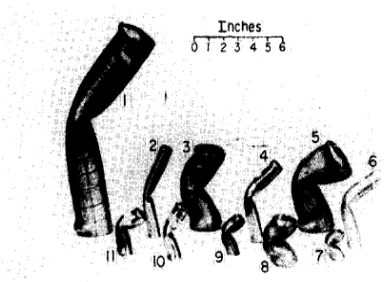

(b) (See Table 1 for specimen details)

FIG. 1. (a) Axial load–axial displacement curve and (b) typical examples of Euler collapse mode.

TABLE 1. DETAILS OF SPECIMENS IN CHARACTERISTIC GROUPS

Euler Collapse Mode (Figure 1)

No.*	Length (L) mm	Internal Diameter (D) mm	Wall Thickness (t) mm	L/D	t/D
1	381	57.15	3.18	6.67	0.0556
2	152.4	19.05	0.92	8.0	0.0483
3	203.2	41.28	4.76	4.92	0.1154
4	152.4	19.05	1.51	8.0	0.0793
5	228.6	47.63	4.76	4.8	0.1
6	152.4	19.05	1.98	8.0	0.1039
7	76.2	12.7	3.18	6.0	0.25
8	127	25.4	4.76	5.0	0.1875
9	88.9	12.7	3.18	7.0	0.25
10	101.6	19.05	1.69	5.33	0.0887
11	101.6	19.05	2.18	5.33	0.1144

*These numbers refer to those shown against each specimen in the appropriate figure.

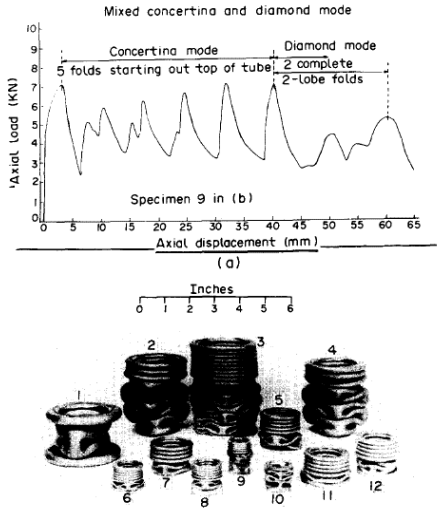

(b) (See Table I for specimen details)

FIG. 3. (a) Axial load–axial displacement curve and (b) examples of the concertina with diamond mode of collapse.

Concertina with Diamond Collapse Mode (Figure 3)

No.	Length (L) mm	Internal Diameter (D) mm	Wall Thickness (t) mm	L/D	t/D
1	177.8	53.98	4.76	3.294	0.0882
2	355.6	57.15	3.18	6.222	0.0556
3	457.2	72.95	1.63	6.267	0.0223
4	279.4	57.15	3.18	4.889	0.0556
5	177.8	35.66	1.22	4.986	0.0342
6	114.3	23.37	0.91	4.849	0.0388
7	114.3	38.66	1.22	3.205	0.0342
8	101.6	23.6	0.9	4.306	0.0382
9	101.6	19.05	0.95	5.333	0.0499
10	76.2	23.65	0.93	3.236	0.0393
11	139.7	35.66	1.22	3.918	0.0342
12	165.1	35.66	1.22	4.630	0.0342

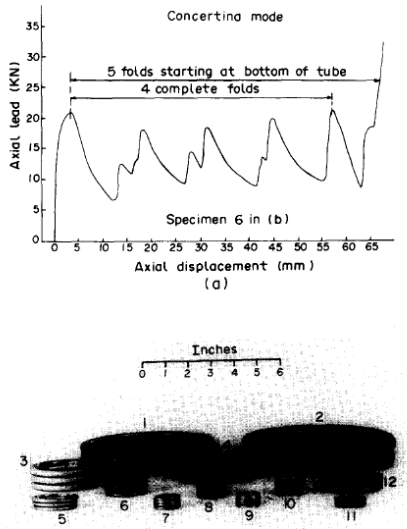

(b) See Table I for specimen details)

FIG. 2. (a) Axial load–axial displacement curve and (b) typical examples of the concertina collapse mode.

Concertina Collapse Mode (Figure 2)

No.	Length (L) mm	Internal Diameter (D) mm	Wall Thickness (t) mm	L/D	t/D
1	152.4	139.7	6.35	1.091	0.0455
2	127	146.1	3.18	0.870	0.0217
3	76.2	57.15	3.18	1.333	0.0556
4	101.6	53.98	4.76	1.88	0.0882
5	76.2	35.66	1.22	2.137	0.0342
6	88.9	35.66	1.22	2.493	0.0342
7	50.8	19.05	1.19	2.667	0.0628
8	63.5	23.57	0.91	2.694	0.0388
9	50.8	19.05	0.92	2.667	0.0483
10	50.8	23.57	0.91	2.115	0.0388
11	38.1	23.57	0.91	1.616	0.0388
12	63.5	44.45	3.18	1.429	0.0714

Appendix E

Model#1 video using Abaqus/Explicit

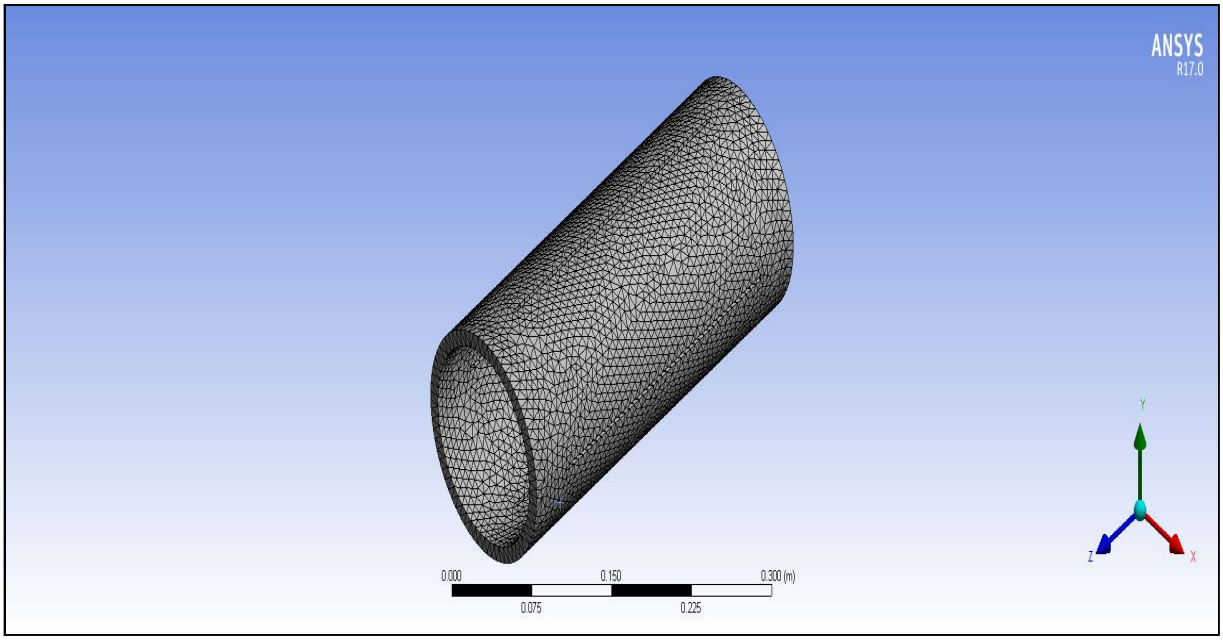

Model#2 video using Abaqus/Explicit

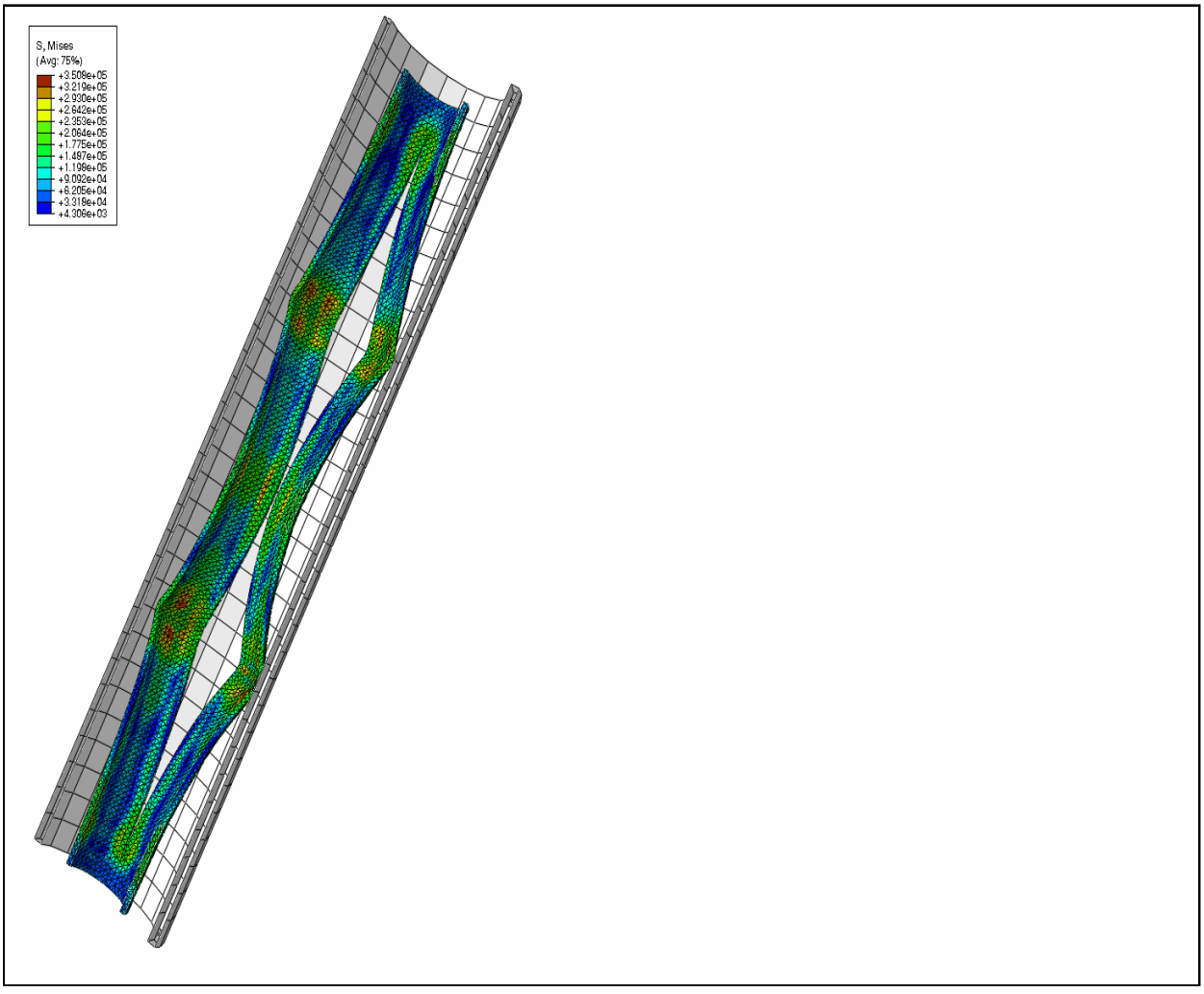

Model#3 video using Abaqus (at the top: tubing top, in the middle: the whole tubing joint, at the bottom: tubing bottom.)